

**OPTIMIZATION OF THE SQUEEZE CASTING PROCESS FOR
ALUMINUM ALLOY PARTS**

Final Report

David Schwam
John F. Wallace
Qingming Chang
Yulong Zhu

Case Western Reserve University

July 2002

Work Performed Under Contract DE-FC07-98ID13613

For

U.S. Department of Energy
Assistant Secretary for
Energy Efficiency and Renewable Energy
Washington D.C.

CONTENT

1. Abstract.....	4
2. Introduction.....	6
3. Squeeze casting technology.....	8
3.1 Literature background.....	8
3.2 Principles of squeeze casting.....	10
3.3 Main processing parameters.....	22
4. Equipment.....	26
5. Experimental results and discussion.....	29
6. Summary and Conclusions.....	45
7. References.....	47

FIGURES

50

ACKNOWLEDGEMENTS

This research investigation was supported by the Department of Energy, Office of Industrial Technology through the Cast Metal Coalition program. Guidance for this work was provided by the High Integrity Castings committee of the North American Die Casting Association. The efforts of Mr. Stephen Udvardy of NADCA and these committees are gratefully acknowledged.

UBE Machinery in Ann Arbor, MI made a substantial contribution to the project by providing the Squeeze Casting System, training and technical support with operation and maintenance. Visi-Track contributed the shot monitoring system for the Squeeze Caster. Ford Motor Company donated the 75kW Lindberg electrical melting furnace. The Case Alumni Association provided \$100,000 towards the installation costs of the unit.

The technical support and advise from industrial squeeze casting operations at CMI, Hayes Lemmerz and Internet are gratefully acknowledged.

This publication was prepared with the support of the U.S. Department of Energy (DOE), Award No. DE-FC07-98ID13613. However, any opinions, findings, conclusions or recommendations expressed herein are those of the authors and do not necessarily reflect the views of the DOE.

1. ABSTRACT

This study was initiated with the installation of a new production size UBE 350 Ton VSC Squeeze Casting system in the Metal Casting Laboratory at Case Western Reserve University. A Lindberg 75kW electrical melting furnace was installed alongside. The challenge of installation and operation of such industrial-size equipment in an academic environment was met successfully. Subsequently, a Sterling oil die heater and a Visi-Track shot monitoring system were added. A significant number of inserts were designed and fabricated over the span of the project, primarily for squeeze casting different configurations of test bars and plates. A spiral “ribbon insert” for evaluation of molten metal fluidity was also fabricated. These inserts were used to generate a broad range of processing conditions and determine their effect on the quality of the squeeze cast parts.

This investigation has studied the influence of the various casting variables on the quality of indirect squeeze castings primarily of aluminum alloys. The variables studied include gating design, fill time and fill pattern, metal pressure and die temperature variations. The quality of the die casting was assessed by an analysis of both their surface condition and internal soundness. The primary metal tested was an aluminum 356 alloy.

In addition to determining the effect of these casting variables on casting quality as measured by a flat plate die of various thickness, a number of test bar inserts with different gating designs have been inserted in the squeeze casting machine. The mechanical properties of these test bars produced under different squeeze casting conditions were measured and reported. The investigation of the resulting properties also included an analysis of the microstructure of the squeeze castings and the effect of the various structural constituents on the resulting properties. The main conclusions from this investigation are as follows:

- The ingate size and shape are very important since it must remain open until the casting is solidified and pressure is maintained on the solidifying casting.

- Fanned gates, particularly on the smaller section castings avoid jetting effects at the ingate end. The fan type ingate helps accomplish a rapid fill without high velocities.
- The molten metal has to fill the cavity before localized solidification occurs. This is best accomplished with a larger ingate to attain rapid filling without excessive velocity or jetting that occurs at high metal velocities.
- Straight gates are prone to cause jetting of the metal stream even at low velocities. Fanned gates allow use of higher fill velocity without excessive jetting.
- A higher metal pressure provides a more complete fill of the die including improved compensation for solidification shrinkage.
- With the proper filling pattern, ingates, overflows and die temperature for a given die, very good tensile properties can be attained in squeeze casting. In general, the smaller squeeze castings require higher die temperatures.
- Computer models using the UES Procast and MagmaSoft finite element software can, after suitable adjustments, predict the flow pattern in the die cavity.

2. INTRODUCTION

The squeeze casting of aluminum alloys and to a more limited extent, magnesium alloys is a rapidly developing technical process that offers the potential for widespread utilization and growth. The process has the capability of producing near net shape castings that are essentially pore free. This permits the solution heat treatment of the castings so that after selective aging, excellent mechanical properties can be attained. It also allows the squeeze castings to be welded, as needed for different structures, without outgassing or blistering.

These advantages and the improved mechanical properties result from several features of squeeze casting. The steel dies used have the close dimensions and details of conventional high pressure die castings. However, thicker runner systems and particularly, larger ingates are used compared to regular pressure die castings. The proper locations of the ingates and maintaining high pressure on the molten alloy and the use of pressure pins (when needed) during solidification permits the casting to be solidified under sufficient pressure to avoid nearly all shrinkage. The high pressure during solidification keeps the molten metal in direct contact with the die surface providing true to die dimensions in the casting. The filling speeds or ingate velocities are relatively low, generally less than five feet per second, so that trapped gas in the casting may be usually avoided with proper venting. The vertically oriented shot sleeve on the equipment employed on this project is filled before the forward stroke of the plunger starts, so that entrapped gas from this source is avoided. The net result is a pore-free or nearly pore-free part.

The close contact with the die surface during solidification results in rapid solidification of the casting. This rapid solidification produces a fine secondary dendrite arm spacing in the castings, so that good strength and ductility can be attained. These excellent properties are relatively high in the as cast condition and are enhanced further in the heat treatable alloys by the excellent response to solution heat treatment. Since the process minimizes both gas porosity and shrinkage cavities, excellent properties are attained. These properties have been shown to be equivalent to wrought alloys in many instances.

Although this process has many obvious advantages in producing parts of light metals that can be utilized in structural applications, the full potential can only be realized after the process has been optimized. This project was undertaken to investigate the variables that will affect the quality of squeeze cast parts and to indicate the best combination of properties to provide castings of the desired quality. Appropriate control of the process requires that the influence of a number of factors on casting quality be evaluated. These include: design and location of ingate, ingate velocity, optimum filling time for a casting, pressure used in filling and molten metal and die temperatures. Other factors such as venting, molten metal quality, die lubricant and die life are being considered but not in the primary thrust of the experimentation.

Some of this information is presently known for other associated casting procedures such as permanent molding and high velocity, high pressure, die casting. However, the direct translation of information from these processes will not provide the optimum for squeeze casting because of the different gating, die filling and solidification patterns that apply.

3. ALUMINUM SQUEEZE CASTING TECHNOLOGY

3.1 LITERATURE BACKGROUND

The A356 aluminum alloy is a widely used aluminum-silicon casting alloy. It provides an attractive combination of excellent castability, corrosion and wear resistance, pressure tightness and particularly high strength-to-weight ratio ^[1-3]. The microstructure and mechanical properties of this alloy depend strongly on the composition, melt treatment, efficiency of feeding system, cooling rate and heat treatment. In general, the mechanical properties are controlled by the cast structure. The mechanical properties of A356 are governed by casting soundness, the amount, size and morphology of the constitutive phases, such as the α -Al phase, eutectic Si-particles, and the distribution of micro-porosity. These factors are in turn influenced by how the Al-Si binary eutectic nucleates and grows during solidification and by the heat treatment process ^[4-6]. Sand casting, permanent mold and die casting (including squeeze casting) are the main processes used to produce castings of Al-Si-Mg alloys. The squeeze casting process yields the highest mechanical properties among these processes ^[7-9].

The earliest reports on squeeze casting originate in the 1878 Russian literature that suggested pressure should be applied to molten metals whilst they solidify in a mold. The commercial development of squeeze casting began to take place in Europe, North America and Japan ^[10-12] only after 1960. Two different types of squeeze casting technology have evolved, based on different approaches to metal metering and metal movement during die filling. These have been given the names “direct” and “indirect”. Both the direct squeeze casting and indirect squeeze casting have advantages and disadvantages. In the case of the direct squeeze casting, the melt is poured directly into an open die, and a hydraulic ram is moved down into the melt to apply the pressure. The biggest advantage of direct squeeze casting process is that pressure is applied to the entire surface of the liquid metal during freezing, producing castings of full density. This technique, inevitably, gives the most rapid heat transfer, yielding the finest grain structure but does not control the die filling stage. This leads to turbulent flow and the entrapment of brittle surface oxide films. The inherent time delay occurring after the metal is poured and prior to

pressurization with the ram often leads to premature solidification. A highly accurate metering system is needed to control the dimensions of the casting. In indirect squeeze casting the pressure is more difficult to apply compared to direct squeeze casting. The melt is injected into the bottom of the die cavity with a hydraulic ram. The metal flow can be controlled via the injection speed and pressure application begins as soon as the die is filled. The casting forms inside a closed die cavity and the dimensions of the casting are easier to control. The use of a highly accurate metering system is not required. As a result, the indirect squeeze casting process has seen more commercial use than the direct process in die casting industry ^[13-14].

Squeeze casting is a process by which molten metal solidifies under applied pressure that is maintained until the end of solidification. The closed dies are positioned between the plates of hydraulic press. By pressurizing liquid metals while they solidify, near-net shapes can be achieved in sound, fully dense castings. The dimensional accuracy of squeeze castings is similar to those of die-casting, 0.25 mm in 100 mm to 0.6 mm in 500 mm ^[8]. The applied pressure and the instant contact of the molten metal with the die surface produce a rapid heat transfer condition that yields a pore-free fine-grain casting with mechanical properties approaching those of a wrought product. However, the process is much simpler, more economical and more efficient in its use of raw material . Due to the high pressure, porosity is eliminated and microstructural refinement is achieved to a much greater extent than in permanent mold casting and any other casting processes. The microstructure refinement and integrity made possible by squeeze casting allow a variety of secondary operations to be conducted, including welding and solution heat treatment ^[15].

The current emphasis on reducing materials consumption through close to net shape processing and the demand for both higher-strength and high ductility parts the emergence of squeeze casting as a production process has provided a new impetus. In recent years, squeeze casting has found production applications in the United States, in the United Kingdom and in Japan ^[16, 17].

3.2 PRINCIPLES OF SQUEEZE CASTING

This section is based on the UBE training manuals. It provides the background and the principles of the squeeze casting process as applied to the Vertical Squeeze Casting unit at CWRU. Also, some guidelines on the selection of the processing parameters for sound squeeze cast products. These guidelines were generally applied, sometimes with minor modifications in the present work.

3.2.1. Casting Theory

In squeeze casting the die cavity is filled with molten aluminum at a low-speed, using a plunger operated by a hydraulic cylinder. High pressure is applied on the metal during solidification. The following section outlines principles of fluid mechanics as applied to the squeeze casting process.

3.2.1.1 Outline of Fluid Dynamics (units and symbols)

The pressure P is defined as force per unit area (psi). When pressure is applied to an area A (in^2) the force is $F = P \times A$.

3.2.1.2 Pascal's Law

If the area of the small piston is A_0 , and the force applied to the small piston is F_0 , the pressure applied to the liquid can be calculated as F_0/A_0 . See illustration in Figure 3.1. By applying Pascal's Law we can deduce that the force required at F_1 to keep the larger piston from moving is $F_1 = \text{pressure} \times \text{area of plunger } (A_1)$

The pressure P is calculated from $F_o = P \times A_o$

$$P = F_o / A_o$$

The force on plunger A_1 is $F_1 = P \times A_1 = F_o \times A_1 / A_o$.

The above relation is known as the Pascal's Law, and can be used to calculate injection pressure, casting pressure and die opening force.

3.2.1.3 Fluid Flow

From a theoretical point of view, there are two types of fluid flow: laminar filling flow and turbulent flow. During squeeze casting filling is accomplished with laminar flow. The flow speed during the transition from laminar filling flow to turbulent flow is referred to as the "critical speed." During laminar filling flow, one regular line of movement is followed at a fixed speed. During turbulent flow, an average flow velocity value is calculated. For example, if the sectional area is A (in²) the flow is Q (in³/sec.), the average speed is v (in/sec):

$$v = Q/A$$

3.2.1.4 Law of Continuity

When a specific area is being filled with fluid in a fixed amount of time, the inflow and outflow of fluids to this area are equal.

In figure 3.2, if the amount of fluid flowing is Q , the area of sections 1-1', 2-2', 3-3', & 4-4' is represented by A_1 , A_2 , A_3 , A_4 , and the velocity of fluid flow is v_1 , v_2 , v_3 , & v_4 , then:

$$Q = A_1 v_1 = A_2 v_2 = A_3 v_3 = A_4 v_4$$

The volume V of fluid flowing within a set time t is:

$$V = Qt = A_1 v_1 t = A_2 v_2 t$$

The above equations can be used to calculate the fluid flow velocity in aluminum die casting (see figure 3.2.)

3.2.2. Processing Parameters for Squeeze Casting

The size and shape of the product- as well as the following items must be taken into consideration when determining the die system, machine size, and injection conditions for squeeze casting:

3.2.2.1 Casting Pressure (Metal Pressure)

Casting is generally carried out in the pressure range of 10-14 ksi, the average being approximately 12 ksi. The casting pressure is calculated by dividing the injection force of the squeeze machine by the area of the plunger tip.

In figure 3.1 the casting pressure P is :

$$P = F_o/A_o = 4P_o \pi D^2/4\pi d^2 = P_o \times D^2/d^2$$

The maximum injection force of the squeeze casting machine is determined by the machine design. The applied injection force can be controlled by adjusting the cylinder pressure. The injection force also depends on the inner diameter of the plunger tip, so selection of a proper tip diameter is important.

3.2.2.2 Projected Casting Area

The casting area A_1 shown in Fig. 3.3 is the area calculated by adding the projected casting area of the biscuit, the runner, and the over-flows to the projected area of the cast product. The projected areas of the biscuit, the runner, and the over-flow well are approximately 30- 50% of the projected area of the product.

3.2.2.3 Necessary Die Clamping Force

The necessary die clamping force is obtained by multiplying the casting pressure by the casting area:

$$F_1 = P \times A_1$$

The actual die opening force varies according to such conditions as the casting capacity and injection speed. Squeeze casting machines are able to compensate for these conditions, adding a 20-50% safety factor to this die clamping force.

F_1 -Clamping force (lbf)

P_0 - Hydraulic pressure (psi)

P -Metal pressure (psi)

F_0 -Injection force (lbf)

A -Injection Area (in^2)

A_1 -Projected Casting Area (Including Biscuit,
Runner, and Overflow well) in^2

D - Injection Cylinder Diameter(in)

d -Plunger Tip Diameter (in)

3.2.2.4 Force Applied by Plunger Tip

$$\text{Injection Force } -F_o = P_o \times A = P_o \times \pi D^2/4$$

Example

If the hydraulic pressure is 995 psi, the injection cylinder diameter is 8.26 in and the plunger tip diameter is 2.76 in.

$$\begin{aligned} F_o &= 995 \times \pi \times 8.26^2/4 = 995 \times 53.586 \\ &= 53,019.57 \text{ lbf} \end{aligned}$$

Calculation of Casting Pressure

The metal pressure is calculated by dividing the applied force (F_o) by the plunger tip area (A_o).

$$P = F_o / A_o = P_o \times \pi D^2 / \pi d^2 = P_o D^2 / d^2$$

Example:

$$P = 53,000 \text{ lbf}$$

$$P = 53,000 / (\pi \times 2.76^2 / 4) = 8860 \text{ psi}$$

Calculation of the Force Necessary for Die Clamping

Die Clamping Force = Metal Casting Pressure x Projected Casting Area

$$F_i = P \times A_i = 8860 \times 42 \text{ (projected casting area)} = 372,120 \text{ lbf}$$

The die opening force varies according to such conditions as the machine size, plunger speed, etc. Casting machines with a 20-50% safety margin are desirable. In UBE squeeze casting machines an additional 20% safety margin is common.

3.2.5 Filling Conditions

In squeeze casting, filling and solidification takes place under, low speed (gate velocity less than 16 in/sec) and high pressure (10-14 ksi) conditions. Since products can vary widely in shape, selection of filling conditions requires some preliminary testing. Processing conditions should be determined while taking into account the shape and composition of the product, as well as past experience with casting similar alloys.

3.2.6 Gating

Because squeeze casting employs a slow shot speed, the metal is prone to solidify in the runners. The gate section must therefore be as large as possible. The relation between gate speed, gate area, and filling time are illustrated in figure 3.4 and described below:

The volume of liquid metal passing through the gate is given by:

$$v=Q \times t$$

The total volume of a casting equals to the metal volume that has flows through the gate. The relationship between volume of the casting V, flow Q, gate velocity (v_g) and filling time (t) is:

$$Q=V \times A = v_g \times A_g$$

v- Injection Speed (in/sec)

A- Plunger Tip Are (in²)

v_g -Gate Velocity (in/sec)

A_g -Gate Area (in²)

The volume (V) of metal passing through the gate is:

$$V = v \times A \times t = v_g \times A_g \times t$$

Product weight:

$$W = \rho \times V$$

Gate area:

$$A_g = V / v_g \times t = W / \rho \times v_g \times t$$

ρ -specific gravity of aluminum alloy 0.0975g/cm³

3.2.7 Gate Velocity

16 in/sec is a common gate velocity for squeeze casting. If this speed is increased, more air is entrained in the product. When performing test castings, it is recommended to begin testing using this speed.

*If the fill velocity is too fast, molten metal can jet and bounce back from the walls of the cavity, causing flow lines and filling defects.

3.2.8 Filling Time

The optimum filling time is selected as a compromise between conflicting needs:

(a) Filling the cavity fast to prevent premature solidification before the cavity is completely filled; (b) Filling the cavity slowly to minimize the amount of entrained air.

To help solve this problem, the tilting injection system has been designed to reduce the filling time from the moment the molten metal leaves the ladle. (see figures 3.5 and 3.6). This is accomplished by tilting the injection system while the die is being closed (rather than after die closing, as is the case in many direct squeeze casting machines).

3.2.9 Example of setting gate area, casting speed and filling time:

W_F -Total weight of metal passing through the gate (lb)

v_g -Gate Velocity(in/sec)

t_F -Filling Time (sec.)

0: Good products

X: Bad products

Figure 3.5 shows the effect of gate velocity on porosity. A gate velocity of $v_g = 4-12$ in/sec is recommended condition for this part.

If v_g approaches 16 in/sec, internal porosity increases considerably.

Figure 3.6 shows the range in which viable products were produced. Gate area and casting speed should be determined from these two diagrams.

$W_F = 2.2$ lb cast product

$d = 2.76$ in (sleeve diameter)

$v_g = 4-12$ in/sec

$V_{AVE} = 7.87$ in/sec (from fig. 2.2)

$t_F = 0.8-2.2$ sec.

$t_{AVE} = 1.5 \text{ sec.}$ (from fig. 2.3)

W_F - Weight of metal passing gate(lb)

v_g - Gate velocity (in/sec)

t_F -Filling time (sec.)

A_g - Gate area(in²)

$$W_F = A_g \times v_g \times t_F \times \rho \text{ (lb)}$$

ρ - Al density = 0.0921 lb/in³

$$A_g = W_F / (0.0921 \times v_g \times t_F)$$

$$A_g = 2.2 / (0.0921 \times 7.87 \times 1.5)$$

$$A_g = 2.0 \text{ in}^2$$

From this, the control range of the plunger tip speed (V_p) can be determined:

$$\pi d^2 \times V_p / 4 = A_g \times v_g$$

$$V_p = 4 A_g \times v_g / \pi d^2 = 4 \times 2 \times v_g / \pi 2.76^2 = 0.334 \times v_g$$

In terms of porosity, the desirable v_g range is 4 - 12 in/sec, and the range of the plunger tip speed is $V_p = 1.34 - 4 \text{ in/sec.}$

3.2.3. Injection Conditions

The injection conditions needed to cast sound products are determined not only by factors such as part shape and composition, but also by other factors such as the die design (gate position, air vents, temperature, lubrication, etc.). When carrying out preliminary casting trials, one must take all of these factors into consideration.

3.2.3.1 Injection speed

In squeeze casting, the plunger tip is moved forward at a high speed (7.874 in/sec) until the molten metal reaches the gate. At this level, the speed is reduced and metal is pushed into the cavity at a gate velocity of approximately 16 in/sec. See figure 3.16.

The fill speed is calculated from the metal flow (Q_a) using the following equation:

$$Q_a = V_p \times A_p = v_g \times A_g$$

$$V_p = v_g \times A_g / A_p$$

The precise time the change in speed occurs is very important to the quality of the product.

As mentioned earlier, there are basically four speeds in the filling process. V_1 is the approach speed, and V_{2-4} indicates the filling speeds. In general the speeds are as follows:

1. Docking speed - 8-12 in/sec
2. V_1 (approach speed)- 8 in/sec
3. V_2 - V_4 (filling speed)- maximum 16 in/sec (recommended)

Figure 3.7 illustrates the docking process. The shot tip should be set at a point where the surface of the metal is approximately 1.5-2.0 in below the top of the shot sleeve. This position can be

changed by altering the length of the tip joints (the tip joint is a cylindrical part, threaded at both ends that connects the plunger tip to the injection rod). If the gap between the level of the molten metal and the top of the shot sleeve is too large, more air is allowed to enter the molten metal during casting. The molten metal will have contact with a longer section of the shot sleeve, causing the temperature of the metal to drop more and forming a thicker layer of solidified metal near the wall of the shot sleeve. The amount of metal changes with the product being cast and the tip diameter therefore the optimum tip joint length should be customized for every part.

*To avoid spillage of molten metal while the injection sleeve is tilted for ladling (15°), about a 1.5 –2.0 in distance from the metal surface to the sleeve top is necessary. When the tip diameter is larger, as in the case of the HVSC350 ton machine (tip diameter is 2.756 - 3.15 in) the safety distance must be increased proportionally.

The position of P_1 at the time of docking (sleeve ascending limit) should be set -0.118 in from the position indicated on the shot control unit panel after manual docking under normal temperatures. This is necessary because the sleeve temperature rises during casting. The approach phase (B in fig. 3. 7) is defined as the motion from the start of the injection motion to the point when the molten metal reaches the gate. The P_2 position should be set 0.4 - 0.8 in below the approach position, to allow time for a change in shot speed. If P_2 is set without this time allowance, metal will enter the cavity at a higher V speed.

The filling speed (C, D, E in fig. 3. 7) should be less than 16 in/sec to avoid excessive gas entrapment. Also, if a choked section exists in the product, the casting conditions should be set after the injection speed has changed to avoid gas entrapment.

*For smaller sized machines (HVSC500 and below) with shorter shot strokes, most castings involve only two speeds.

*With HVSC machines, the molten metal is slowed just before it enters- the gate, and then is increased again once the metal is entering the cavity; this helps prevent mixing .of air with the molten metal; this is in effect a porosity reducing measure.

*The pressure intensification process is initiated once the final inject speed (V_4) has been completed. The hydraulic pressure on the molten metal is increased during intensification. The timing of intensification is determined by the degree of valve opening during V_4 . Intensification is complete once the shot pressure increasing signal is received, and hydraulic pressure from the rod is returned to the tank.

3.3 PROCESING PARAMETERS

The main process parameters that need to be controlled to produce a successful squeeze cast component are outlined below:

3.3.1 Metal Casting Temperature

The temperature at which the molten metal is poured into the die cavity has a significant effect on the quality of the casting and the die life. Since the gates and runners are short, lower pouring temperatures can be employed with respect to other casting methods. The filling details of the mold are primarily accomplished by pressurization. Too low a pouring temperature has to be avoided, as it can cause incomplete die fills especially in sections, and cold laps. Too high a casting temperature may result in plunger problems if metal is trapped between the plunger and in hot tearing. The die life is adversely affected by high pouring temperatures.

For aluminum alloys, casting temperature may range between 20°C and 100°C above liquidus. Narrow freezing range alloys tend to form solid layers immediately upon making contact with the die wall, and therefore a higher superheat is used for these alloys.

3.3.2 Tooling Temperature

The die temperature has to be monitored within close limits. Too low a die or plunger temperature may result in premature solidification, and cold laps in the casting. Too high a die temperature can cause surface defects and welding of the casting to the die. Temperatures above 300°C are generally not recommended for aluminum alloys. The correct operating temperature has to be determined for each alloy and product design. Currently this is a trial and error

process. The information gathered in this project provides a rationale that can be applied to determine the necessary die, shot sleeve and plunger temperatures.

3.3.3 Melt Quality and Quantity

Metering precise quantities of molten metal into the die cavity is an essential step in the process. Various methods have been suggested to address this problem. Excess metal can be poured into biscuit size increased or the casting allowed to oversize in a non-critical area. Another variation suggested by Lynch uses a compensating hydraulic piston and cylinder to control the exact quantity of metal in the die. The excess metal is accommodated by allowing formation of an appendage to the component. It is also possible to use an overflow system into the die set for close control of dimensions.

3.3.4 Temperature for Pressure Application

Some investigators suggest that the best time for highest pressure to be applied is when the metal is midway between the liquidus and solidus temperatures. At that time, a continuous solid phase skeleton has been formed, and the metal has lost much of its fluidity.

Others recommend that the metal be mostly liquid when the pressure is applied. Control of the temperature is mainly by delay time, i.e. the time interval between the pouring and pressure application. This time will vary depending on melt temperature and component temperature. For large aluminum components this delay time could reach one minute.

3.3.5 Specific Pressure Level and Duration

Experimental evidence indicates that the minimum required pressures to eliminate shrinkage and gas porosity are within the range of 30 to 108MN/m² for the majority of non-ferrous materials. Actual pressure levels depend on the alloy characteristics and component geometry. The factors that determine the pressure level are:

- Flow stress of the alloy near the freezing temperature.
- The growth morphology of the alloy grains.
- The freezing range of the alloy.

Pressure application timing is determined by the alloy type, casting configuration and heat transfer conditions. Once solidification is completed, pressure is no longer necessary. Extended holding times may cause wall cracking and problems with plunger withdrawal due to thermal contraction of the casting. A rule of thumb for maximum holding time is about one second per mm of section thickness. The present investigation has established quantitative relationships between pouring temperature, mold and plunger temperature and recommended pressure holding times. These relationships are based on experimental data as well as heat transfer finite element analyses of specific component geometries.

3.3.6 Plunger Speed

For most practical purposes, the plunger speed when contact is made with the metal should be 0.5 m/sec or less. Higher velocities can have adverse effects on the inclusions in the casting or the dilation of die parts and flash at joints and parting lines. When the distance between the die and plunger is large, a two-speed action may be used, with a rapid approach to the metal surface followed by a slower impact speed.

3.3.7 Die Coating and Lubrication

Some release agents used in pressure die casting work reasonably well in squeeze casting applications. Some customized coatings with higher thermal resistance are also being marketed specifically for squeeze casting. A common used lubricant is water based colloidal graphite, sprayed onto the die and the plunger between each cycle. Limiting the thickness of the coating/lubricant under 50 microns can prevent surface contamination of the parts with coating residues stripped from the die surface. For more severe conditions, a ceramic agent can be sprayed on the die. A mixture of alumina powder or mica with a binder have also been studied.

4. EQUIPMENT

The squeeze casting system comprises the squeeze casting machine and auxiliary equipment including a melting furnace, an oil die heater and data acquisition equipment. Following is a brief description of the squeeze casting machine and the auxiliary equipment.

4.1 UBE 315 VSC Squeeze Casting Machine

This is a vertical squeeze casting (VSC) machine with a clamping force of 315 metric tons and an injection force of 60 metric tons. The machine is shown in figure 4.1. Front and top views of the squeeze casting machine are shown in figures 4.2 and 4.3 respectively. Note that the dies open vertically (the parting line is horizontal) and the injection is also vertical. In HVSC squeeze casting machines the dies open horizontally (vertical parting line) but the injection is also vertical. The technical specifications of the machine are summarized in figure 4.4. The main subsystems of the squeeze casting machine include:

(a) Robotic Pouring Ladle - Scoopes a fixed amount of molten metal from the crucible and pours it into the shot sleeve. The amount of metal can be closely controlled by programming the exit angle of the ladle from the molten metal. The capacity of the ladle is about 10-11 pounds. A cast-iron ladle coated with a refractory coating was used in this investigation. The pouring ladle is shown in figure 4.5: (a) scooping molten metal from the melting crucible. (b) transferring it to the shot sleeve (c) pouring it into the shot sleeve.

(b) Injection Shot Sleeve - The vertical shot sleeve tilts to accept the molten metal from the ladle. It then returns to the vertical position and docks to the shot block. A copper beryllium of H13 plunger tip pushes the molten metal into the cavity. At the end of the stroke, a high-pressure intensification is applied. This pressure is intended to feed molten metal to compensate for the solidification shrinkage. When the solidification is completed, the ejector die opens and moves up, while the plunger moves along keeping the casting in the ejector die. The plunger and the

shot sleeve are then retracted for the next cycle. The shot sleeve is shown in Figure 4.6. Figure 4.7 shows the sequence of the shot sleeve operation.

(c) Receiver and Die Lubricant Spraying Unit - moves in between the cover and ejector dies to receive the casting and apply die lubricant. The ejector plate pushes the ejector pins that release the casting onto the receiver. While retracting, the spraying unit applies lubricant to the dies. This unit is also equipped with compressed air lines and water lines. Both can be sprayed on the dies as needed. The unit is shown in Figure 4.8. A manual die spraying unit shown in figure 4.9 was used in some of the experiments.

(d) Shot Sleeve Lubrication Unit - The shot sleeve lubrication unit extends forward while the shot sleeve is in the tilted position and applies a lubricant inside the shot sleeve. The unit is depicted in figure 4.10.

(e) Controls - The squeeze casting machine is controlled by a Sharp Programmable Logic controller (PLC). The PLC program comprises elaborate commands that control the precise sequence and timing of events during the squeeze casting process. This program essentially controls the valves that operate the hydraulic and pneumatic pistons of the machine. It also includes many safety interlocks. In order for any command to be executed, all the systems have to be in their correct position. For instance, unless the dies are closed, the plunger can not apply the intensification force. To determine position of the cylinders, both limit and proximity switches are used. The PLC program has to be modified only when an entirely new part design is involved. A special PLC programming computer is required for this purpose.

The robotic pouring ladle and the injection shot sleeve have their own controllers. Unlike the main PLC program these are frequently accessed by the operator to adjust the motion of the pouring ladle and the shot sleeve or modify it for new parts.

4.2 Melting Furnace

A 75kW Lindberg electrical melting furnace is used to provide the molten aluminum alloy. The furnace is equipped with an 800lb silicon carbide crucible.

4.3 Oil Die Heater

A 35kW Sterling oil die heater is used to maintain the dies at the desired processing temperature. This oil die heater circulates oil at 50 psi through the dies. It can heat the oil up to 550 degrees Fahrenheit. It also has a water cooled heat exchanger that can cool the oil. The oil die heater is shown in figure 4.11.

4.4 Data Acquisition System

4.4.1. Shot Control

A Visi-Track shot control system is used to monitor the position of the shot sleeve during the process, the velocity of the injection and the intensification pressure. The Visi-Track system is shown in figure 4.12. Also shown figure 4.13 is a typical shot profile, with the approach, docking, shot and intensification pressure. The shot monitoring system provides valuable information on the process parameters that can be correlated to the quality of the squeeze cast parts.

4.4.2 Temperature Control

Thermocouples are used to monitor the temperature of the molten metal and the dies during the process. The thermocouples are attached to a Yokogawa hybrid recorder that plots the temperature curves and also downloads them into a file for further processing. An infrared thermometer is used to monitor the temperature at the surface of the die.

5. EXPERIMENTAL RESULTS AND DISCUSSION

5.1 Preliminary "Hub" Experiments

Along with the squeeze casting machine UBE Machinery provided a two cavity die holder and a set of inserts. These inserts were used to fabricate a hub for a mainframe computer tape drive. The casting is shown in figure 5.1. Every casting comprises a biscuit, two runners and two hubs. A few hundred parts were made with these inserts as part of the commissioning of the machine and the training of the CWRU personnel. With few exceptions these parts had cold laps and did not feed adequately. It was apparent that some modifications to the process were required. However, at that point in time no data acquisition was available to indicate what was wrong.

5.2 Preliminary "Plate" Experiments

To facilitate a systematic study of the squeeze casting processing parameters two plate inserts were designed. Both plates were half inch thick. Plug inserts were also designed and fabricated for the cover die and the ejector die. The gates on the cover insert and the ejector insert are different in depth. Each insert can be used in combination with a plug to fabricate a half inch plate. When used together the two inserts can make a one inch plate.

At first, one inch thick plates were cast. The first problem encountered was flashing at the parting line on the plate side of the die. This flashing was attributed to the imbalance in the applied forces. Note that only one side of the die was being pressurized with molten metal, while the other side had a plug. Consequently, the die had a tendency to separate at the parting line, on the plate site. As a remedy for this problem a hub insert was mounted instead of the plug. In this manner, molten metal is pressurized on both sides of the die resulting in a more balanced condition. With this set up the flashing problem was alleviated but not completely

eliminated. It should be noted that the projected area of the plate is a relatively large. When multiplied by the maximum injection pressure, it yields a force that is relatively large to the clamping force available. However, high-quality plates can be made with lower injection pressures that do not cause flashing.

Another problem encountered early on was the presence of entrapped gas. A spike in the velocity of the plunger was noticed on the Visi-Track profile of the. Considerable effort was invested in identifying the source of this spike. Eventually, the origin of the spike was identified in the programming of the shot control motion. The motion of the shot sleeve is controlled by a dedicated PLC. The user can enter position limits for the plunger positions at which the slow fill **injection velocity** should start and the plunger position at which the fast plunger **approach velocity** should be restored. The later was assigned an incorrect position. Rather than completing the injection at the low velocity, the plunger resumed its high, approach velocity before the cavity was completely filled. This spike in velocity forced the metal into the cavity at a high gate velocity. The metal stream coming from the gate hit the opposite wall of the cavity and bounced to the sides as two separate streams while trapping pockets of air. Once the programming of the shot profile was corrected the spike disappeared, and the quality of the castings improved considerably.

5.3 Test Bar Experiments

A number of different designs were employed to produce test bars, as depicted in the flow chart shown in figure 5.2.

5.3.1 Standard ASTM Test Bar Insert

The initial tensile specimens insert produced two ASTM type test bars with internal dimensions of 0.380", diameter, 1.40" gage length and a .505" gage diameter, 2.00" gage length

as illustrated in Figure 5.3 and 5.4. This insert is equipped with large runners, ingates and overflows as shown in this figure. Three equally spaced cooling lines were drilled in the insert, across the test bars: one in the center and two near the grip ends. A series of sixty tensile bars were initially produced using this insert with the configuration labeled Design #1 as shown in figure 5.5. The inserts were kept at 450°F. A white die lubricant with a dilution ratio of 1:10 was utilized. For these experiments, the gate velocity was 46.85 in/sec. These test bars were then examined by X-ray to determine their soundness and selected test bars were heat treated by the conventional T6 treatment for a 356 alloy (1000°F for 12 hours, age at 310°F for 4 hours) and tested. The tensile properties that were obtained in these 356 alloy test bars i.e. UTS of 30 ksi for the small diameter 0.38” bars and 37 ksi for the large diameter 0.505” bars were lower than those reported on similar tests conducted on production squeeze casting equipment for this alloy. The strength of the test bars is shown in figure 5.6 and the elongation in figure 5.7 respectively. The lower strength of the small test bar is attributed to the more difficult feeding of the small 0.38” diameter in the gage length due to premature freezing.

To improve the quality of the test bars castings the modified Design #2 shown in figure 5.5 was fabricated. The ingate diameter was increased; so was the size of the overflows. Vents were added past the overflows, to allow for venting of any trapped air. The dilution of the die lubricant was reduced to 1:5 to allow for better thermal insulation. The temperature of the insert was increased to 550°F. With the new design, the UTS of the small diameter, 0.38” bars increased to 34 ksi and for the large diameter 0.505” bars the UTS increased to 40 ksi.

In the third round of test bar experiments the ingate velocity was reduced to 20in/sec and the white die lubricant was replaced with a black, graphite based die lubricant with a dilution ratio of 1:5. This change resulted in a further increase in the strength of the 0.38” bars to 40 ksi; for the large diameter 0.505” bars the UTS increased to 42 ksi. It is interesting to notice that along with the increase in the strength, the difference between the strength of the small and the large diameter bars has also been minimized. This is an indication that the premature solidification caused by the smaller diameter of the small test bar is no longer as severe under the modified conditions of the third experiment.

The elongation of the test bars produced in these experiments is depicted in figure 5.7. While the elongation of the small test bars has been very good, holding steady around 14-15%, the large test bars show a steady decline from 13% for Design #1 to about 8% for Design #3. Part of this decline may be attributed to a slower cooling rate. However, there may be another factor at play that has not been identified yet.

The changes in the processing conditions clearly led to markedly improved properties. Much of this improvement can be attributed to elimination of casting defects. The statistical bar chart in figure 5.7 depicts the decrease in typical defects found in the 0.380” test bar. The occurrence of shrinkage defects in the grip section decreased significantly from Design #1 to Design #2. So did the occurrence of cold shuts near the overflow. As a matter of fact these disappeared completely in Design #2. Hot tearing was reduced by a significant amount. A similar trend was noted for the 0.505” test bars as depicted in Figure 5.8. In this case, the occurrence of defects was lower to start with, because of the better feeding and slower cooling rate facilitated by the larger diameter. The improved Design #2 eliminated all the defects, yielding perfectly sound test bars. Figures 5.9 and 5.10 summarize the tensile mechanical properties obtained with this insert for the 0.505” and 0.380” bars respectively.

Figures 5.11 and 5.12 illustrate the results of the flow computer simulation for this insert. An interesting feature revealed by the simulation is the bounce-back of the molten metal jet from the wall of the overflow. This bounce-back is believed to interfere with filling and cause some of the defects described earlier.

5.3.2 “U” Test Bar Insert

To prevent the bounce-back, a new test bar design was initiated and fabricated – the “U” test bar. This design is illustrated in figures 5.14 and 5.15. The overflow has been substituted

with a U shaped extension of the grip section and another test bar, along the first one. This modification accomplishes two objectives:

1. The U shaped bend prevents bounce-back of molten metal into the incoming flow.
2. The second test bar serves as an overflow while also providing additional heat to the insert. The additional heat is important for this insert, and for small die cast parts in general.

The prevention of the bounce-back was verified with a flow computer simulation, as shown in figure 5.16. The mechanical properties obtained with the “U” test bars are depicted in figures 5.17 and 5.18. Figure 5.19 summarizes the strength and elongation obtained with the “U” test bars in the T6 condition. Noteworthy is the very small scatter in properties, a good indication that we have stable, robust processing conditions that favor good properties.

5.3.3 Two-gate Test Bar Insert

Another design of test bars was attempted, in which the molten metal was fed into each bar from two ingates. The insert and the 3-D rendering of the casting are shown in figures 5.20 and 5.21 respectively. The results obtained with this insert design were inferior to the previous designs. The computer flow simulation revealed the source of the problem: the two molten metal fronts advancing from the ingates into the gage section meet there and form a “weld” line that is detrimental to the properties of the bar. Based on this observation, the ingate closer to the gate was modified so that it would only accept metal after the gage section is completely filled. Results with the modified insert were not available at the time of this writing.

A summary of the UTS tensile strength and elongation for all the test bar designs is shown in figure 5.22. While the strength level is generally above 40ksi with the exception

of the two-gate test bars, the elongation varies over a wide range. The best test bars have elongations of over 14% while the worst are below 6%.

In practice it is possible to increase the elongation at the expense of strength and vice-versa, by controlling the aging process during heat treating. Figure 5.23 illustrates this trend. However, the results shown for the test bars indicate similar strength levels of 40 ksi, with wide variations in elongation. It is concluded that the improvement of the tensile properties result from the better design and casting conditions rather than heat treating.

5.4 Plate Experiments

Plates that are 5.0" x 5.5" with thickness of 0.25, 0.5", 0.75" and 1.0 inches have been cast in the order shown in figure 5.24. The changes in plate thickness and gate dimension are accomplished by removable inserts for the runner, ingate and thickness of the casting. A Visi-Trak die casting monitoring system was used with the squeeze casting machine to record the velocity of filling and intensity pressure, with plots for every casting. In addition, the temperature of the molten metal, cover and ejection half of the die was monitored continuously. The temperature of the molten metal in the holding pot was measured with an immersion thermocouple inserted about 20 inches below the surface. All tests were conducted with 356 metal that had about 0.5% iron content. The die temperatures were measured with thermocouples inserted into the center and side of the die at a distance of 1/8 inch below the surface of the holder.

5.4.1 Quarter Inch Plate Experiments

A series of over 200 one-inch thick plate castings using the insert shown in Figure 5.25 were cast from the 356 alloy using variable metal velocities, fill times and pressures. The casting is shown in figures 5.26 and 5.27. These castings were examined to determine their density using the Archimedes procedure and the surface finish of the cover die and ejection die

surfaces. The quality was evaluated by visual examination and rated on a scale of six for a perfect casting and one for a defective casting. Examples of this visual rating system are shown in figure 5.28. During casting a conventional squeeze cast die lubricant was sprayed on the die before each shot.

The casting quality parameter was subsequently plotted as a function of the ingate velocity as shown in figure 5.29. The experimental conditions are typical to squeeze casting of aluminum: molten metal at 1350°F, die temperature 550°F squeeze pressure ca.8,000 psi. The least mean square curve in this plot has an inverted parabolic shape with a maximum in the center and lower values at the two extremes of the experimental range. At slow ingate velocities the drop in the quality rating is caused primarily by cold shuts. In other words, below a certain velocity threshold of about 12 ips, it becomes difficult to fill a quarter inch plate under the experimental conditions that were employed. . At high ingate velocities the drop in the quality rating is caused by the jetting of the molten metal into the cavity. This jet of molten metal tends to bounce off the wall opposite to the gate and create two swirling streams of metal, while trapping air in the center of the vortex. At times, this results in more than two large voids as depicted in figure 5.29. We conclude that for thin plates and shapes, the dominating factors in the attainment of sound castings are filling and jetting. Ingate velocity and filling time need to be fast enough as to ensure complete filling before the metal solidifies, yet slow enough to prevent jetting and bounce-back. The window of favorable ingate velocities will become narrower as the plate becomes thinner. A fanned gate will be less prone to cause bounce-back than a straight ingate.

5.4.2 Half Inch Plate with Straight Ingate Design

A series of half-inch thick plate castings using the insert with a straight ingate shown in Figure 5.30 were cast from the 356 alloy using variable metal velocities, fill times and pressures. The casting is shown in figures 5.31 and 5.32.

Based on the previous experience with the quarter inch plates, it was anticipated that the straight gate would exacerbate the jetting of the molten metal. A series of computer simulation were undertaken to study the effect of the ingate velocity on the jetting. Figure 5.33 illustrates the flow pattern in the half inch plate when the ingate velocity is high, 28ips. The molten metal jet bounces off the back wall creating two metal streams that flow along the side walls and then looping around into the incoming stream. In doing so, the two streams trap two pockets of air that may remain as partial voids or even through holes in the plate. When the ingate velocity is reduced to 7 ips, the computer model predicts a less violent bounce-back. However, partial voids in the plate are still forming, as illustrated in figure 5.34. Only when the ingate velocity is reduced to 5 ips is the bounce-back completely eliminated, as shown in figure 5.35.

The computer simulation results are shown again for a high ingate velocity of 50 ips in figures 5.36 (a), (b), (c) side by side with castings made at the same conditions. At 0.2 seconds, a well formed molten metal jet has reached the back wall and is starting to bounce back. At 0.5 sec the jet has split into two metal streams that start flowing back along the side walls. Finally, at 1.4 sec the plate is filled but has two through holes due to air trapped between the metal streams. For a low ingate velocity of 6.1 ips the computer simulation are shown in figures 5.37 (a), (b), (c) side by side with castings made at the same conditions. At this ingate velocity the metal fills the cavity slowly, while “mushrooming” from the ingate inwards. The end result is a sound plate with no voids in it.

The quality of the half inch plates was evaluated by visual examination and rated on a scale of six for a perfect casting and one for a defective casting, and plotted as a function of the ingate velocity as shown in figure 5.38. The experimental conditions are typical to squeeze casting of aluminum: molten metal at 1350°F, die temperature 550°F squeeze pressure ca.8,000 psi. The curve that best fits the experimental data has a maximum around 7 ips and lower values at the two extremes of the experimental range. At slow ingate velocities the drop in the quality rating is caused primarily by cold shuts. In other words, below a certain velocity threshold of about 6 ips, it becomes difficult to fill a half inch plate under the experimental conditions that were employed. At higher than 10 ips ingate velocities the drop in the quality rating is caused

by the jetting of the molten metal into the cavity. This jet of molten metal tends to bounce off the wall opposite to the gate and create two swirling streams of metal, while trapping air in the center of the vortex as depicted in figure 5.38. Just like in the case of the quarter inch plate, the dominating factors in the attainment of sound castings are filling and jetting. Ingate velocity and filling time need to be fast enough as to ensure complete filling before the metal solidifies, yet slow enough to prevent jetting and bounce-back. A straight gate promotes jetting more than a fanned gate. As a result, the window of ingate velocities that is conducive for sound plates is quite narrow. The steep drop in the quality rating as ingate velocity increases is evident in the plot.

5.4.3 Half Inch Plate with Fanned Ingate Design

A series of half-inch thick plate castings using an insert with a fanned ingate shown in Figure 5.39 were cast from the 356 alloy using variable metal velocities, fill times and pressures. The casting is shown in figure 5.40.

A series of computer simulation were undertaken to study the effect of the ingate velocity on the jetting. Figure 5.41 illustrates the flow pattern in the half inch plate when the ingate velocity is high, 28ips. Due to the fanned ingate, the molten metal advances across the entire section of the plate cavity and fills it smoothly even at this high velocity. The only exception are the two corners near the gate that fill last, and may possibly show some cold laps. When the ingate velocity is reduced to 7 ips, the computer model also predicts a sound casting as illustrated in figure 5.42.

The quality of the half inch plates with a fanned gate was evaluated by visual examination and rated on a scale of six for a perfect casting and one for a defective casting, and plotted as a function of the ingate velocity as shown in figure 5.43. The experimental conditions are typical to squeeze casting of aluminum: molten metal at 1350°F, die temperature 550°F squeeze pressure ca.8,000 psi. The curve that best fits the experimental data has a maximum around 7 ips and lower values at the two extremes of the experimental range. At slower ingate

velocities the drop in the quality rating is caused primarily by cold shuts. In other words, below a certain velocity threshold of about 6 ips, it becomes difficult to fill a half inch plate under the experimental conditions that were employed. At higher than 10 ips ingate velocities there is a gradual drop in the quality rating. However, this drop is not as steep as the half inch plate with the straight ingate. The dominating factors in the attainment of sound castings are still the same, i.e. filling and jetting. Ingate velocity and filling time need to be fast enough as to ensure complete filling before the metal solidifies, yet slow enough to prevent jetting. The fanned gate prevents severe jetting. As a result, the window of ingate velocities that is conducive for sound plates is wider than for a straight gate and drop in the quality rating as ingate velocity increases is much milder.

5.4.4 3/4 Inch Plate

A series of $\frac{3}{4}$ inch thick plate castings shown in figure 5.44 were cast from the 356 alloy using variable metal velocities, fill times and pressures. The dimensions of the casting are shown in figure 5.45. The quality of the $\frac{3}{4}$ inch plates with a fanned gate was evaluated by visual examination and rated on a scale of six for a perfect casting and one for a defective casting, and plotted as a function of the ingate velocity as shown in figure 5.46. The experimental conditions are typical to squeeze casting of aluminum: molten metal at 1350°F, die temperature 550°F with the oil die heater, squeeze pressure ca.8,000 psi. According to this plot the best plates were obtained at the lowest ingate velocities. However, the defects responsible for the drop in the quality of the plates are different than in the thinner plates, and include shrinkage as a major factor. It was concluded that in the $\frac{3}{4}$ inch plates the critical factors for attaining sound castings have shifted from flow related to solidification related. To further accentuate these factors we decided to follow up with one inch plate experiments. (Please proceed to next section 5.4.5 and return to this section). The lessons learned from the one inch experiment were subsequently applied to the $\frac{3}{4}$ inch plates: at the conclusion of the one inch experiments, the $\frac{3}{4}$ inch plates were cast with the oil heating around the plate substituted with water cooling. Only the gate area

was heated with oil. The result was very sound plates, regardless of the ingate velocity as illustrated in figure 5.47.

5.4.5 One Inch Plates

A series of one-inch thick plate castings using the insert with a long and thin ingate shown in Figure 5.48 were cast from the 356 alloy using variable metal velocities, fill times and pressures. The casting is shown in figures 5.49 and 5.50. Figure 5.51 shows the design side by side with a casting. The primary quality problem with this design is massive shrinkage at the top center of the plate. Evidently, the long and thin gate freezes before the rest of the casting, preventing further feeding of the shrinkage by application of high pressure on the biscuit. The computer simulation reinforced this conclusion as it did not indicate any flow related filling problems as demonstrated in figure 5.52.

To address the premature freezing the thin and long ingate, was substituted with a short and thick gate as illustrated in figure 5.53 and 5.54. The quality of the castings was rated on a 1 to 8 scale using X-Ray images of the plates. The main defects were cold laps and shrinkage. The casting quality parameter was subsequently plotted as a function of the ingate velocity as shown in figure 5.55. The experimental conditions are typical to squeeze casting of aluminum: molten metal at 1350°F, die temperature 550°F heated with the oil die heater, squeeze pressure ca.8,000 psi. The least mean square curve in this plot has an inverted parabolic shape with a maximum in the center and lower values at the two extremes of the experimental range. At slow ingate velocities the drop in the quality rating is caused primarily by cold shuts. At higher ingate velocities the defects are primarily associated with shrinkage.

To address the shrinkage problem, the oil heating around the plate was substituted with water cooling. However, the oil heating was still used in the ingate area. This set-up creates a condition that favors directional solidification from the far end of the plate towards the gate. The plate solidifies before the ingate. The ingate is therefore still open while the plate is still

solidifying, and the pressure applied on the biscuit is effective in feeding the shrinkage in the plate during solidification. The quality rating for these plates is illustrated in figure 5.56. It shows all the plates were of high quality, irrespective of the ingate velocity. It was therefore concluded that for plates thicker than $\frac{3}{4}$ inches, the filling stage is less critical than the solidification sequence. There is sufficient heat in this plate to allow filling without premature solidification with cold laps during filling. However, once filled the plate starts solidifying and will have shrinkage defects unless properly fed. Establishing a directional solidification pattern and maintaining an open gate for efficient application of the pressure feeding is essential for the heavier section castings. The computer simulation of the solidification in the 0.75" confirmed this conclusion. The simulation with run with oil heating around the biscuit and water cooling boundary conditions around the plate.

The results of the plate casting experiments are summarized in table 5.70 and figures 5.71 and 5.72. The bars in figure 5.71 show the window of ingate velocities that produce good castings. In all cases, lower than the minimum velocity will cause premature freezing and cold laps. At the high end of the velocities, the limiting factor that is causing defects can be jetting for the thinner plates or solidification defects for the heavier plates. The information is also plotted as a function of plunger velocity in figure 5.72. These plots convey the information provided earlier in Figures 3.5 and 3.6. However, in the present case the plots are for specific parts rather than generic. While the generic plots provide general guidance, the conditions necessary for casting sound parts need to be refined for each part configuration.

The beneficial effect of applied pressure reported in other studies has been confirmed here. Plots showing the increase in visual rating and density with increased pressure are shown in figures 5.74 and 5.75 respectively. A prerequisite for benefiting from higher pressure is that the gate stays open and does not solidify prematurely.

5.4.6 The Ribbon Insert

Shown in figure 5.75, this insert was fabricated for evaluation of fluidity in different alloys. Multiple thermocouples are embedded in the insert to measure the temperature distribution. Casting obtained with this insert, for increasing gate velocities in a 356 alloy are shown in figure 5.76. Clearly, higher velocities promote filling. The insert is available for future studies.

5.5 Evaluation of the Microstructure

Transverse and longitudinal cross sections were cut from the gauge length of the cast test bars. Specimens were polished and etched in a solution of 1 ml HF (40%)/200 ml H₂O. For as cast samples, the secondary arm spacing (DAS) and silicon particle spacing (λ_{Si}) in the eutectic regions were estimated as a measure of the fineness of the structure. A linear intercept method was used for measuring DAS and λ_{Si} . In this method, an intersecting line is placed normal to the secondary dendrite arms or the relatively parallel silicon particles in the eutectic. DAS and λ_{Si} (both center to center) were taken as the distances divided by the numbers of secondary dendrite arms and silicon particles. For T4 and T6 samples, area (A), perimeter (P) and equivalent area diameter (EAD) were measured to describe the size of the spheroidized silicon particles. For the shape of silicon particles, shape factor (SF) and aspect ratio (AR) were used. SF is roundness and is defined as $SF = P^2 / 4\pi A$. AR is the ratio of the length to the width of a box drawn around each particle and is a measure of circularity. A 100X magnification was used to measure DAS and 1000X magnification was used to measure the λ_{Si} ; 500X and 1000X magnification were used to measure the A, P, EAD, SF and AR separately. These measurements were made with the MSQ Materials Analysis System Software for image analysis and all the results are averaged. A Hitachi S4500 Scanning Electron Microscope was used to analyze the fracture features of impact samples for both squeeze cast and permanent mold test bars in the as-cast and T6 conditions. The as-cast typical microstructures of squeeze cast and permanent mold cast test bars are illustrated side-by-side in figure 5.77 at magnifications of x100, x500 and x1000. The typical impact fractographs are shown in figure 5.78 -a and c at magnification of x1000. The typical

microstructures of squeeze cast and permanent mold test bars in the T4 and T6 conditions are illustrated side-by-side in figure 5.79. The typical impact fractographs are shown side-by-side in figure 5.80-b and d at a magnification of x1000.

Microscopic examination reveals that application of the squeeze pressure during solidification of this alloy affects the microstructure in both the as-cast condition and T4 and T6 conditions. In the as cast condition, squeeze casting refines the primary α -phase and the eutectic silicon phase. The DAS of squeeze cast bars is only half of the permanent mold bars. In the squeeze cast bars, the silicon has a fibrous morphology while in the permanent mold bars silicon has a plate or needle shape. The Si particle spacing in the squeeze cast bars is only $1.25\mu\text{m}$, which is 5 times smaller than that of the permanent mold bars at $7.3\mu\text{m}$. Very low porosity levels are encountered in squeeze cast parts. In the squeeze cast bars in the T4 and T6 conditions, the Si-particles are smaller and rounder. The Si-particles of both squeeze cast and permanent mold castings are spheroidized by the T4 and T6 treatment. SEM fractographs show that squeeze cast bars have a more ductile fracture than permanent mold bars.

The differences in the microstructures of squeeze cast and permanent mold bars result indirectly from the applied pressure. When the die is made of metal, the die/casting interface becomes the greatest resistance to heat transfer. Due to the contraction of most metals and expansion of the mold during solidification, detachment of the casting from the die wall takes place once the initial solid shell of the casting has sufficient strength to hold the remaining molten metal. Consequently, an air gap is formed between the die walls and casting, which considerably increases resistance to the heat transfer. In squeeze casting, the applied pressure of about 70MPa on the casting forces the initial solid shell to remain in contact with the die. The intimate metal-die contact is maintained by the plastic deformation of the casting, throughout solidification. This leads to very fast heat transfer rates, high cooling rates and increased temperature gradients in the casting. The cooling rate in squeeze casting can therefore be much faster than that of permanent molds, depending on applied pressure, die preheat temperature, cooling line location, casting thickness, die lubricate and other factors^[20]. The rapid cooling rates of squeeze cast parts greatly refines the microstructure and changes the silicon phase from the plate or needle shape to

a fibrous morphology. The rapid cooling is a potent Si-modifier, equal to Si-modification by additives during metal melting.

No significant micro-porosity was detected in the squeeze cast bars but some porosity and interdendritic microporosity was found in the permanent mold cast bars as illustrated in Fig.4-a, b. This difference can be explained by the application of pressure to the squeeze cast test bars. The ability of a pore to grow in a solidifying metal, given that nucleation is relatively easy in permanent mold casting, can be best related to the following equation^[21]:

$$P_g + P_s > P_{Atm} + P_H + P_{s-t}$$

Where: P_g : =equilibrium pressure of dissolved gases in the melt

P_s : =pressure drop due to the shrinkage

P_{Atm} : =pressure of the atmosphere over the system

P_H : =pressure due to the metallostatic head

P_{s-t} : =pressure due to surface tension at the pore/liquid interface

In squeeze casting, P_{Atm} is as high as 70MPa, therefore porosity can usually be eliminated. This type of porosity can exist in permanent mold because $P_{Atm} + P_H$ is low compared to squeeze casting.

No coarse intermetallic phases occur in either the squeeze cast or permanent mold bars because this is high quality A356 and the impurity level is controlled, especially the content of iron that is less than 0.2%.

The structural differences between squeeze casting and permanent mold after heat treatment originate from the structural differences in the as-cast condition caused in turn by the different solidification rates. Those findings are similar to the literature^[6, 22, 23] that reports Si morphology after heat treatment to have some relationship to the as cast structure. The finer of the as-cast structures will bring to the lower aspect ratio of silicon particles. The segmentation and spherodization depend on the original, as-cast Si morphology and the solutioning time and temperature^[23]. For the same heat treatment, the rate of the breakdown and spherodisation depends on both the type and size of the Si particles that are predominant in the structure. The fine and fibrous silicon particles in the squeeze casting need shorter times to dissolve. In

contrast, the coarse flakes or plates of Si in the permanent mold cast bars are inherently more resistant and need a longer time to dissolve and to segment. These particles have shorter time to spheroidize so morphological changes beyond an increased degree of roundness are less evident after heat treatment in comparison with that of the squeeze cast parts.

The structural differences between squeeze casting and permanent mold before and after heat treatment originate from the distribution of the silicon phase. The process of spheroidization of eutectic the Si-particles can be divided into two stages⁽²³⁾: the dissolution and segmentation of the eutectic Si-particles and, the spheroidization and coarsening of the segments. The solubility of silicon in solid aluminum at the solution temperature (540°C) is about 1.25% while at room temperature is only 0.05%^[1]. Therefore during solution treatment, some silicon atoms from the eutectic Si phase will dissolve into the aluminum solid solution. Those silicon atoms at thin growth steps and the corners will dissolve easily because of their higher energy. The driving force for spheroidizing and coarsening of the silicon phases is the reduction in the surface area between the silicon particles and the aluminum solid matrix. The size of silicon particles in the T6 condition is slightly bigger than in the T4 condition. Because silicon was supersaturated in the as-quenched α -Al solid solution in the T4 condition, some of the silicon atoms will precipitate during aging on the surface of the previously formed Si-particles. Other atoms may form intermetallic compounds and precipitate as very fine particles such as Mg_2Si . Extremely fine precipitates can be observed between the dendritic silicon. The precipitates in the T4 condition are different from those seen in the T6 condition. The solution treated specimens contain only $TiAl_3$ needles and no Mg_2Si platelets while the aged specimens contain both $TiAl_3$ and Mg_2Si . If the aging temperature and time are optimized^[2] only Mg_2Si will be present. This experiment also demonstrates that components produced by squeeze casting can be heat treated without any blister defects.

SUMMARY AND CONCLUSIONS

A comparison of the results does show that generally, squeeze cast properties are somewhat better than some other casting processes because of the soundness of the tests and the rapid solidification of the test bar producing the fine dendrite arm spacing and the fine distributions of the silicon phase of the eutectic. The same molten 356 alloy used to produce the properties shown above was also poured into a permanent mold die for a .505" diameter test. The results of this test were considerably inferior to the squeeze cast test.

The squeeze casting literature shows that as the pressure exerted on the solidifying metal through the piston is increased, the soundness of the castings increases. This has been observed on the test bars and plate castings produced to date on this project. Increased filling velocity results in more entrapped air in the die and affects this porosity. More rapid filling will break up the stream of metal entering the cavity and entrap more air or gas into the molten metal. Jetting of the metal stream and bounce-back from the cavity walls can also trap pockets of air in the casting

The work that we have conducted on the surface finish of the squeeze casting has also shown that good casting surfaces, at least for the large flat areas of the plate die, are affected mostly by the die temperature. This temperature should be at least 350°F or somewhat higher to avoid laps and rough surface areas.

The work conducted to date on the squeeze casting process permits several observations as listed below.

- Excellent tensile properties of squeeze cast aluminum alloys can be attained compared to other castings processes.
- The density of the squeeze casting is increased by higher pressures maintained on the solidifying metal.

- The density of the squeeze castings also increased with slower fill velocities. This is attributed to the maintenance of a solid part fill with the streamers of molten metal entering the die that reduce the amount of entrapped gas.
- The ingate size and shape are very important since it must remain open until the casting is solidified and pressure is maintained on the solidifying casting.
- Fanned gates, particularly on the smaller section castings avoid jetting effects at the ingate end. The fan type ingate helps accomplish a rapid fill without high velocities.
- The molten metal has to fill the cavity before localized solidification occurs. This is best accomplished with a larger ingate to attain rapid filling without excessive velocity or jetting that occurs at high metal velocities.
- Straight gates are prone to cause jetting of the metal stream even at low velocities. Fanned gates allow use of higher fill velocity without excessive jetting.
- A higher metal pressure provides a more complete fill of the die including improved compensation for solidification shrinkage.
- With the proper filling pattern, ingates, overflows and die temperature for a given die, very good tensile properties can be attained in squeeze casting. In general, the smaller squeeze castings require higher die temperatures.
- Computer models using the UES Procast and MagmaSoft finite element software can, after suitable adjustments, predict the flow pattern and solidification sequence in the die cavity.

REFERENCES

- [1] I. J. Polmear, *Light Alloys—Metallurgy of the Light Metals*, Thomson Litho Ltd, East Killbride, Scotland, 1983.
- [2] M. S. Misra, K. J. Oswalt, Aging Characteristics of Titanium-Refined A356 and A357 Aluminum Castings, *AFS Transactions* 1982, 90:1-10.
- [3] M. Ravi, U. S. Pillai, B. C. Pai, A. D. Damodaran and E. S. Dwarakadasa, Mechanical Properties of Cast Al-7Si-0.3Mg (LM25/356) Alloy, *Int. J. Cast Metals Res.* 1998,11:113-125.
- [4] A. Saigal, J. T. Berry, Study of the Effects of Volume Fraction, Size and Shape of Silicon Particles on Mechanical Properties in Al-Si Alloys Using Finite Element Method, *AFS Transactions* 1985, 93:699-704.
- [5] M. M. Tuttle, D. L. Mclellan, Silicon Particle Characteristics in Al-Si-Mg Castings, *AFS Transactions* 1982, 90:13-23.
- [6] C. W. Meyers, A. Saigal and J. T. Berry, Fracture Related Properties of Aluminum A357-T6 Cast Alloy and Their Interrelationship with Microstructure, *AFS Transactions* 1983, 91:281-288.
- [7] G. Williams and K. M. Fisher, Squeeze forming of Aluminum Alloy Components, *Metal Technology*, July 1981:263-267.
- [8] M. R. Ghomashchi, A. Vikhrov, Squeeze Casting: an Overview, *Journal of Materials Processing Technology* 2000, 101:1-9.
- [9] J. N. Pennington, Squeeze-cast Parts Approach Performance of Forging, *Modern Metal* 1988, 44(1):52,54-56,58,60.
- [10] A. I. Batyshev, E. M. Bazilevskii, Yu. A. Ebstratov and F. A. Martynov, Bush Production by Casting and Solidification Under Piston Pressure and by Liquid Metal Stamping, *Russian Castings Production*, Feb. 1972:76-77.
- [11] W. F. Shaw and T. Watmough, Squeeze Casting: A Potential Foundry Process, *Foundry* 1969(Oct), 97:166-169.
- [12] R. F. Lynch, R. P. Olley and P. C. J. Gallagher, Squeeze Casting of Aluminum, *AFS Transactions* 1975, 83:569-576.
- [13] T. M. Yue, G. A. Chadwick, Squeeze Casting of Light Alloys and Their Composites, *Journal of Materials Processing Technology* 1996, 58:302-307.

- [14] S. W. Kim, G. Durrant, J. H. Lee, B. Cantor, The Effect of Die Geometry on the Microstructure of Indirect Squeeze Cast and Gravity Die Cast 7050(Al-6.2Zn-2.3Cu-2.3Mg) Wrought Al Alloy, *Journal of Materials Science* 1999, 34:1873-1883.
- [15] S. Rajagopal, W. H. Altergott, Quality Control in Squeeze Casting of Aluminum, *AFS Transactions* 1985, 93:145-154.
- [16] S. Okada, N. Fujii, A. Goto, S. Morimoto, T. Yasuda, Development of a Fully Automatic Squeeze Casting Machine, *AFS Transactions* 1982, 90:135-146.
- [17] ASM Handbook, Casting, Vol.15, Formerly Ninth Edition, Metals Handbook, Solidification of Eutectic Alloys, Aluminum-Silicon Alloys.
- [18] J. F. Wallace, D. Schwam, Squeeze Casting of Aluminum and Magnesium Alloys, *World of Die Casting, Transactions* 1999, No.2, 1999:41-45. 49.
- [19] Z. W. Chen, W. R. Thorpe, The Effects of Squeeze Casting Pressure and Iron Content on the Impact Energy of Al-7Si-0.7Mg Alloy, *Materials Science & Engineering A* 1996, A221: 143-153.
- [20] H. Hu, Squeeze Casting of Magnesium Alloys and Their Composites, *Journal of Materials Science* 1998, 33: 1579-1589.
- [21] J. Campbell, *The solidification of Metals*, ISI Publication 110, The Iron and Steel Institute, 1967.
- [22] S. Shivkumar, S. Ricci Jr., B. Steenhoff, D. Apelian, D. Sigworth, *AFS Transactions* 1989, 97():791.
- [23] P. Y. Zhu, Q. Y. Liu, T. X. Hou, Spheroidization of Eutectic Silicon in Al-Si Alloys, *AFS Transactions* 1985, 93: 609-614.
- [24] Q. G. Wang, C. H. Caceres, J. R. Griffiths, Cracking of Fe-Rich Intermetallics and Eutectic Si Particles in an Al-7Si-0.7Mg Casting Alloy, *AFS Transactions* 1998, 107:131-136.
- [25] Q. G. Wang, C. H. Caceres, The Fracture Mode in Al-Si-Mg Casting Alloys, *Materials Science & Engineering* 1998A, A241: 72-82.
- [26] C. H. Caceres, On the Effect of Macroporosity on the Tensile Properties of the Al-0.7%Si-0.4Mg Casting Alloy, *Scripta et Materialia* 1995, No.11,32: 1851-1856.
- [27] C. H. Caceres, C. J. Davidson, J. R. Griffiths, The Deformation and Fracture Behavior of an Al-Si-Mg Casting Alloy, *Materials Science and Engineering* 1995A, A197: 171-179.

- [28] C. Verdu, H. Cercueil, S. Communal, P. Sainfort, R. Fougères, Microstructural Aspects of the Damage Mechanisms of Cast Al-Si-Mg Alloys, *Materials Science Forum* 1996, 217-222: 1449-1454.
- [29] C. H. Cáceres, J. R. Griffiths, Damage by the cracking of silicon particles in an Al-7Si-0.4Mg casting alloy, *ACTA Mater.* 1996, 44:25-33.
- [30] C.H. Cáceres, J. R. Griffiths, P. Reiner, The influence of microstructure on the Bauschinger effect in an Al-Si-Mg casting alloy, *ACTA Mater.* 1996, 44: 15-23.
- [31] D. Lindsey and J.F. Wallace – “Effect of vent size and design, lubrication practice, metal degassing, die texturing and filling of shot sleeve on die casting soundness”, SDCE Paper No. 10372, 1972.
- [32] Private communication from U.S. commercial squeeze casting workshop, 1996
- [33] M. Adachi, Y. Waku, H. Iwai, T. Nishi and A. Yoshida “Microstructure and Mechanical Properties of squeeze cast AC4CH alloy (low in 356) Volume 39 No. 7, Japanese Casting Society, 1989.
- [34] D.E. Croom *A Modern Die Casting Technology - a User's View.* ≡ *British Foundryman*, Dec. 1996 pp. 440-445 (low in 356)
- [35] T. Oeno, M. Uchida, M. Sose - *Squeeze Casting Present and Future.* 1993.

FIGURES

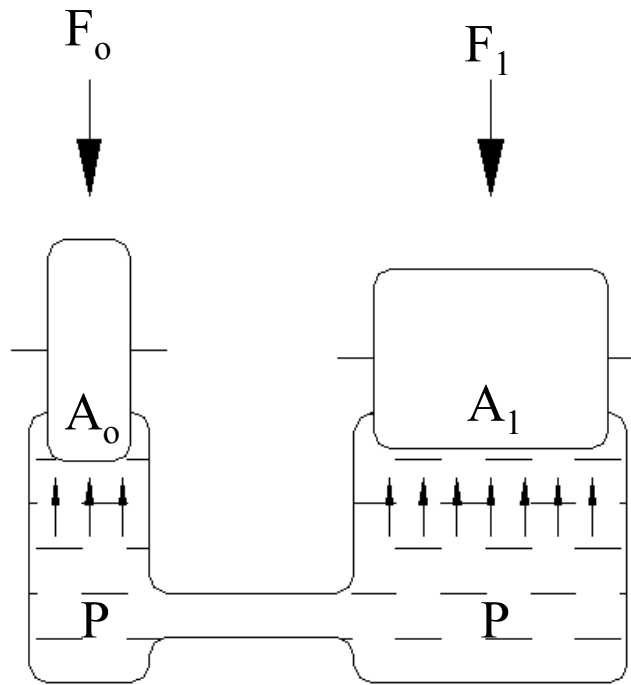


Figure 3.1 Pascal's Principle

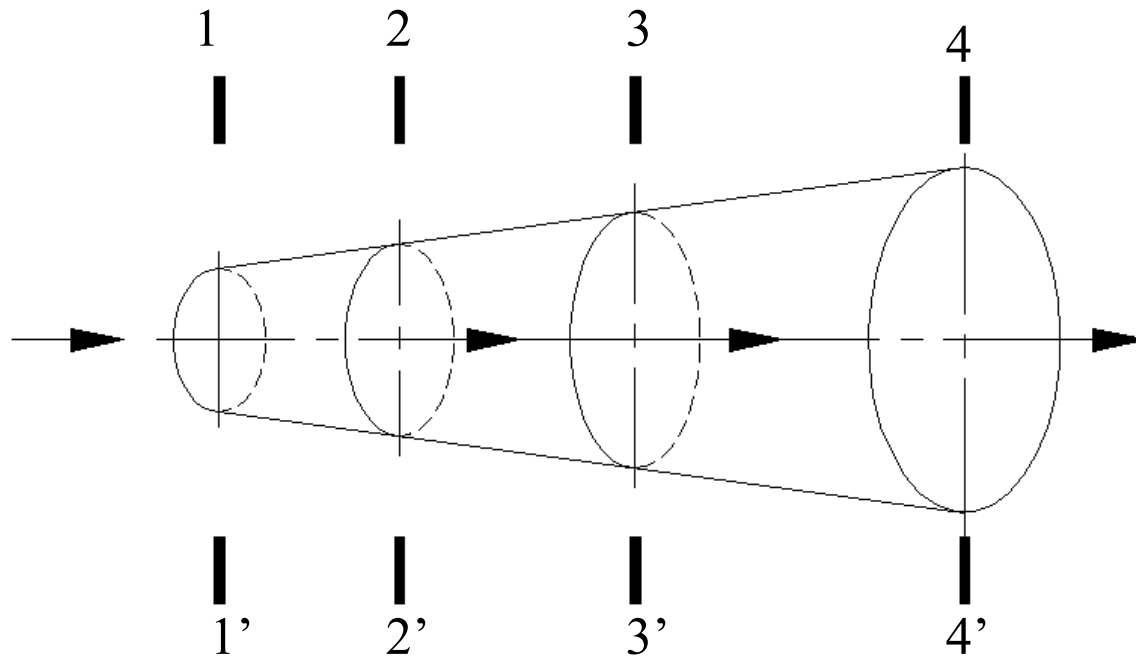


Figure 3.2: Fluid flow in a pipe

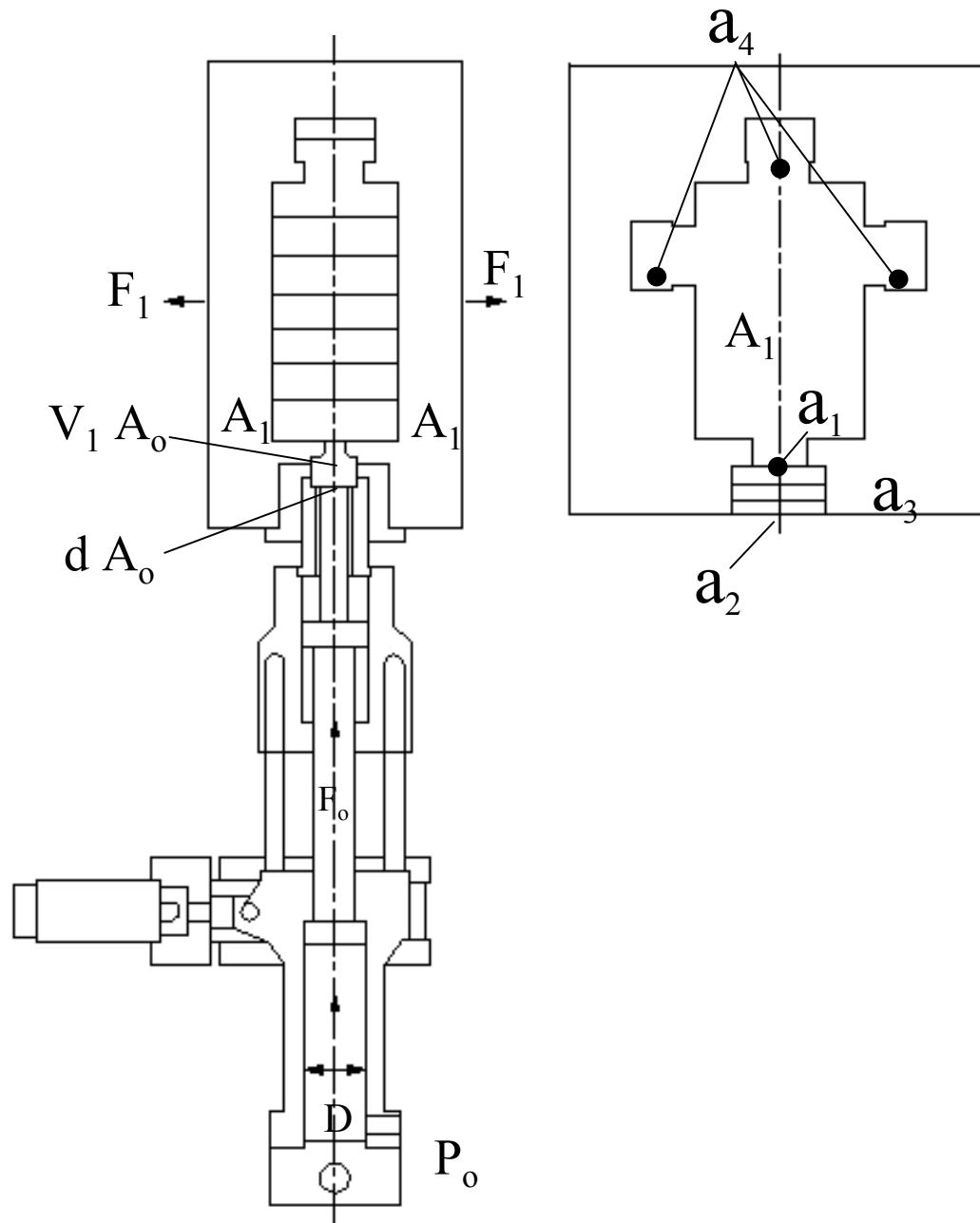


Figure 3.3: Pressure and velocity changes

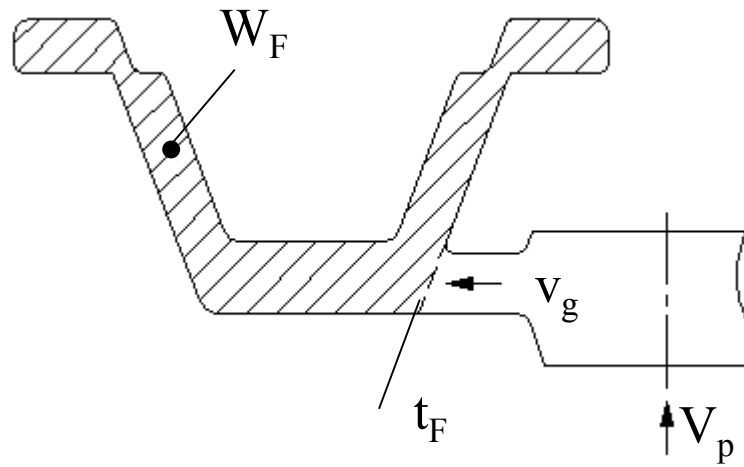


Figure 3.4: Part-gate-plunger filling variables

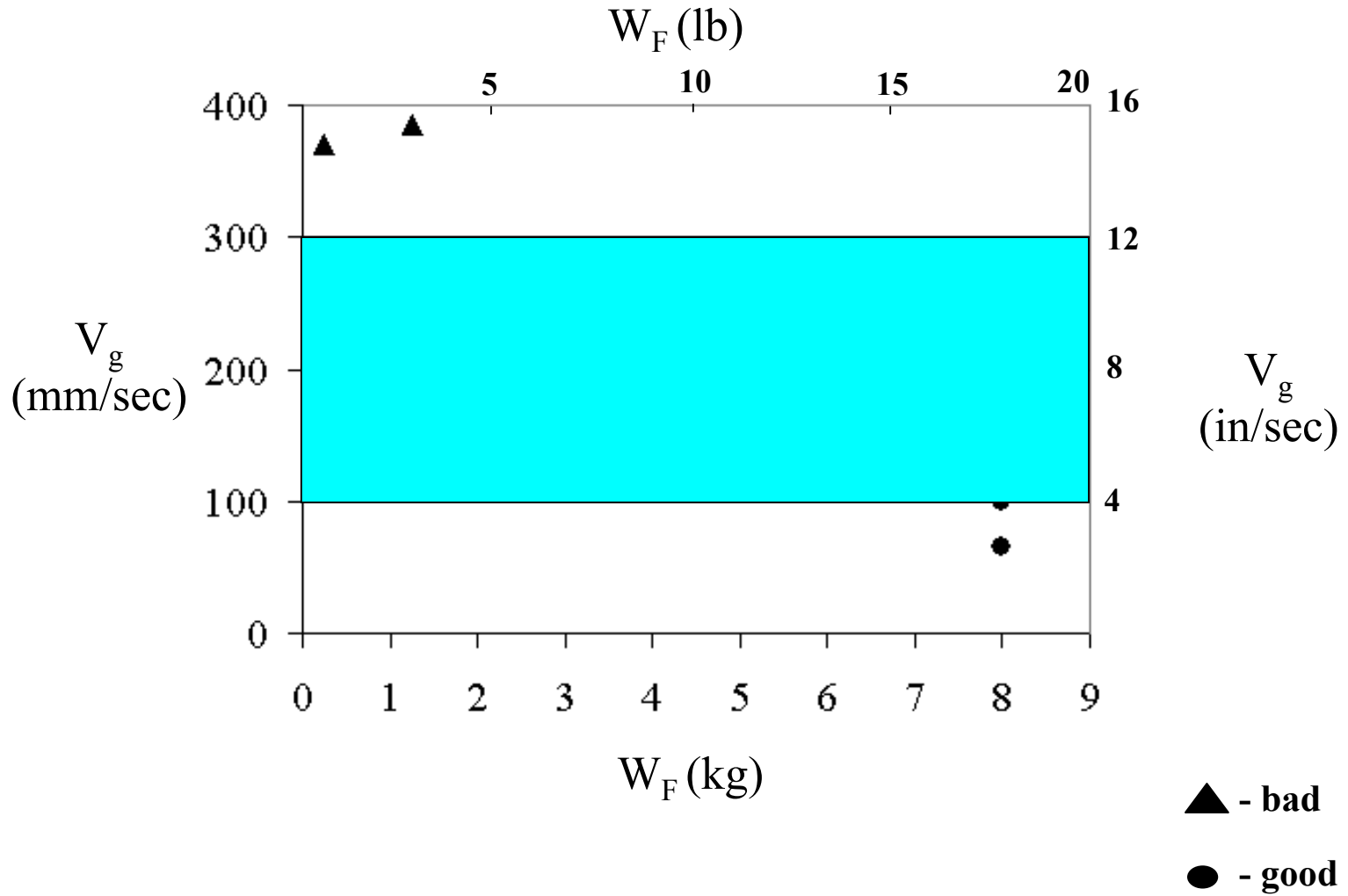


Figure 3.5: Typical gate velocities

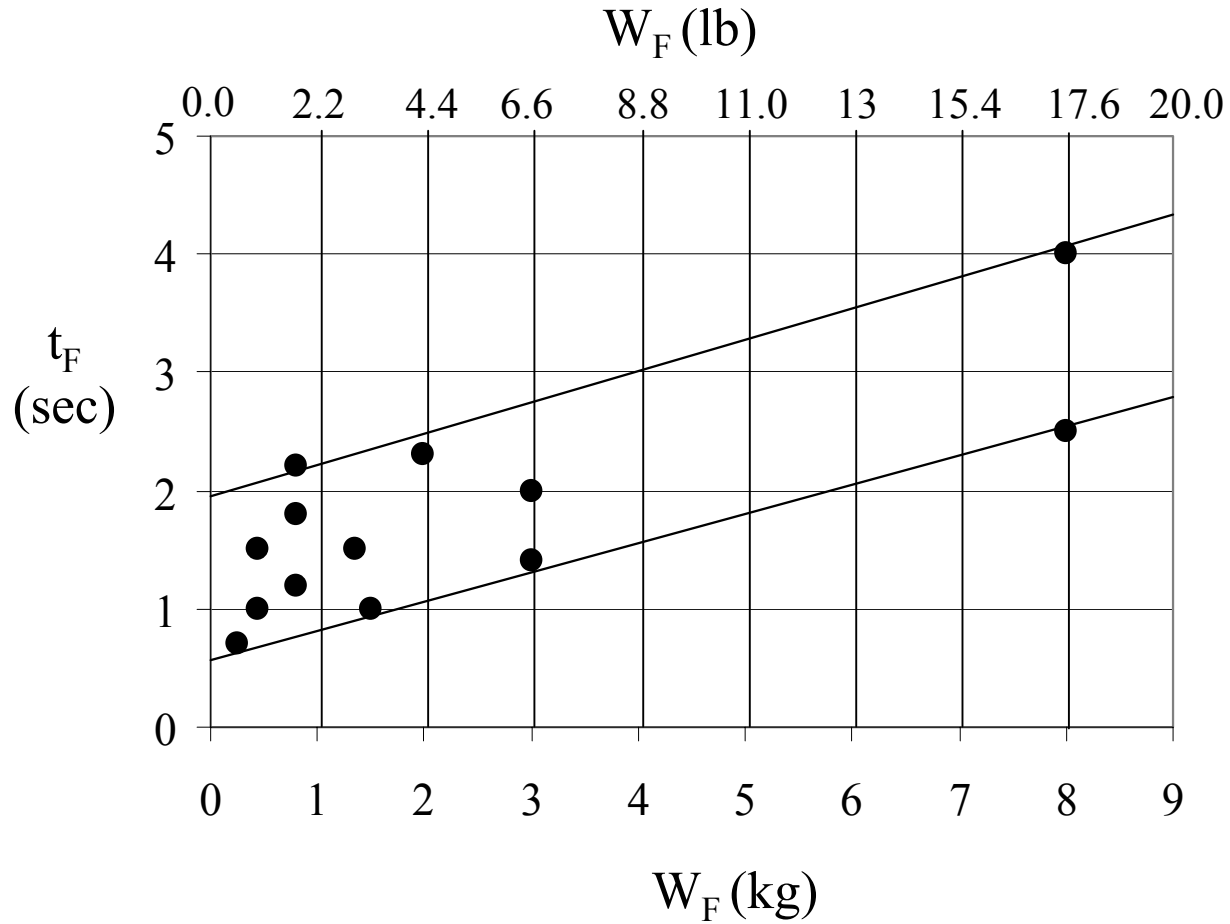


Figure 3.6: Favorable filling times for sound castings

Figure 3.7: Steps in the Injection of Metal Into the Die

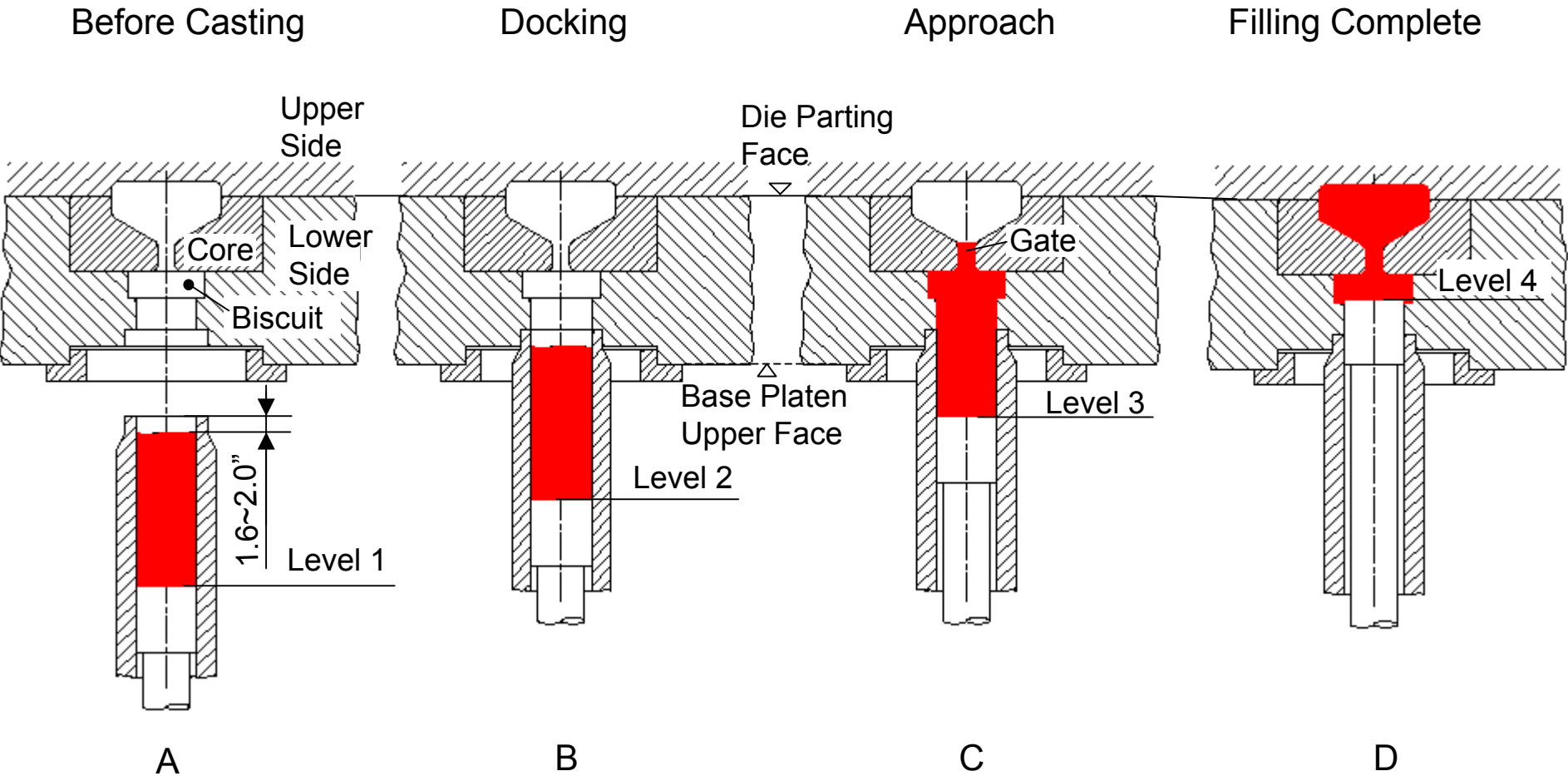


Figure 4.1: UBE VSC 315 Ton Squeeze Cast Machine

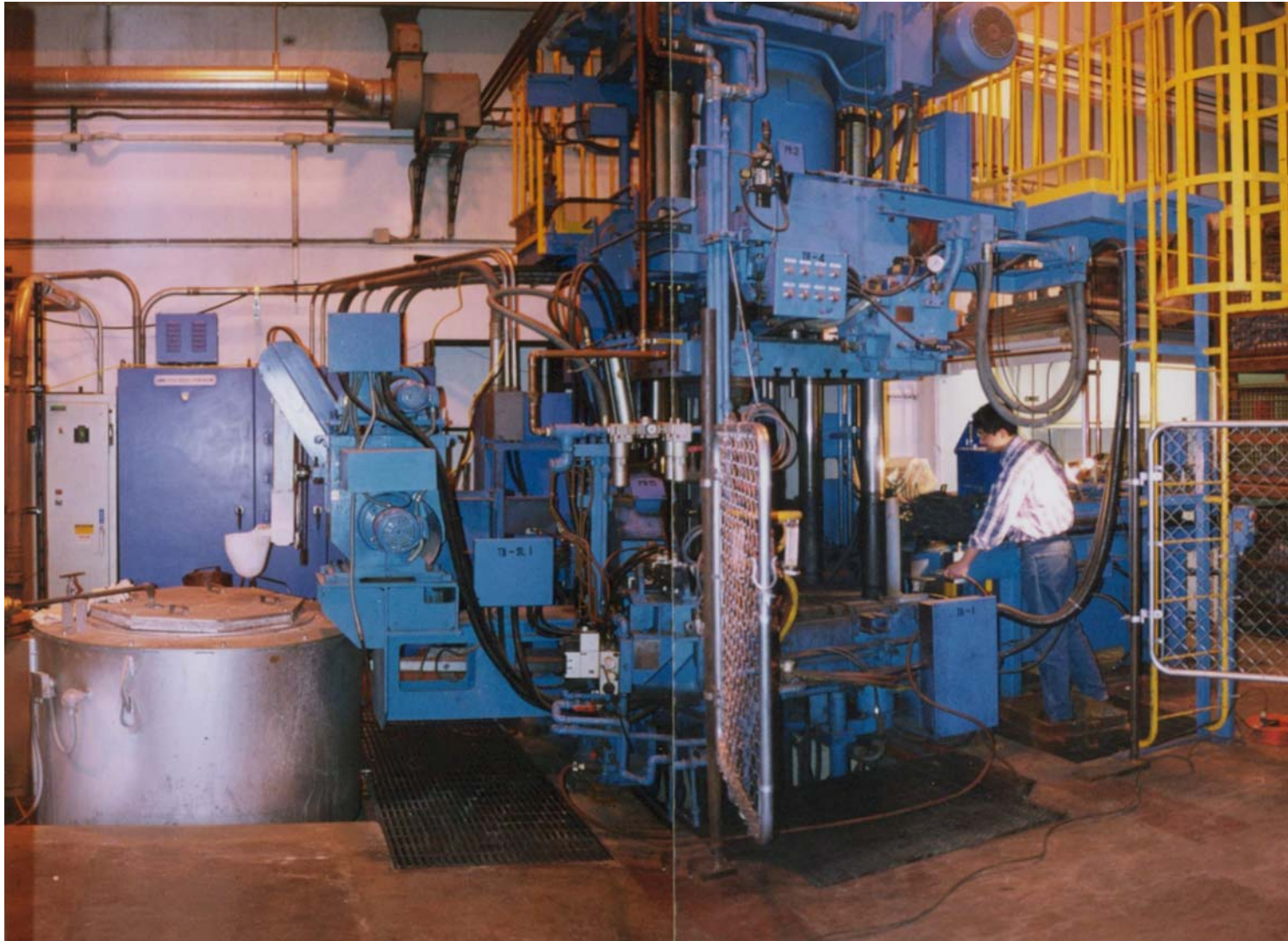


Figure 4.2: UBE VSC Squeeze Caster – Top View Schematic

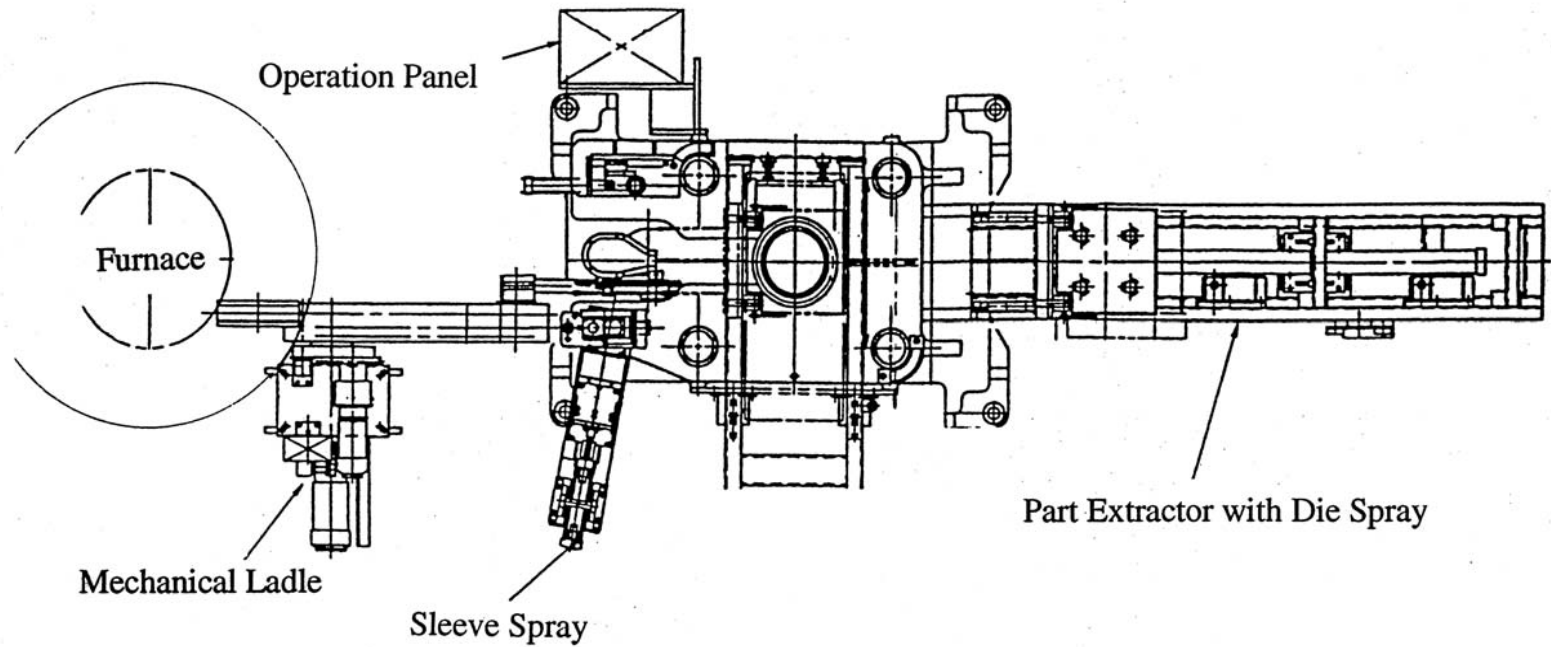


Figure 4.3: UBE VSC Squeeze Caster – Side View Schematic

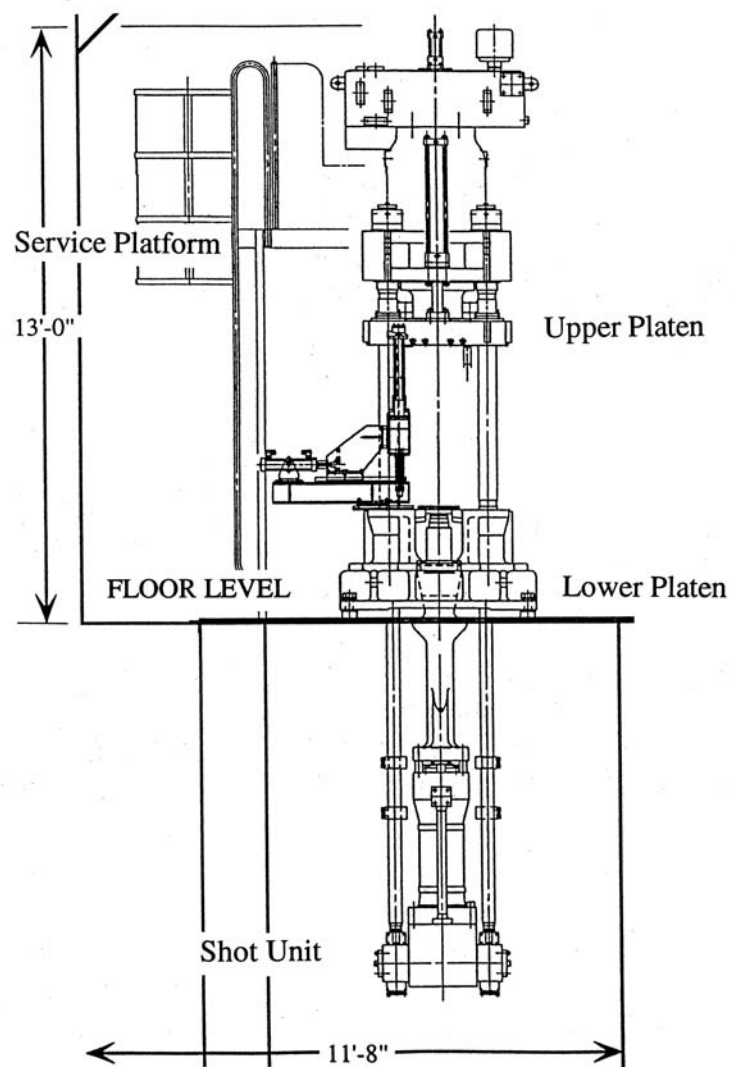


Figure 4.4: CWRU SQUEEZE CASTING EQUIPMENT

TYPE—UBE VCS315

1. DIE CLAMPING UNIT

DIE CLAMPING FORCE	315 TON	
PLATEN DIMENSIONS	42×38 INCHES	1060×950 MM
DIE STROKE (MAX)	24 INCHES	600 MM

2. SHOT UNIT—S63

SHOT FORCE	20 ~ 63 TON	
SHOT STROKE (MAX)	25 INCHES	630 MM
SHOT SPEED (MAX)	3.2 INCHES/SEC	80 MM/SEC

3. CASTING WEIGHT (MAX)	11 LB	5KG
-------------------------	-------	-----

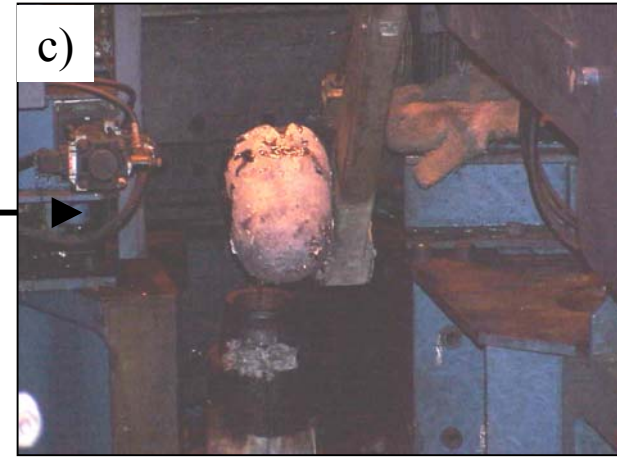
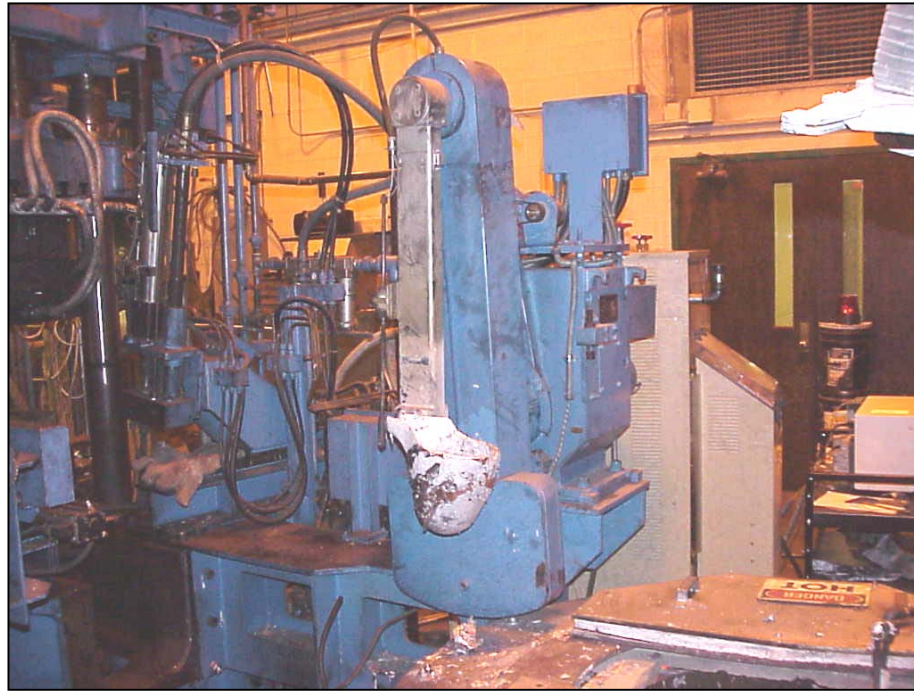
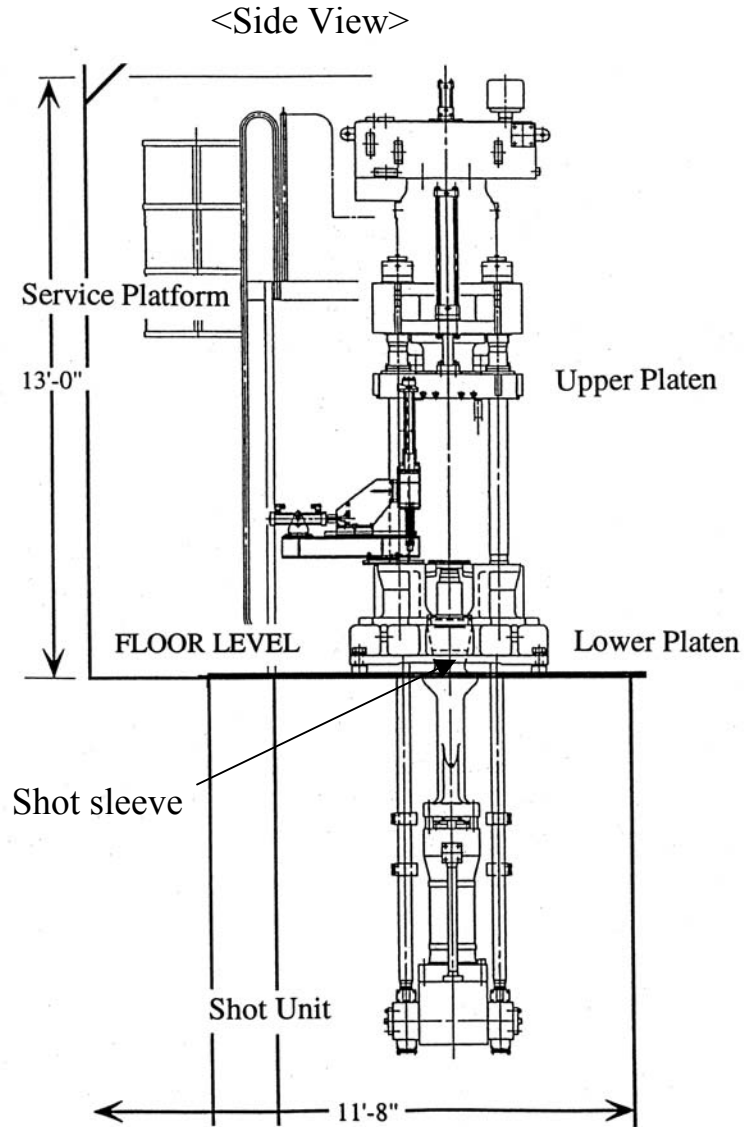
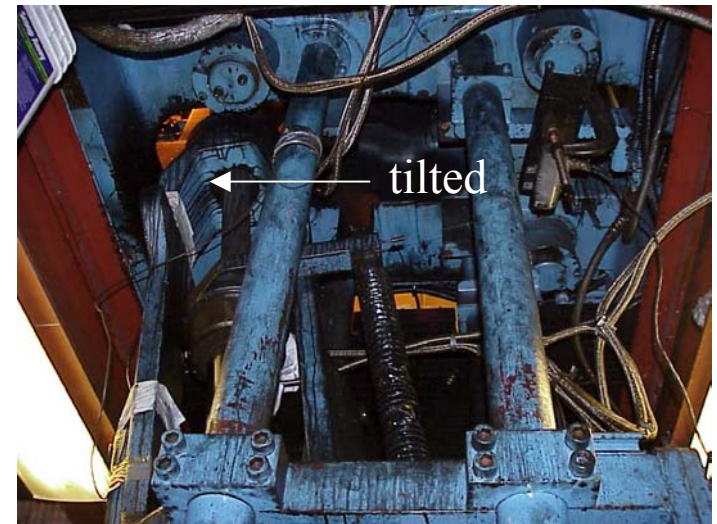


Fig.4.5: Automatic ladling machine

Figure 4.6: View of shot sleeve

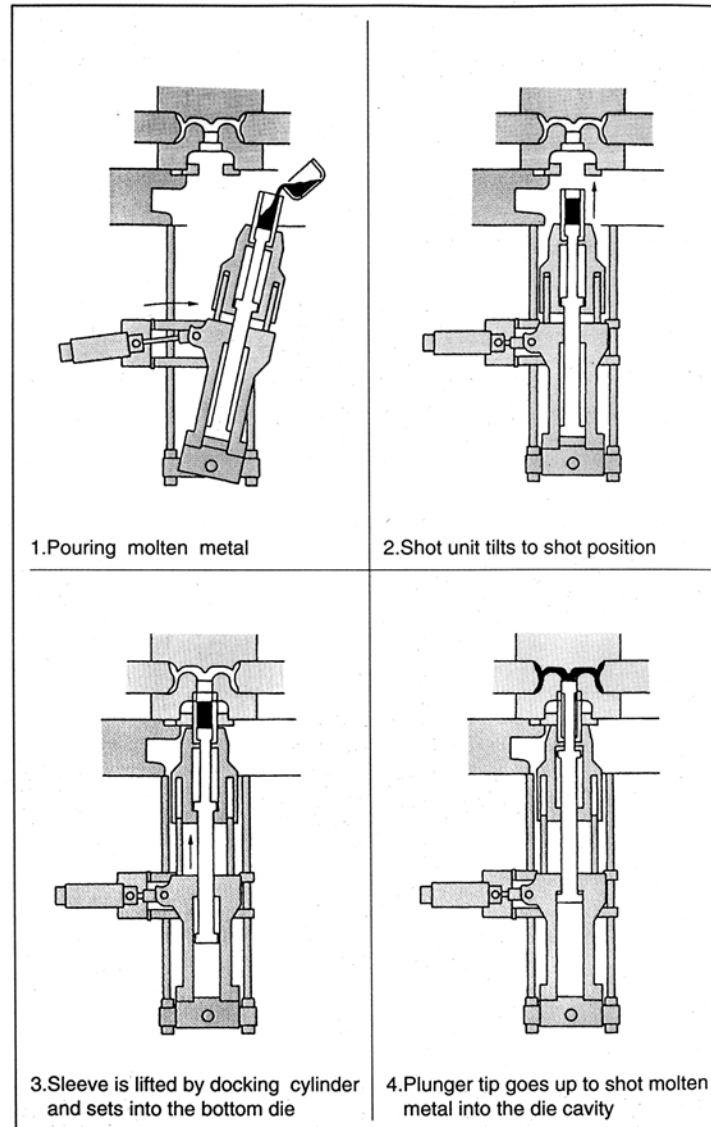


<Top View>

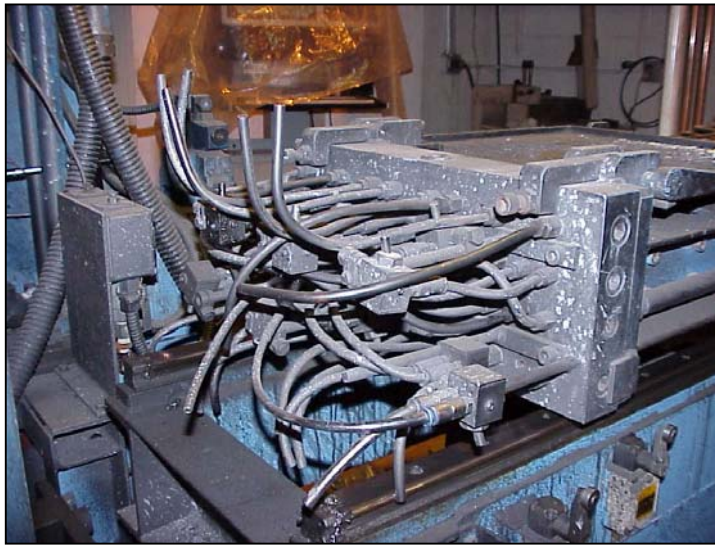
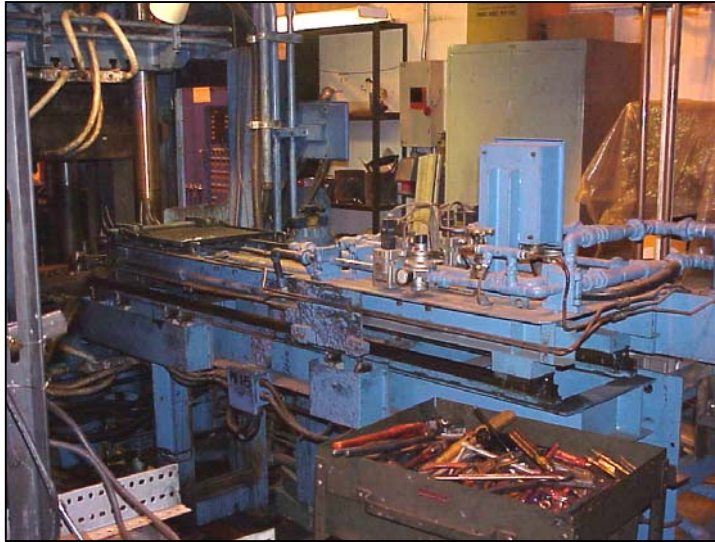


<Bottom View>

Figure 4.7: Sequence of shot sleeve operation



For dies



For shot sleeve

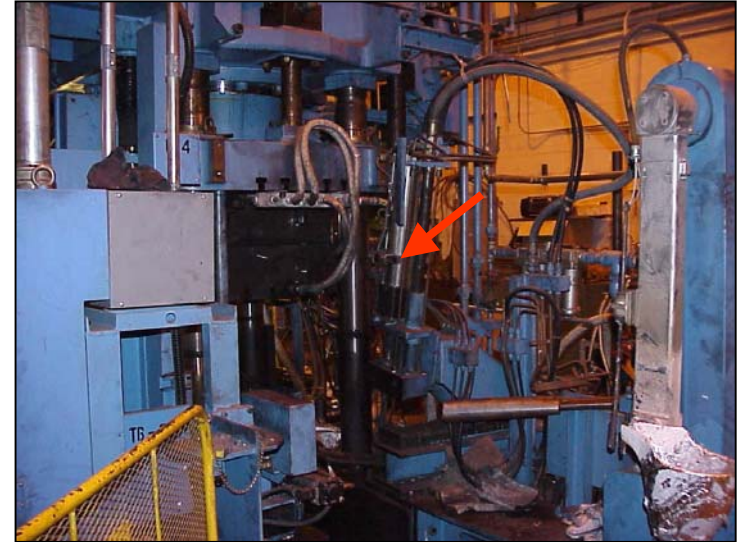
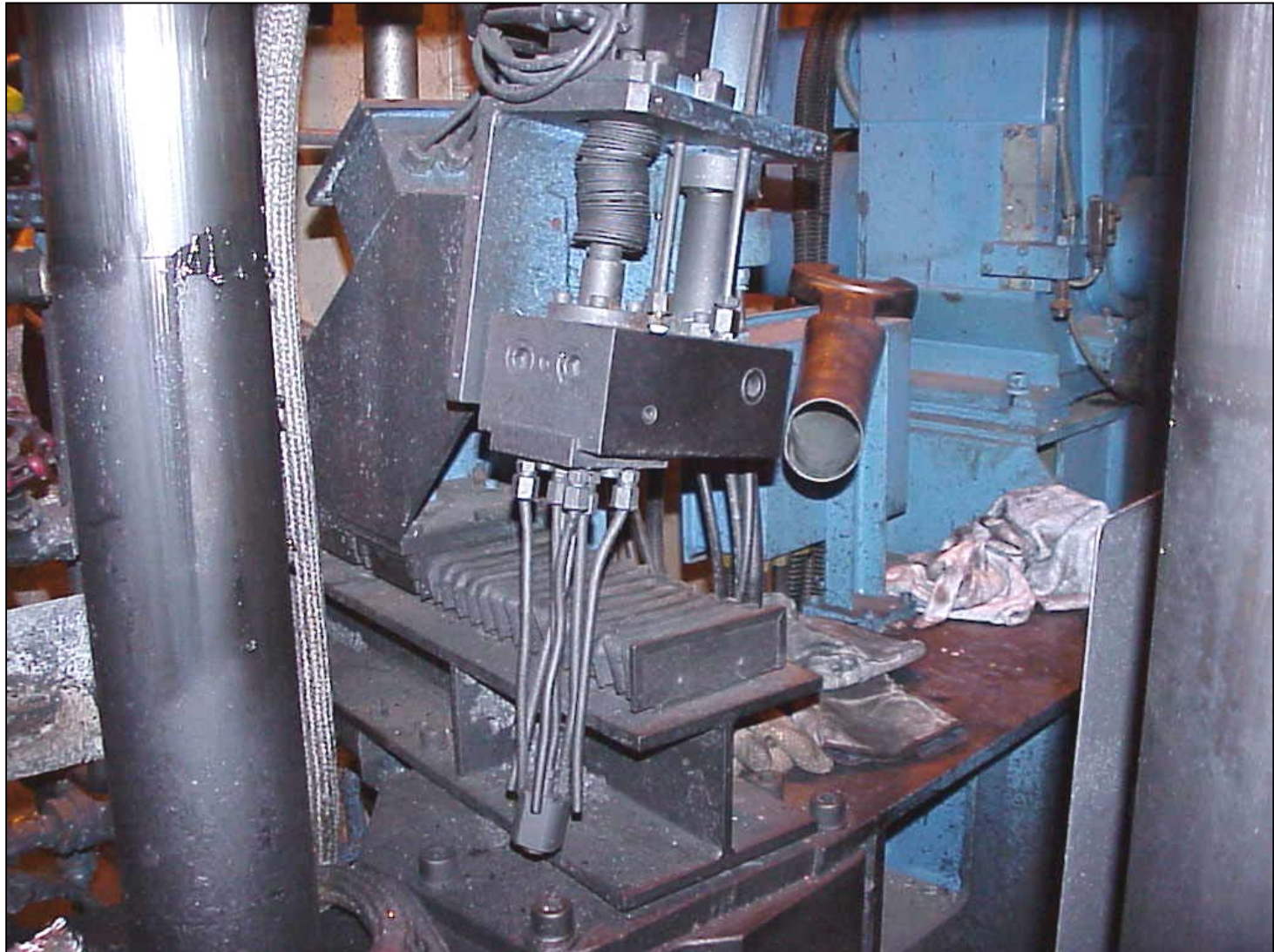


Fig.4.8: Automatic die lubricant spraying units

Fig.4.9: Manual die lubricant spraying unit



Fig.4.10: Die lubricant spraying unit for shot sleeve



Oil Die Heater



(Sterlco, M2B9016-J1)

Infrared Die Heater

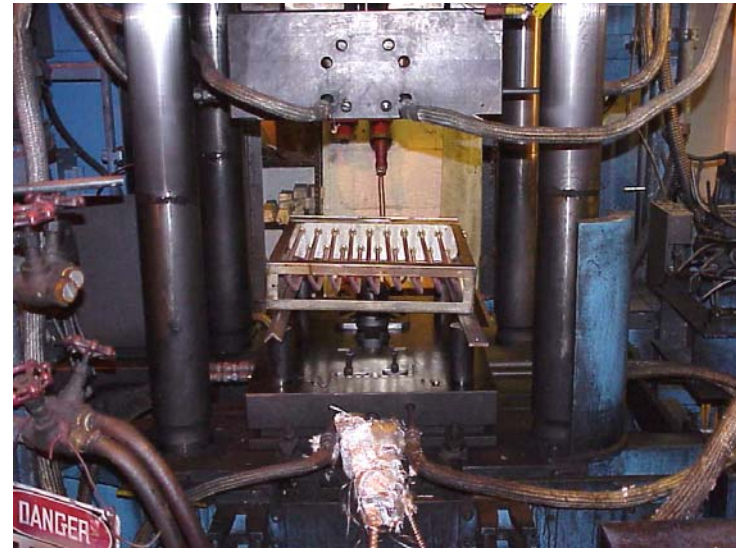


Fig.4.11 Die heating equipment

Fig.4.12: Visi-Track shot monitoring system



Figure 4.13: Typical Visi-Trak Shot Monitoring Plot

1 : apr3199 : SHOT 114 : Thr 04/08/1999 15:51:35

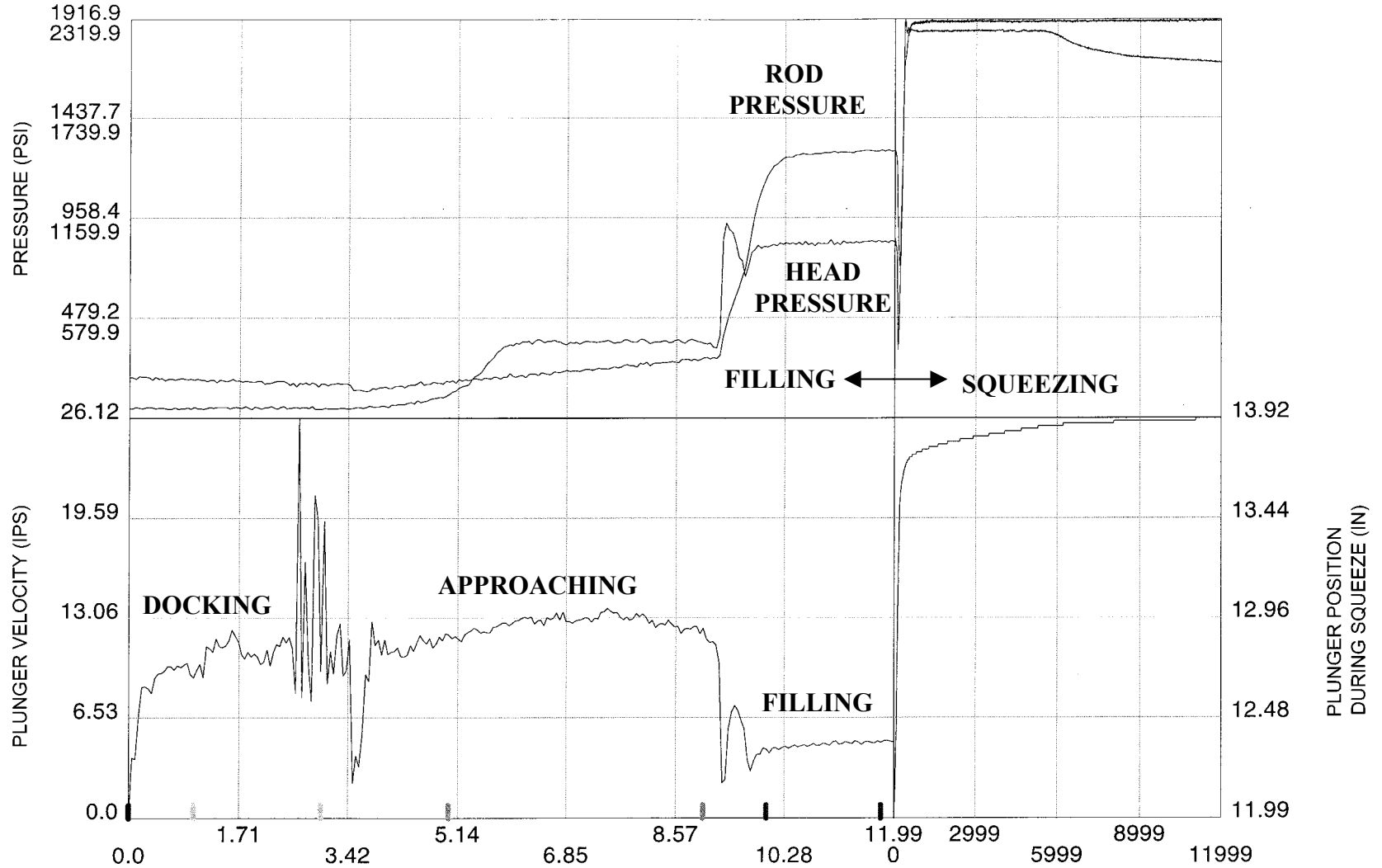


Figure 5.1: Computer Hub Casting (two cavities)

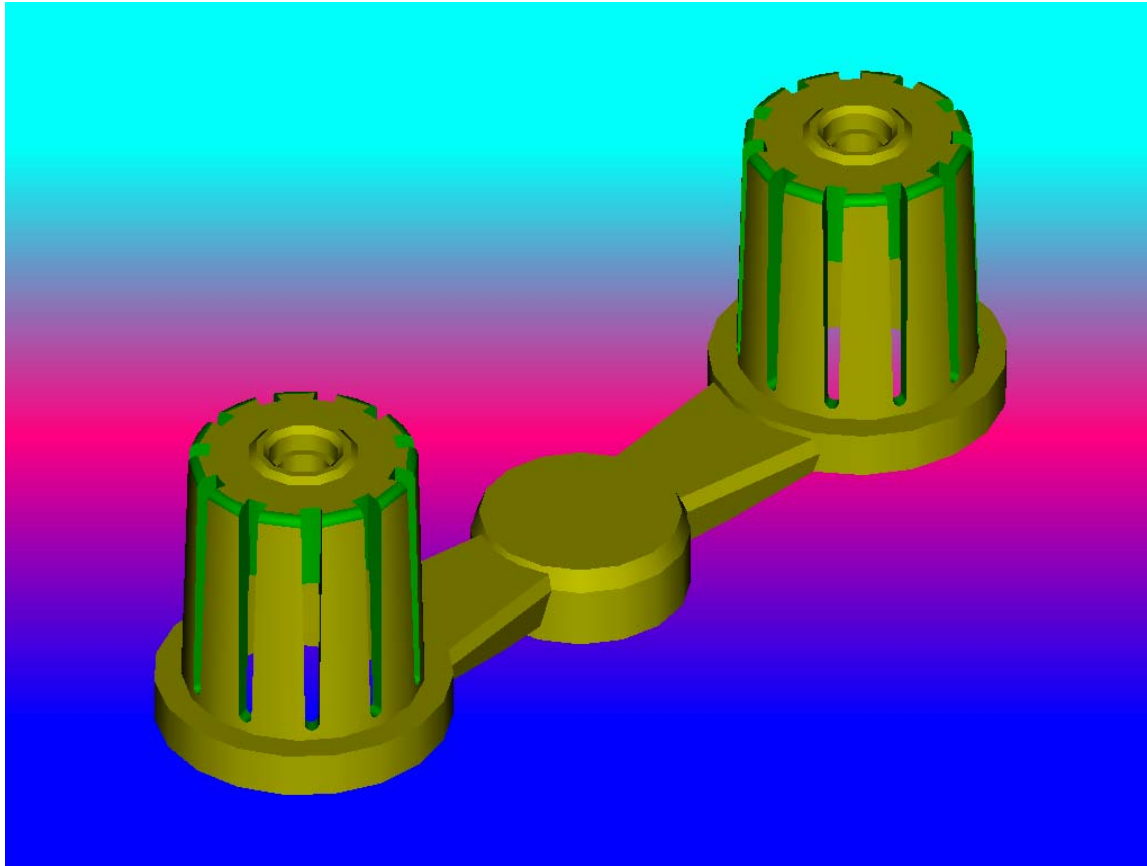


Figure 5.2: TENSILE TEST BAR DESIGNS

Insert #1/Design 1: Two test bars 0.505” and 0.380” diameter.



Insert #1/Design 2: Modified to improve integrity of the bars.



Insert #2: “U” shape with four 0.505” test bars and large overflow.



Insert #3: with runner feeding two test bars from both ends.

Figure 5.3: CWRU Test Bar Inserts (CMI Design)

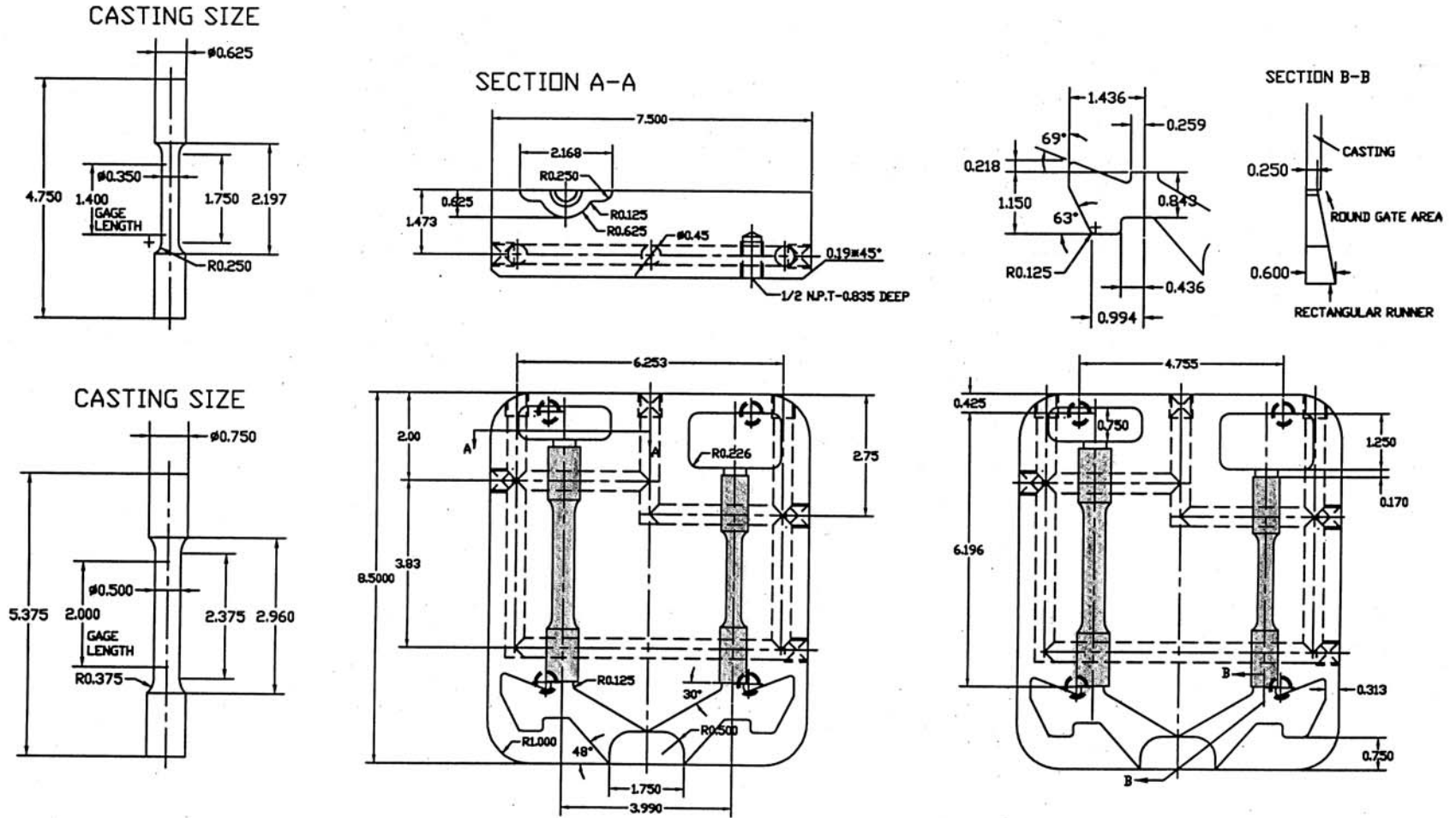
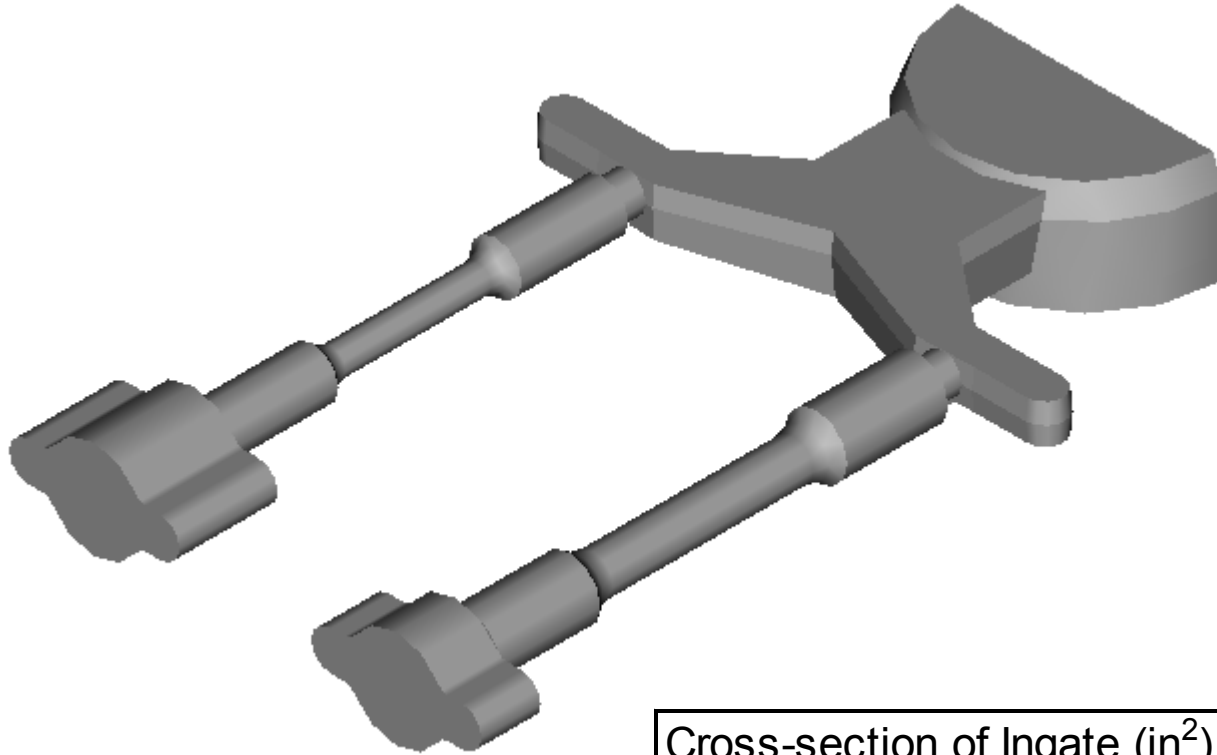


Figure 5.4:CWRU Test Bar (CMI Design)



Cross-section of Ingate (in ²)	0.39
Volume of Casting (in ³)	3.30
Volume of the Overflow (in ³)	3.30

Fig. 5.5: Modification of the Test Bar Insert

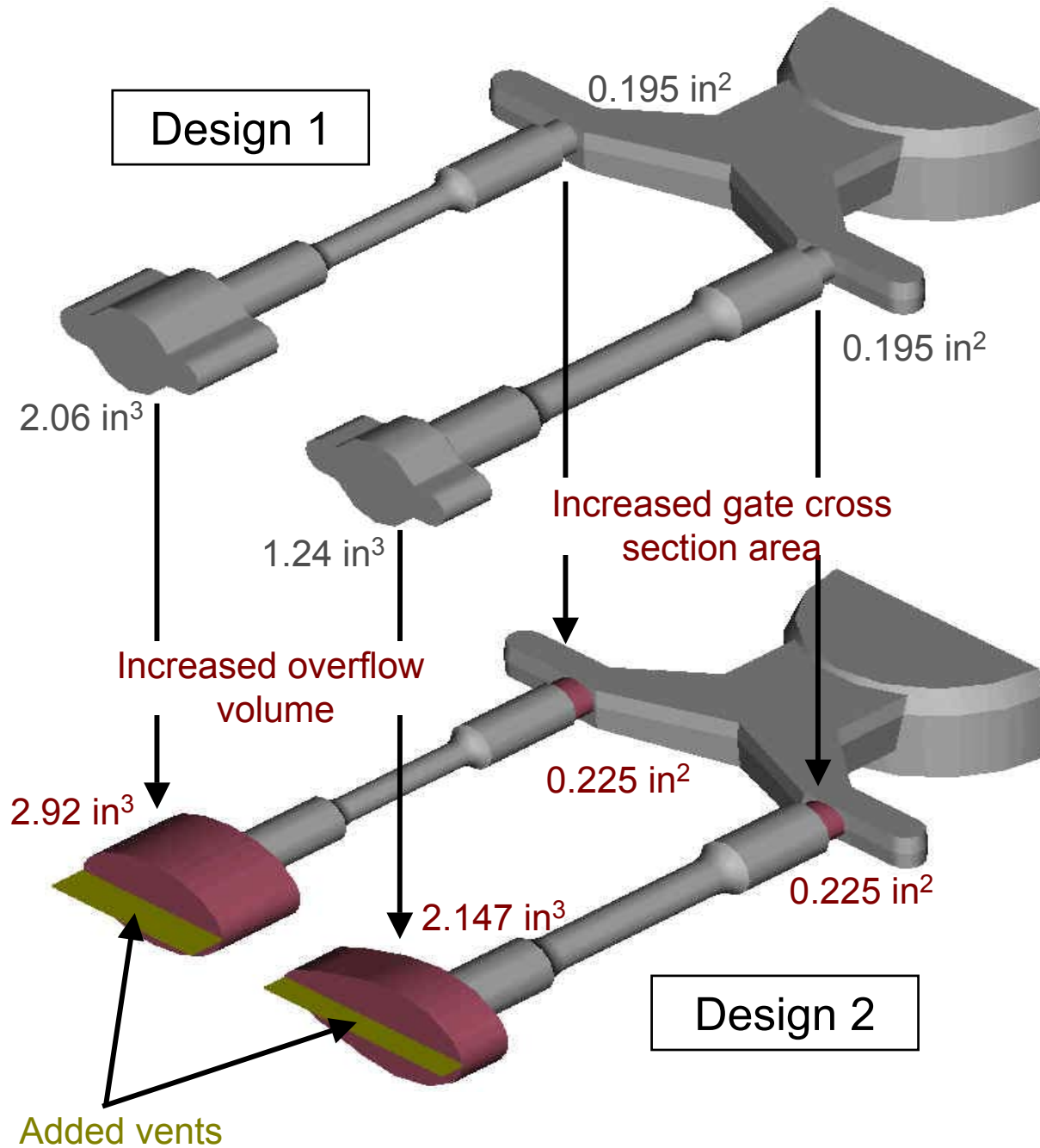


Figure 5.6: Effect of Die Modification on Tensile Strength of 356 Test Bars (T6)

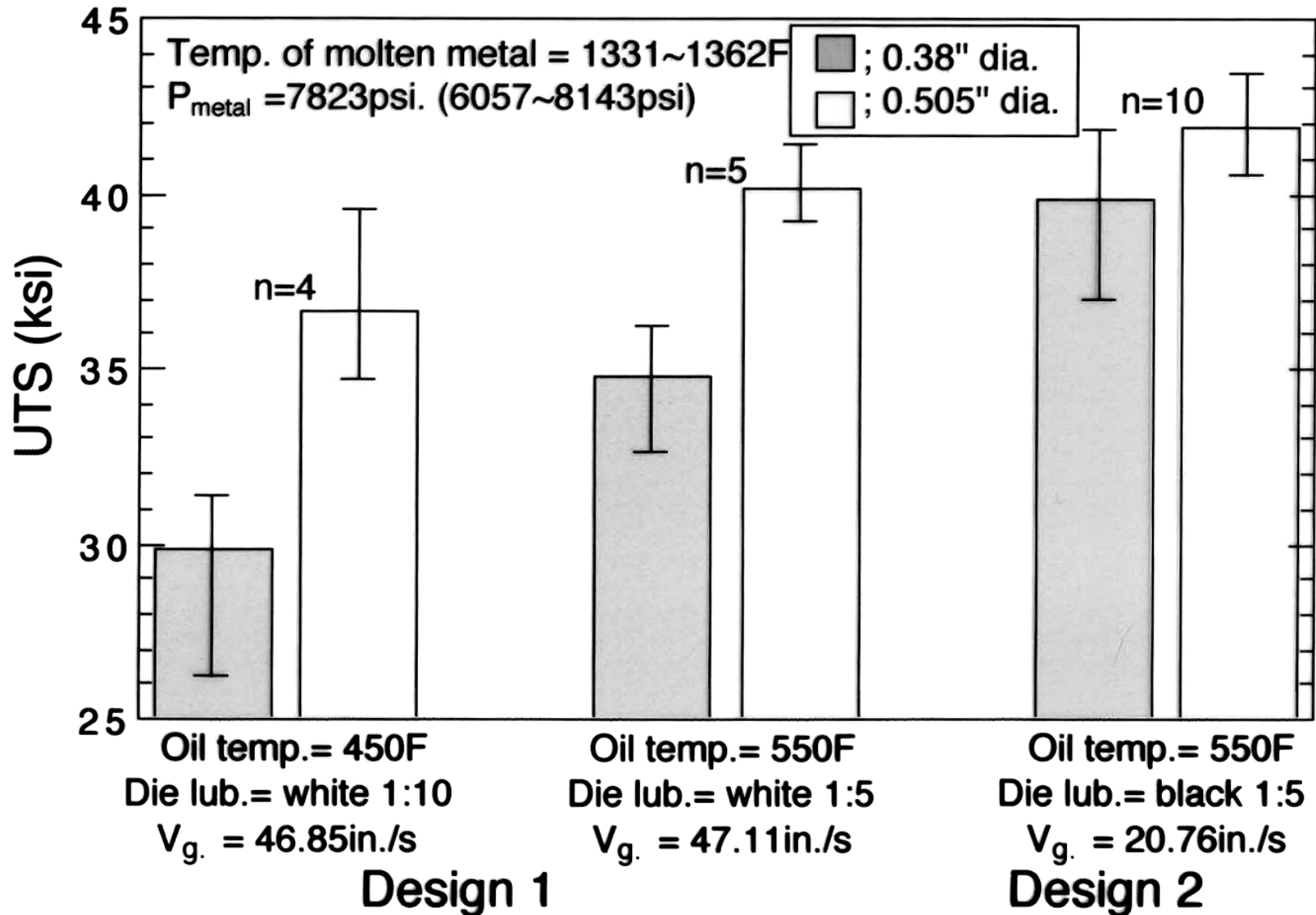


Figure 5.7: Effect of Die Modification on Elongation of 356 Test Bars (T6)

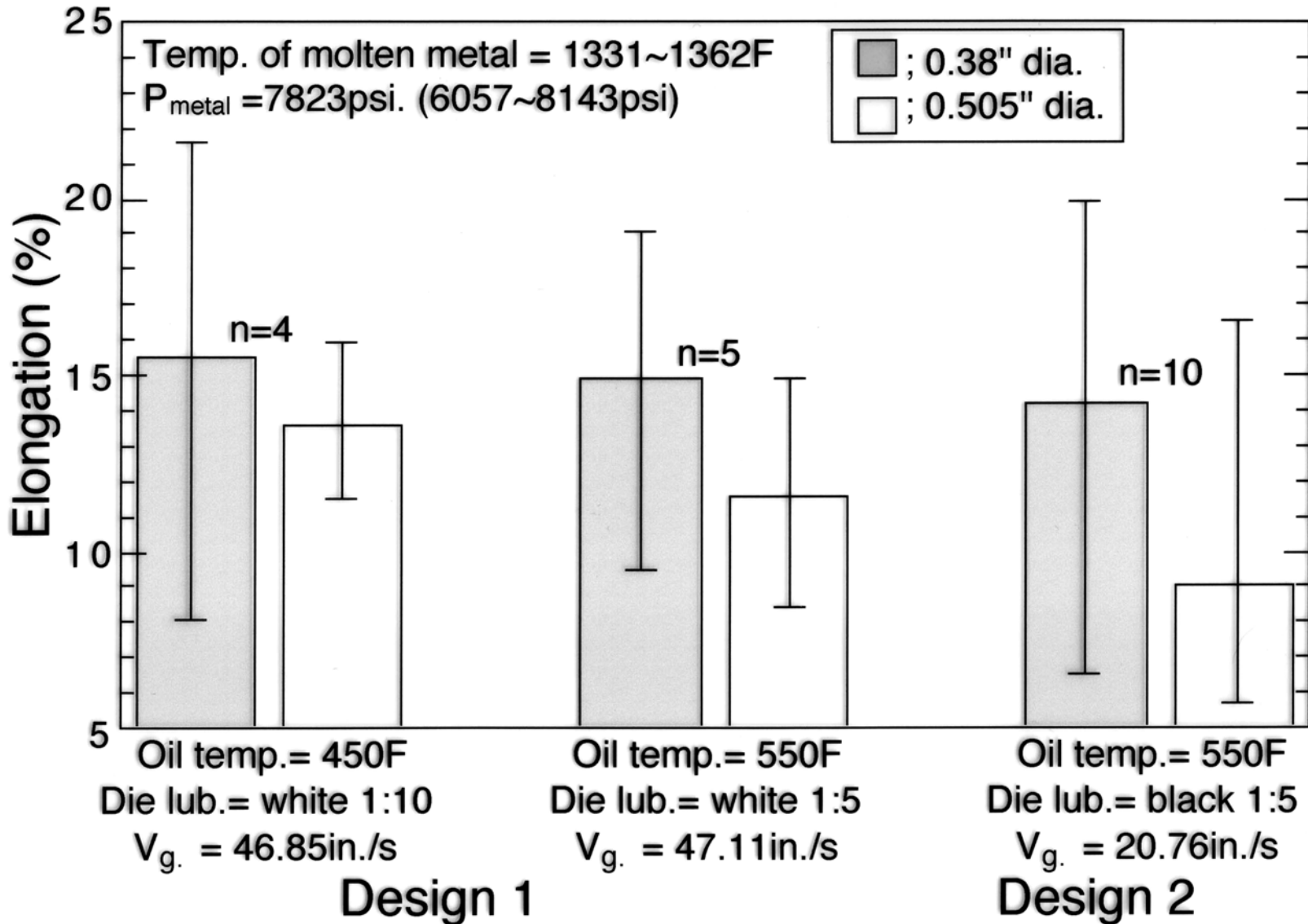


Figure 5.8: CASTING DEFECTS IN 0.380" DIAMETER BARS

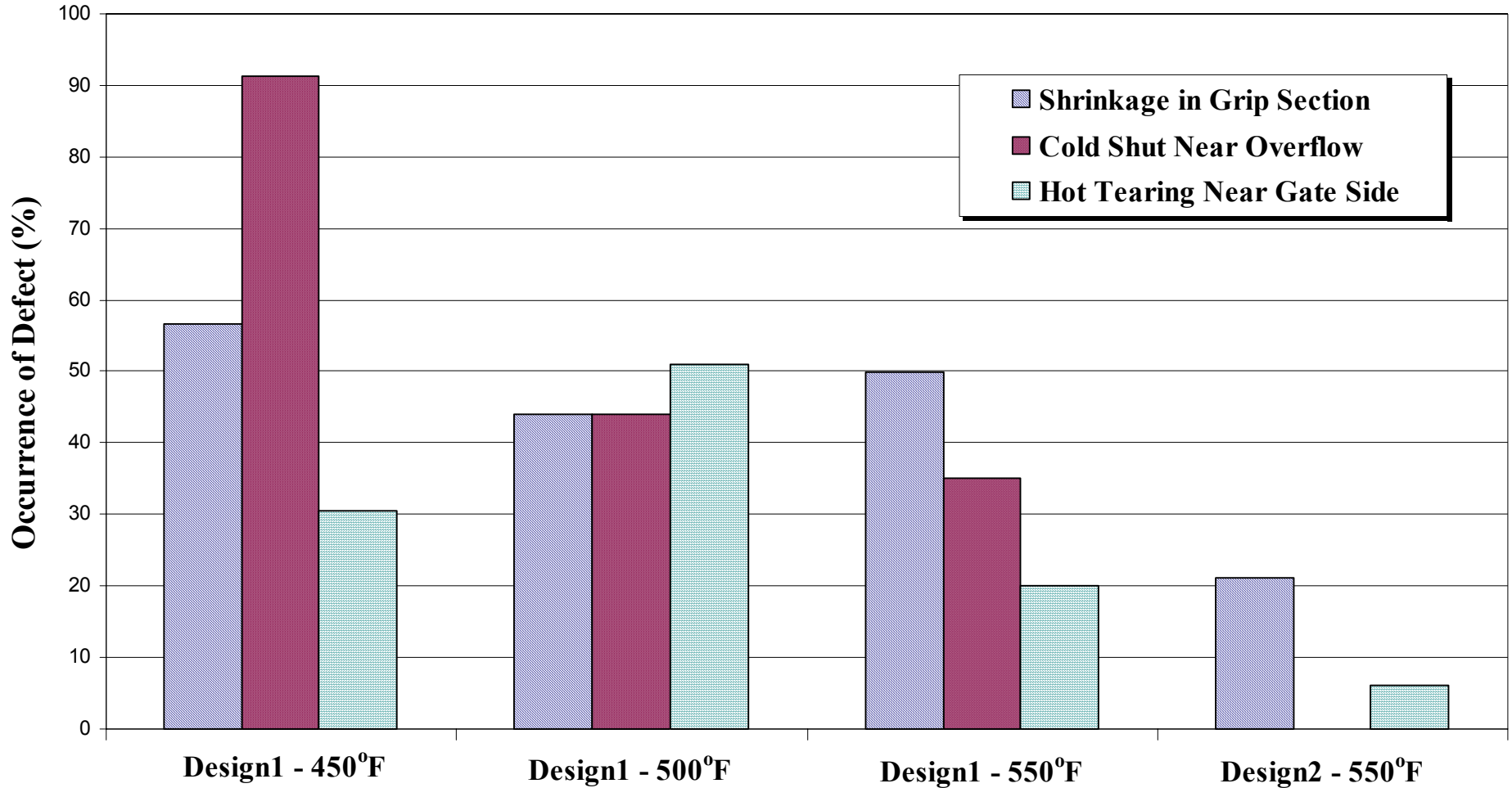
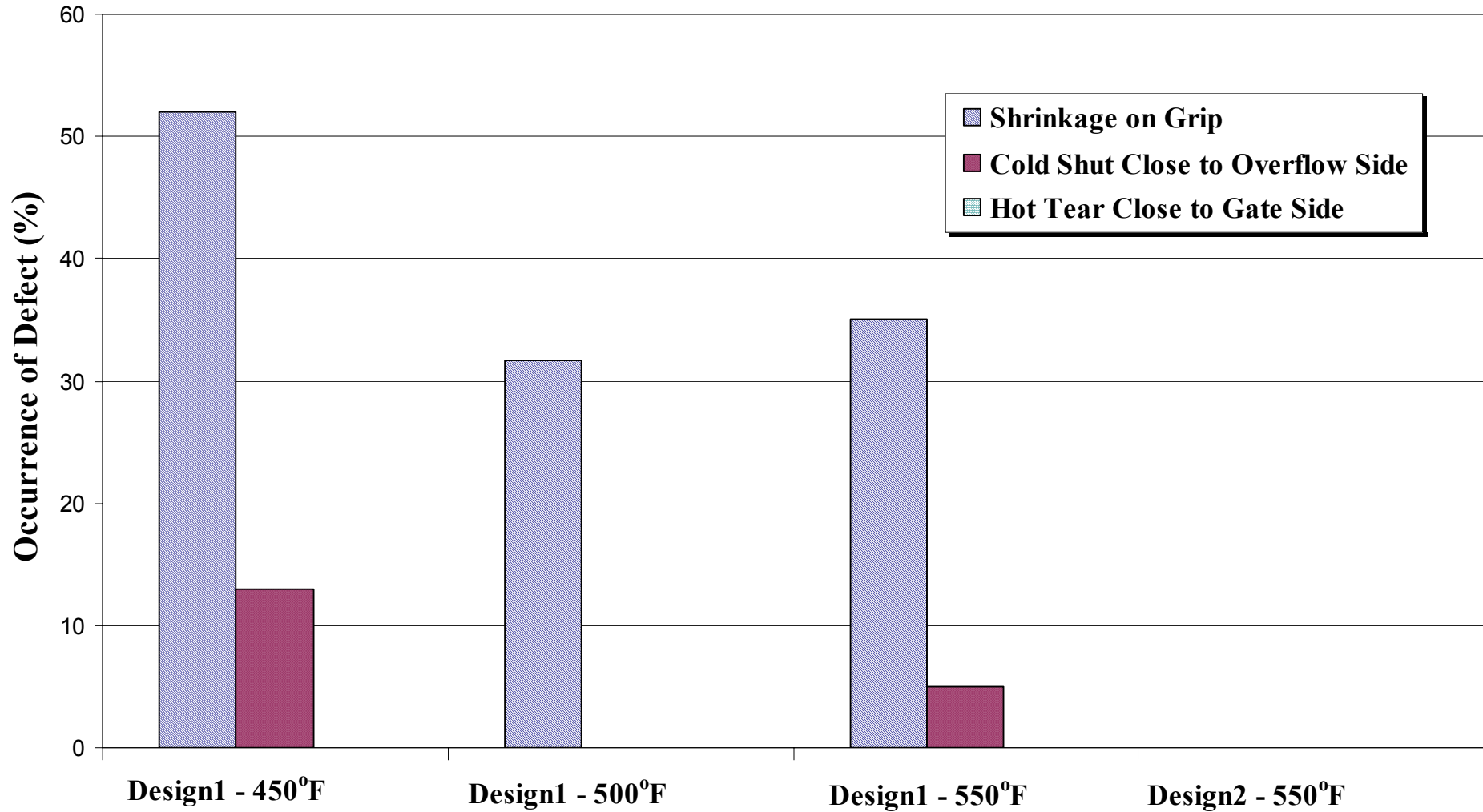


Figure 5.9: CASTING DEFECTS IN 0.505" DIAMETER BARS



**Figure 5.10: TENSILE PROPERTIES OF
VIRGIN ALUMINUM 356 -- .505" DIA
BARS**

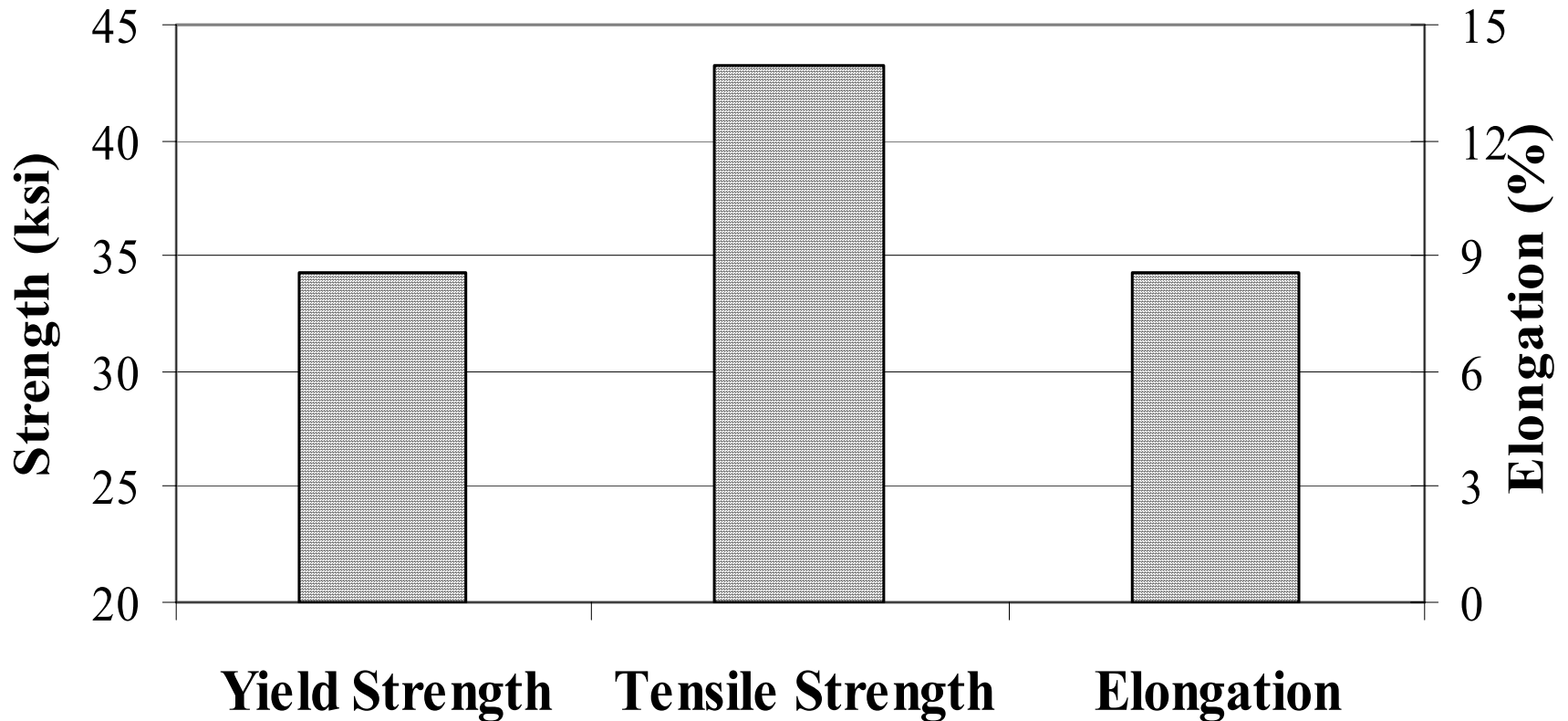


Figure 5.11: TENSILE PROPERTIES OF VIRGIN ALUMINUM 356 -- .380" DIA

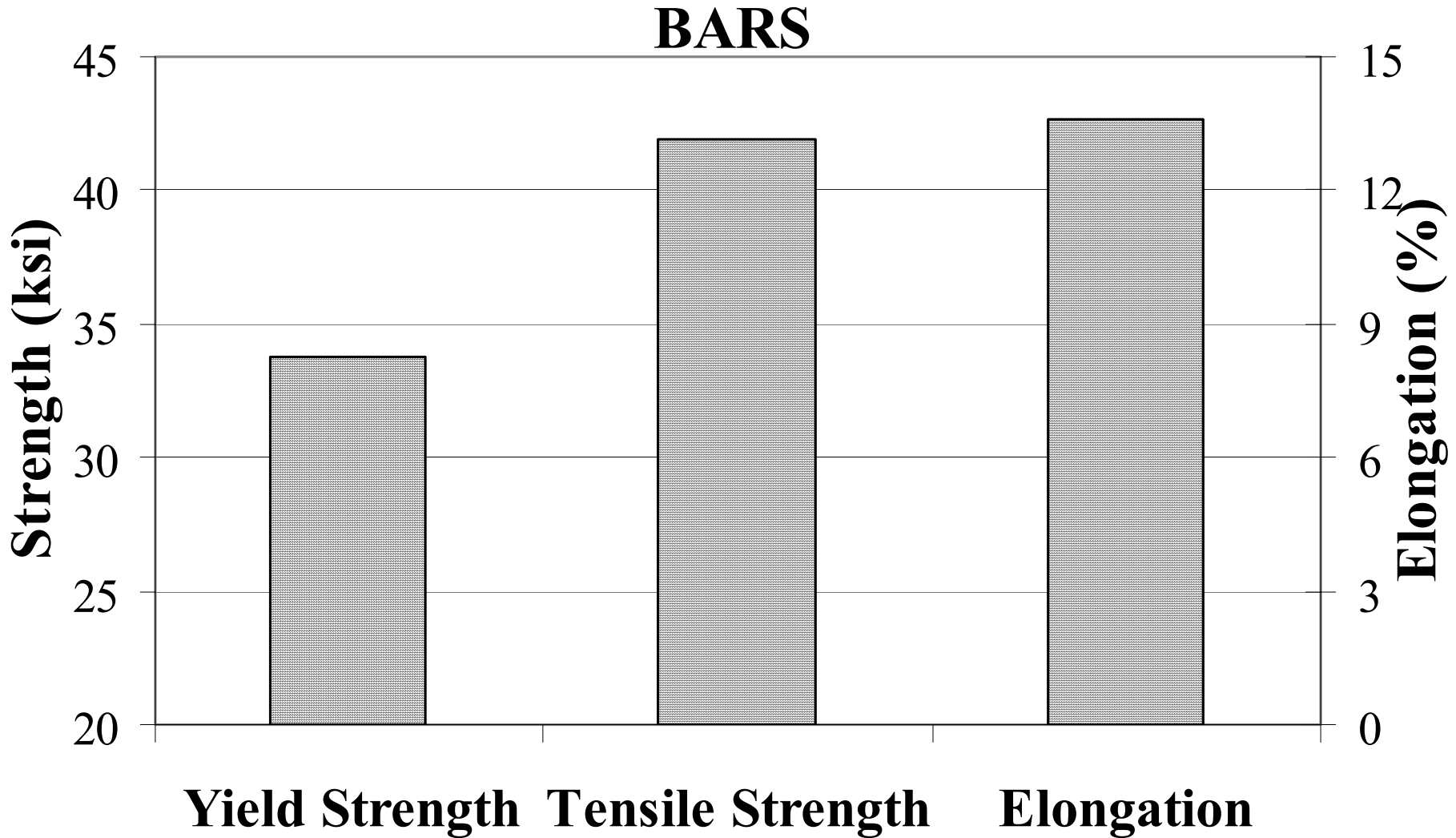
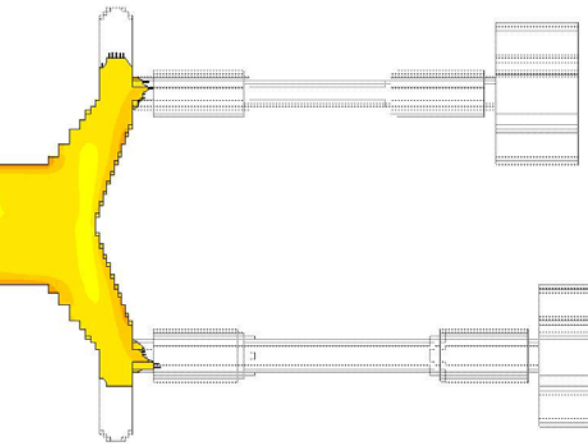
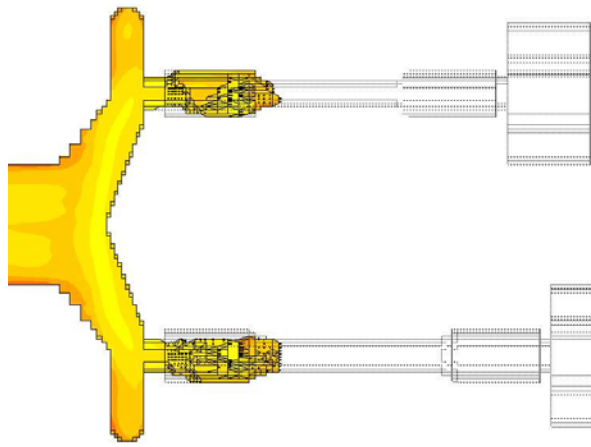


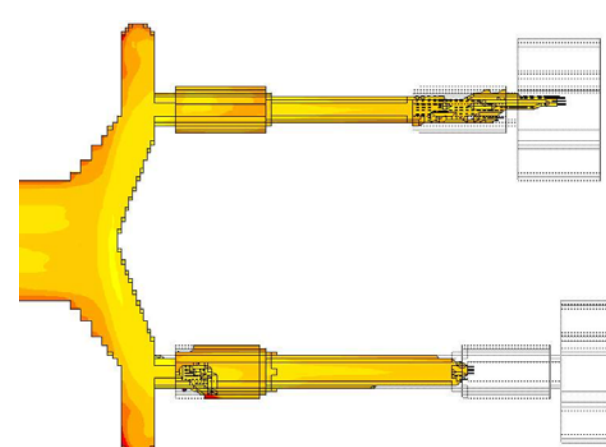
Figure 5.12: Flow Pattern in SC Test Bar (CMI design)
(Design 1, Gate Velocity = 46 in/sec)



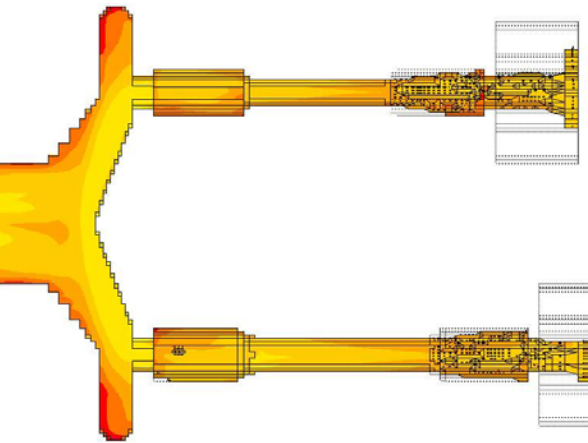
0.665 sec



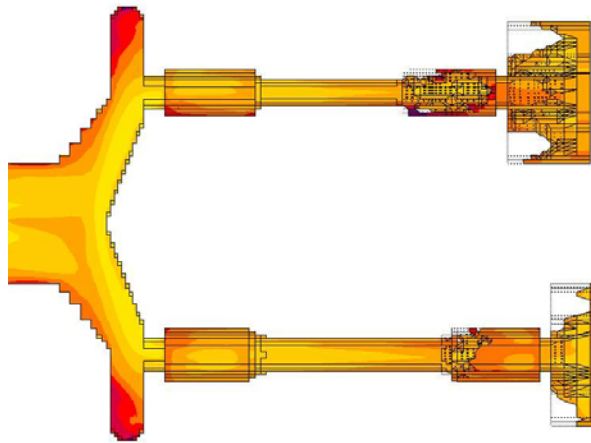
0.712 sec



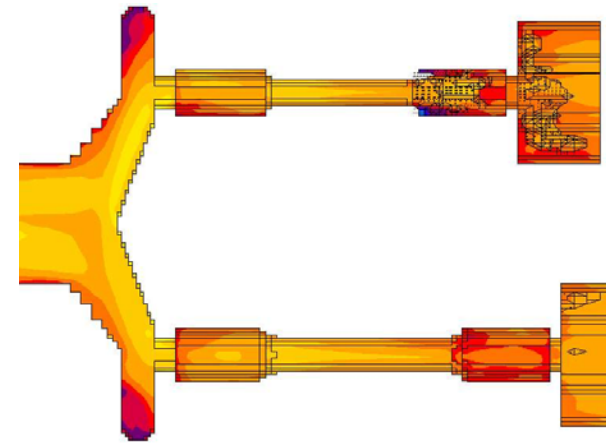
0.760 sec



0.808 sec

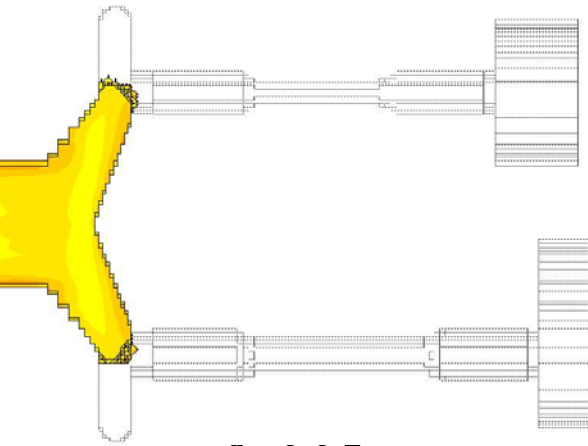


0.855 sec

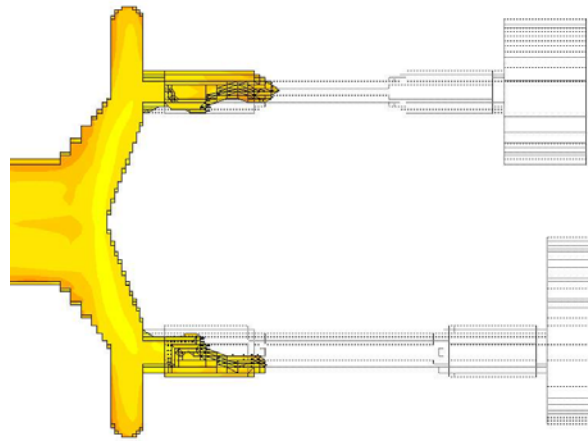


0.905 sec

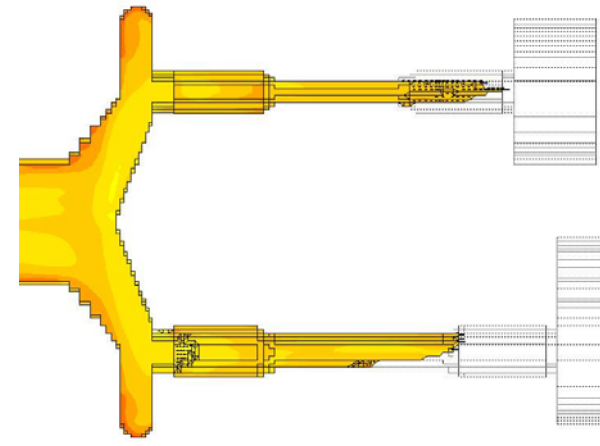
Figure 5.13: Flow Pattern in SC Test Bar (CMI design)
(Design 2, Gate Velocity = 46 in/sec)



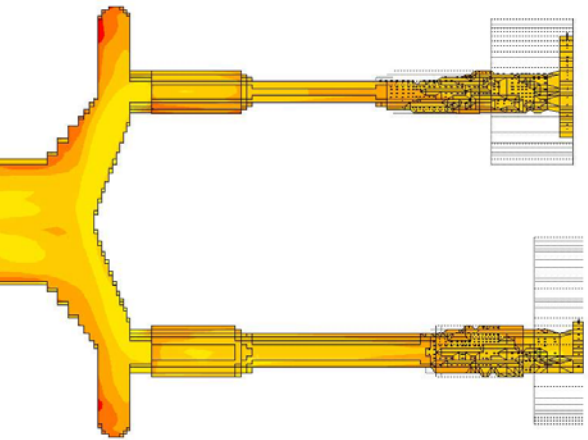
0.665 sec



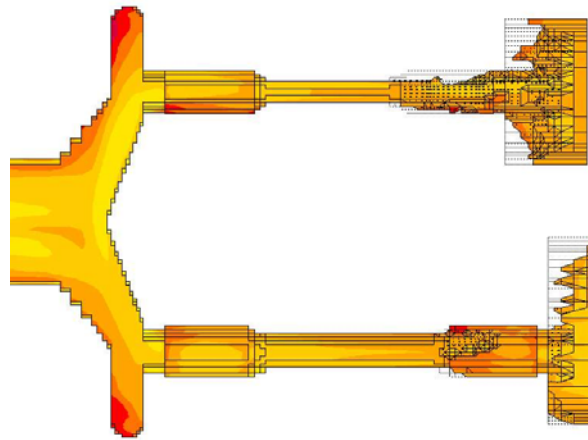
0.712 sec



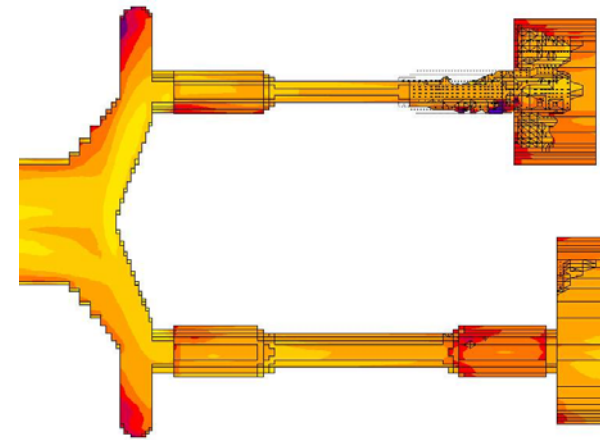
0.760 sec



0.808 sec

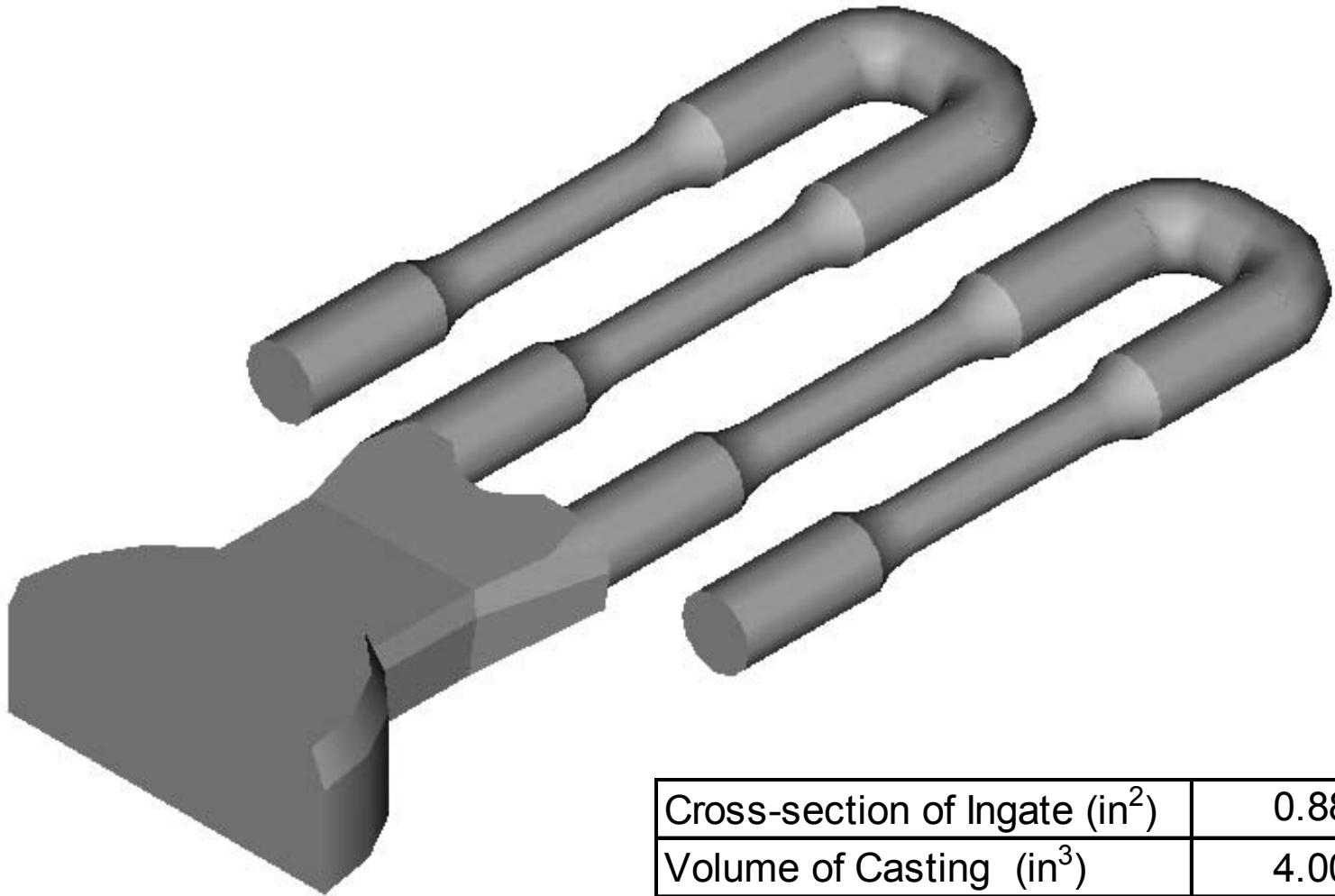


0.855 sec



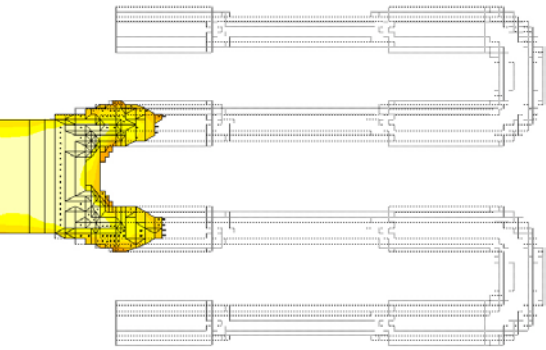
0.905 sec

Figure 5.14: U Test Bar

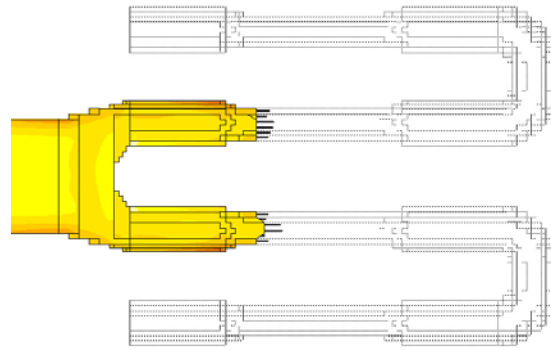


Cross-section of Ingate (in ²)	0.88
Volume of Casting (in ³)	4.00
Volume of the Overflow (in ³)	6.02

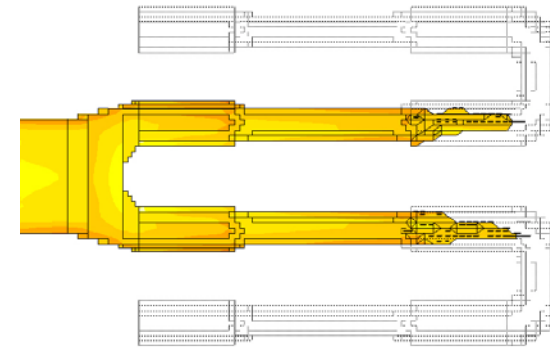
Figure 5.16: Flow Pattern in SC U Test Bar
(Gate Velocity = 20 in/sec)



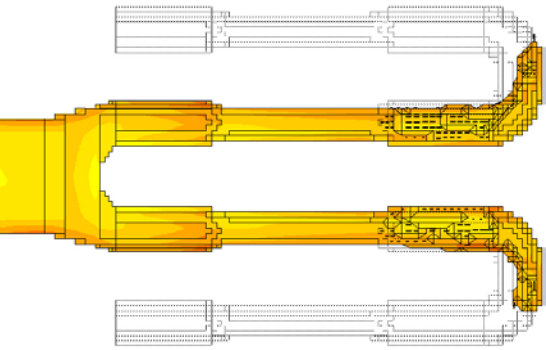
0.50 sec



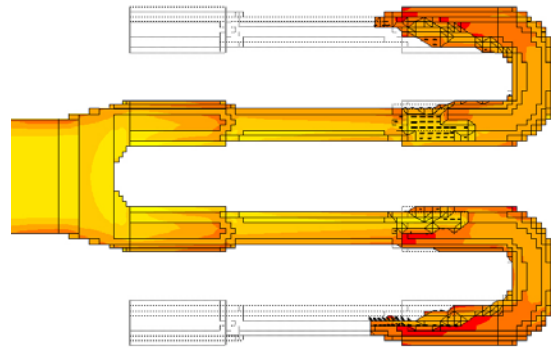
0.65 sec



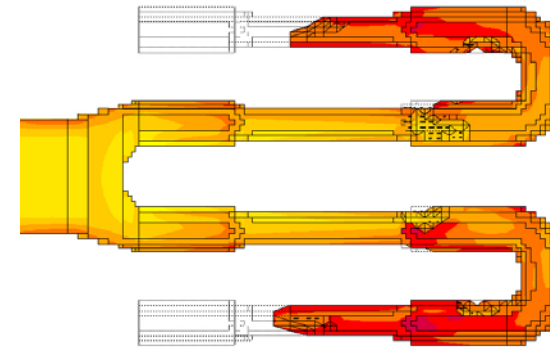
0.70 sec



0.75 sec



0.80 sec



0.90 sec

Figure 5.17: UTS of Squeeze Cast U bar & Permanent Mold Test Bar A356 CWRU12010

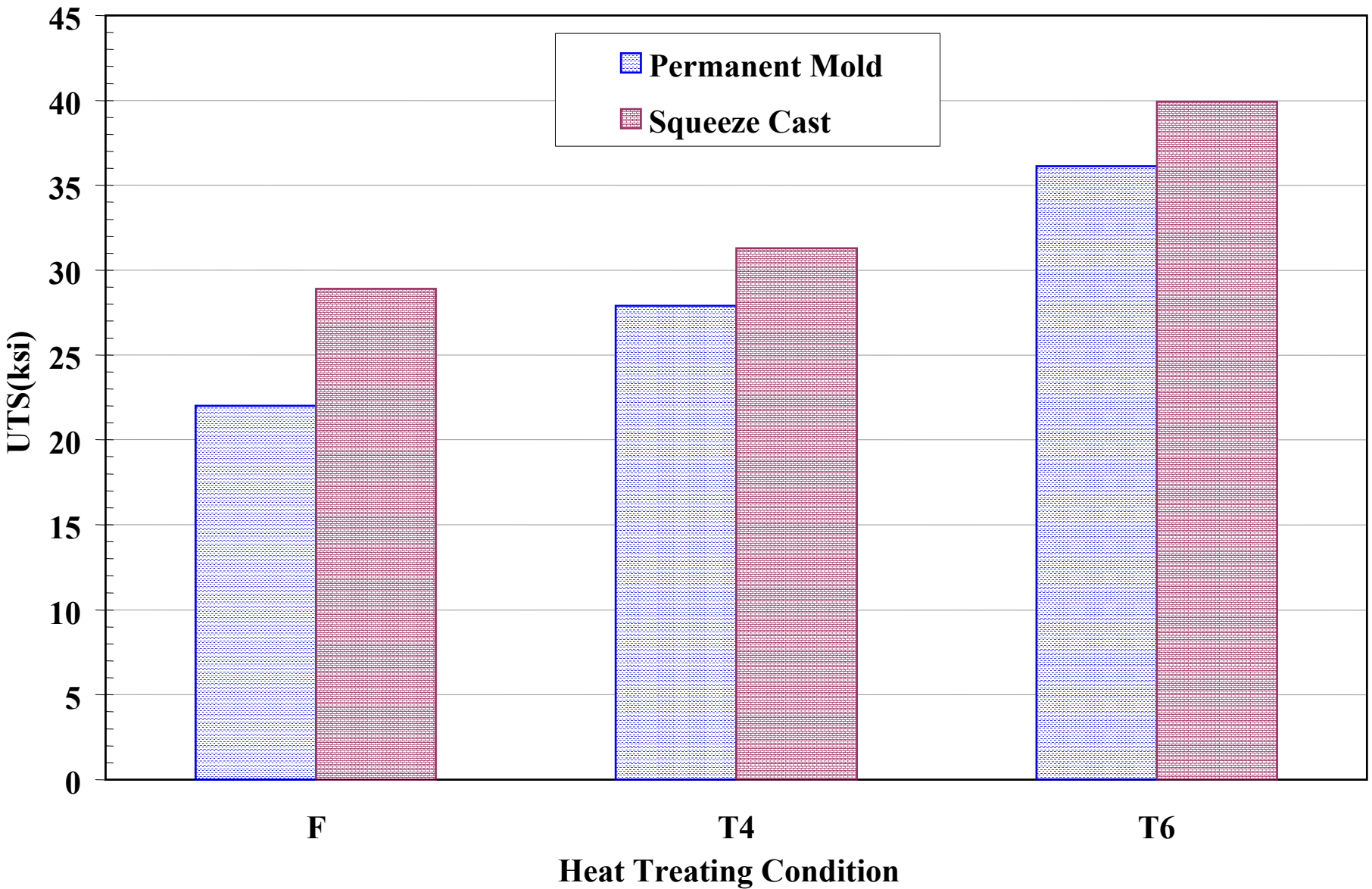


**Figure 5.18: Elongation of Squeeze Cast U bar & Permanent Mold
Test Bar A356 CWRU12010**

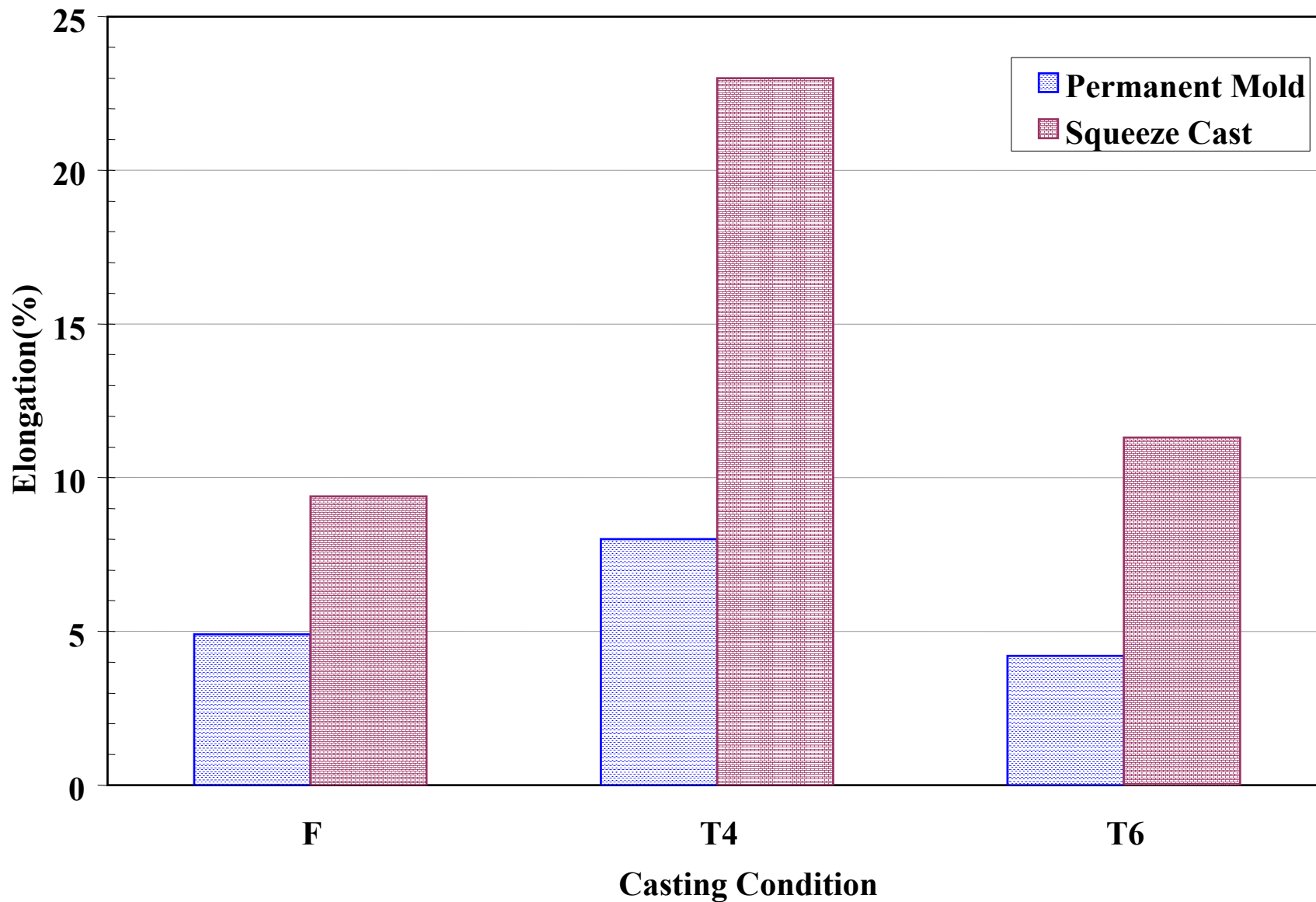


Figure 5.19: UTS and Elongation of SC A356 of U Bars-As Cast

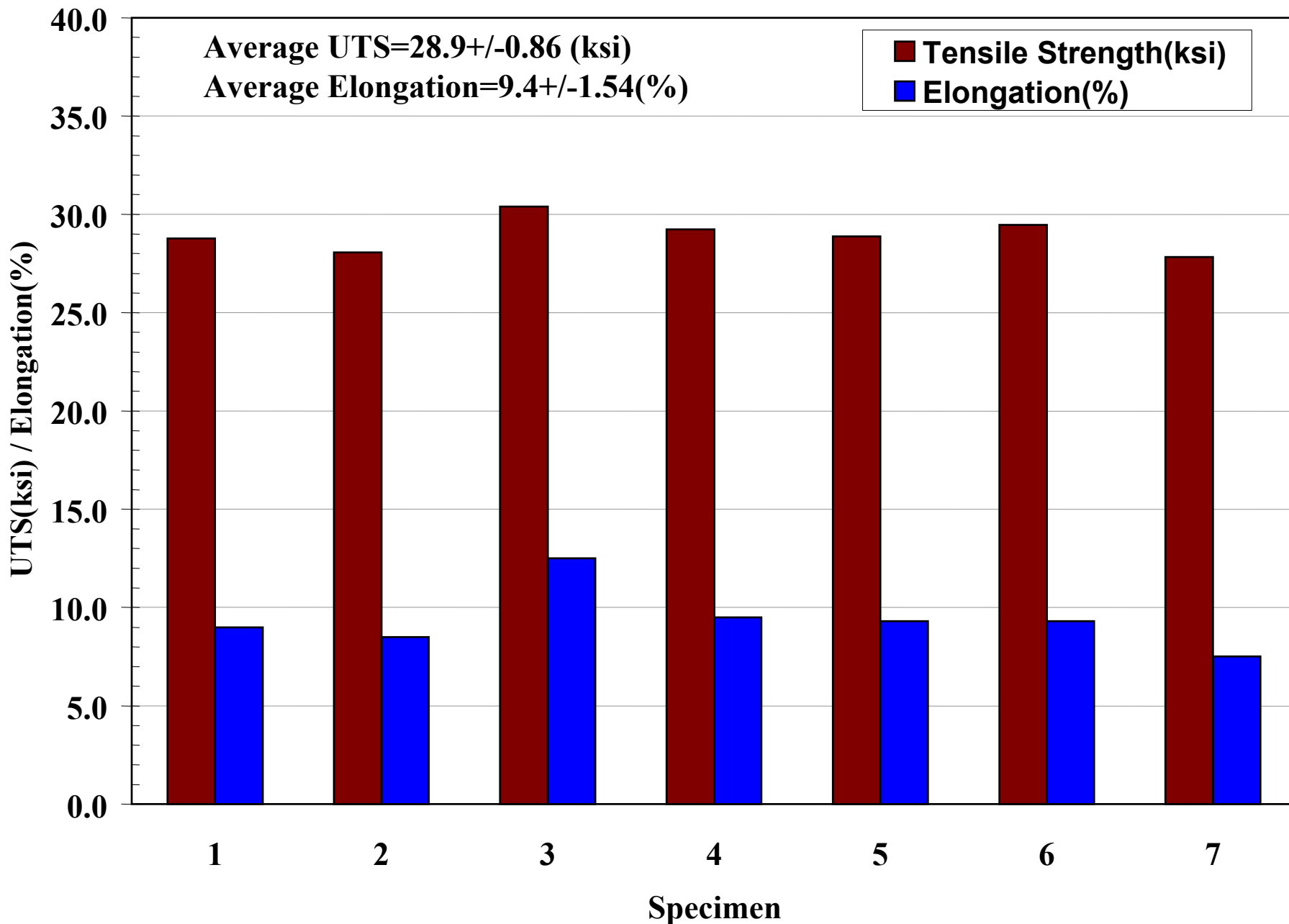


Figure 5.20: UTS and Elongation of SC A356 of U Bars-T6

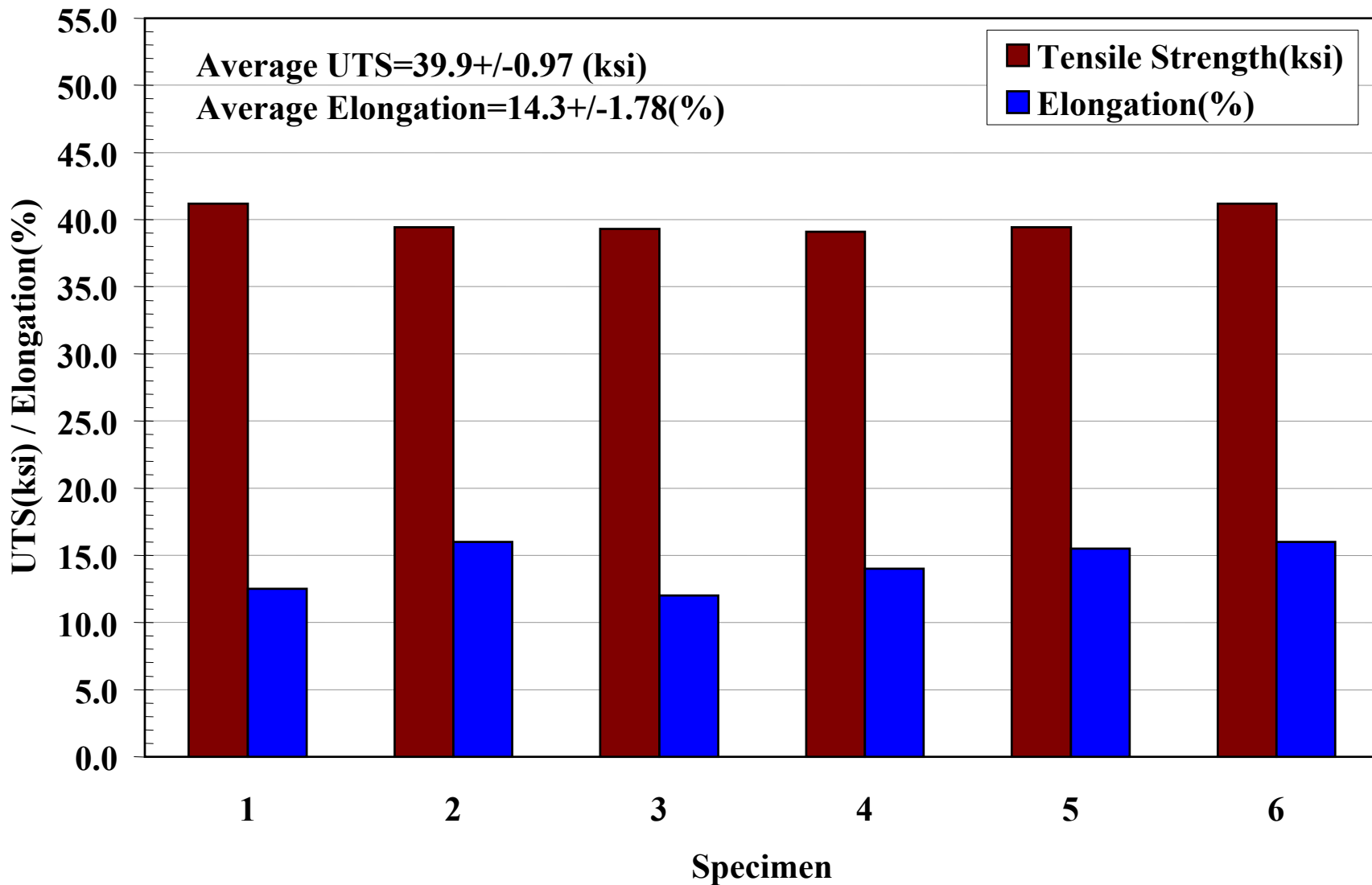
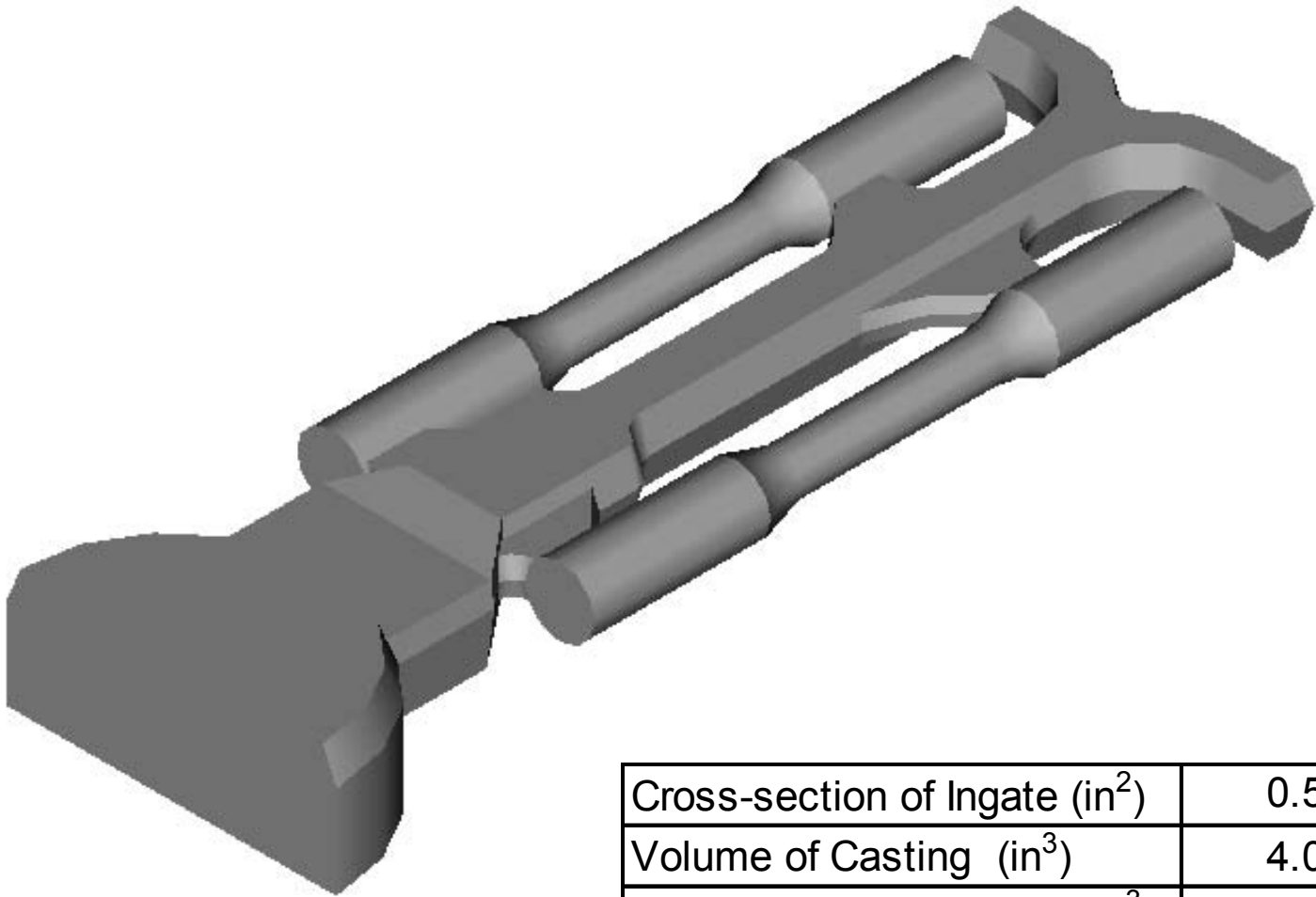
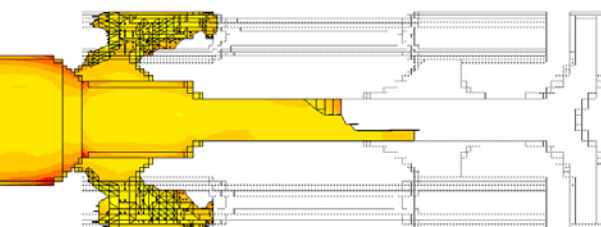


Figure 5.22: Two-gate Test Bar

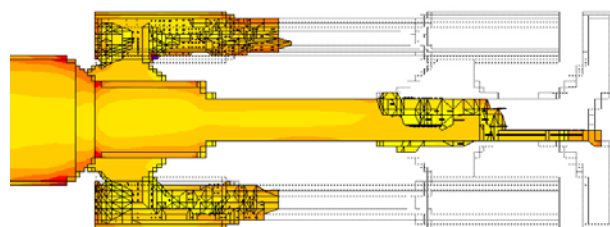


Cross-section of Ingate (in ²)	0.54
Volume of Casting (in ³)	4.00
Volume of the Overflow (in ³)	0.70

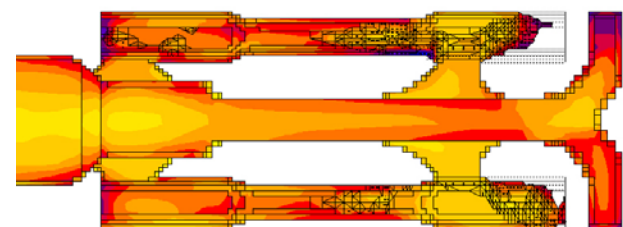
Figure 5.23: Flow Pattern in SC Two-gate Test Bar
(Gate Velocity = 50 in/sec)



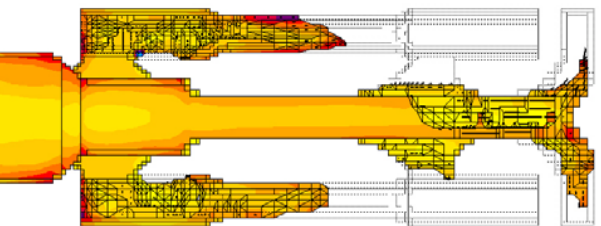
0.665 sec



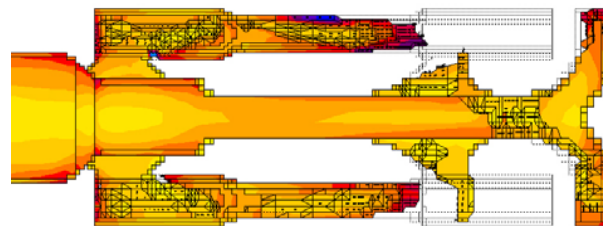
0.712 sec



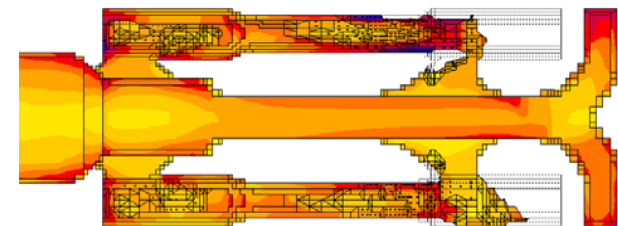
0.760 sec



0.808 sec



0.855 sec



0.905 sec

Figure 5.24: UTS & Elongation of SC A356 of Two Bars-As Cast

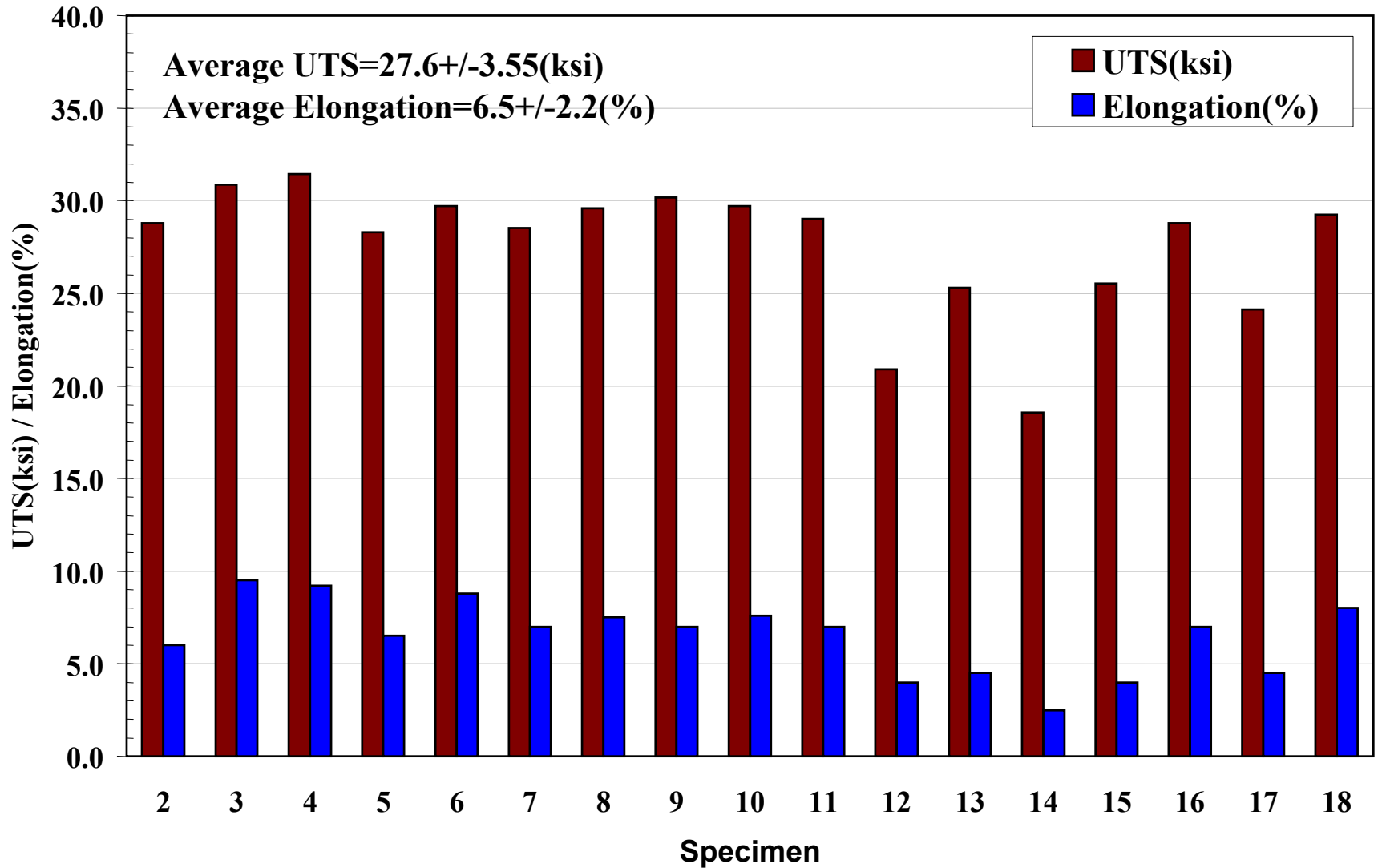


Figure 5.25: UTS & Elongation of SC A356 of Two Gates-T6

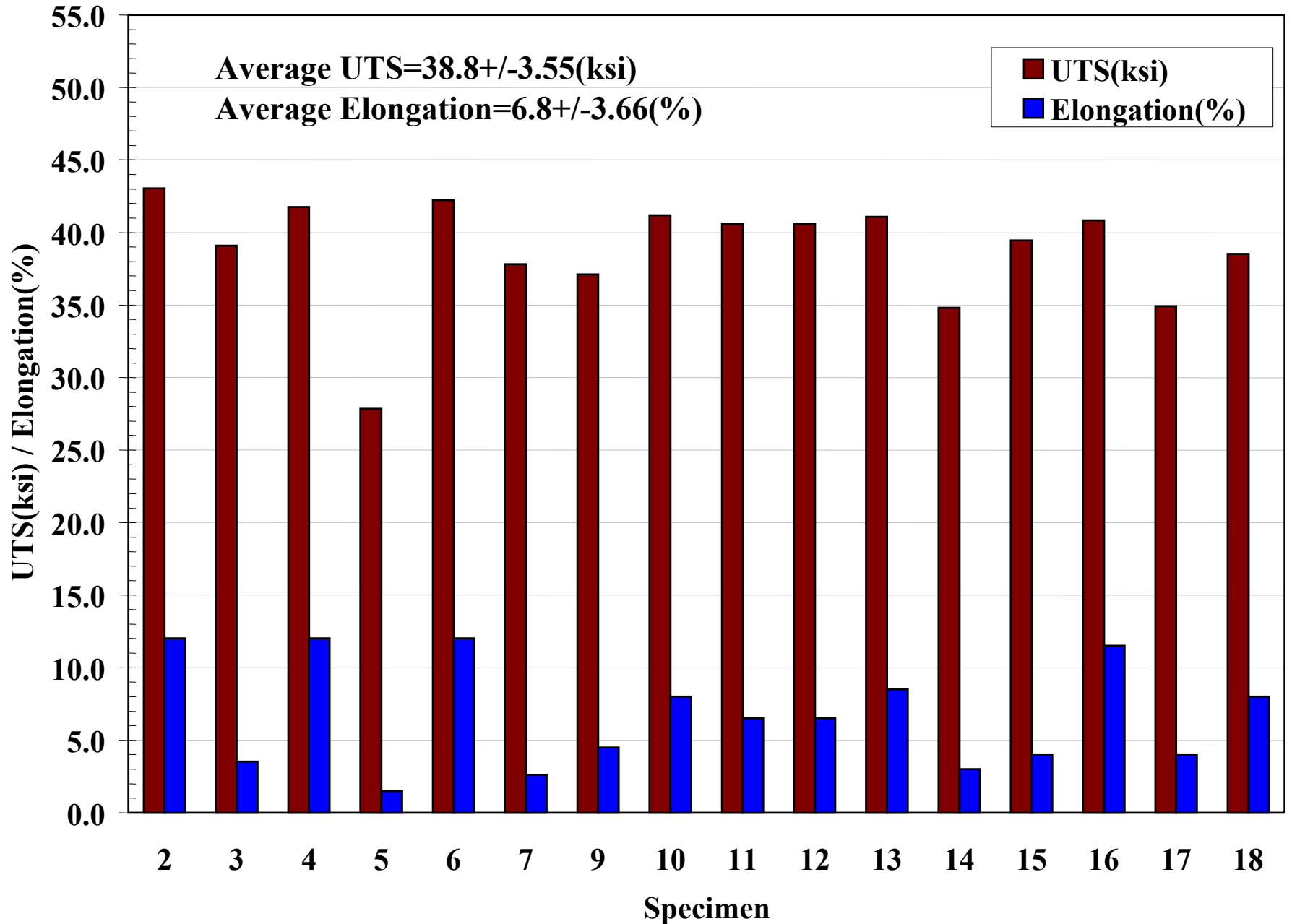


Figure 5.26: Average UTS & Elongation of A356 SC & PM Castings-T6

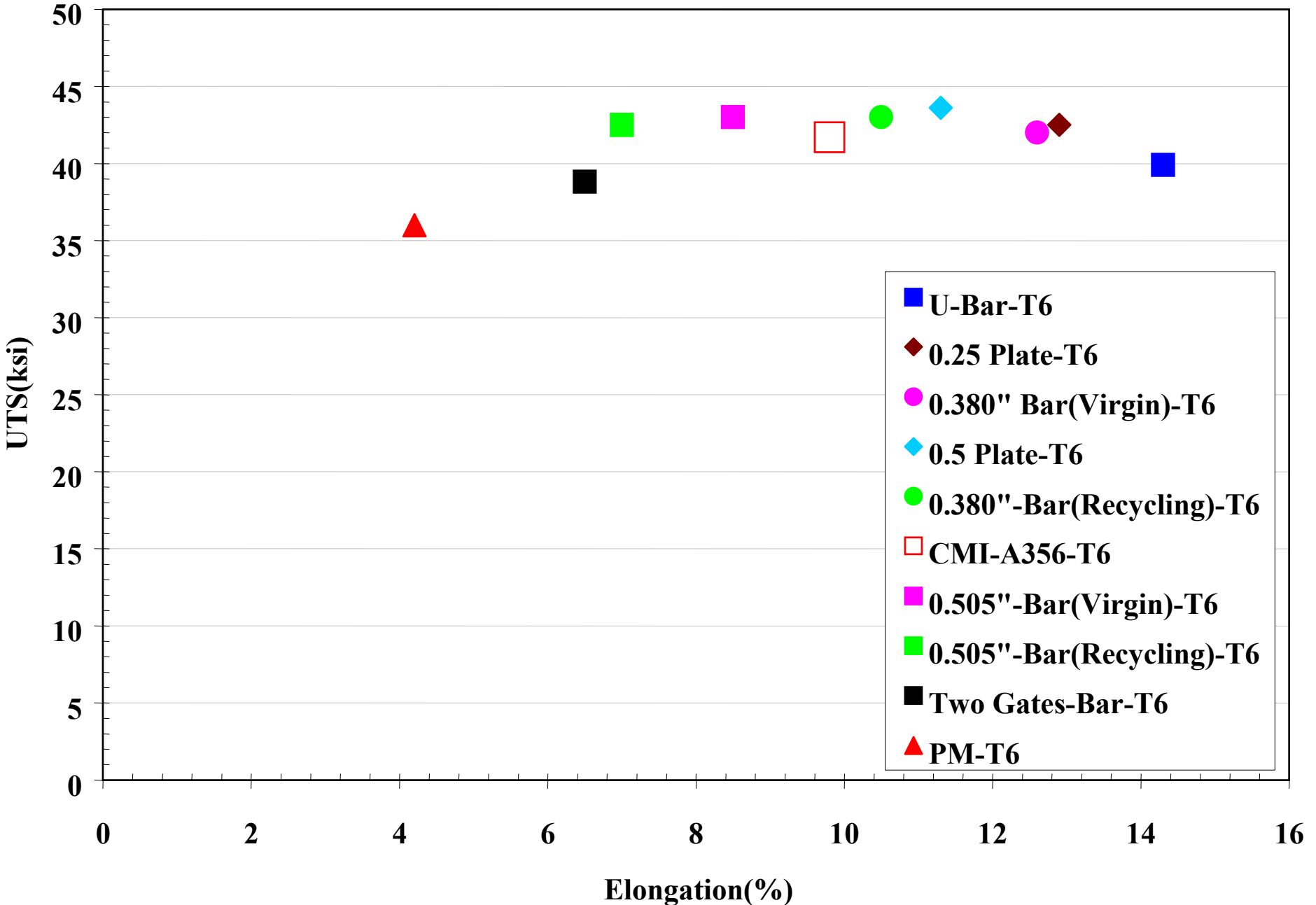


Figure 5.28: PLATE DESIGNS

- 1. 0.25” thick plate with fanned gate.**
- 2. 0.5” thick plate with straight gate.**
- 3. 0.5” thick plate with fanned gate.**
- 4. 1.00” plate with thin gate.**
- 5. 1.00” plate with thick gate (currently being fabricated).**

Figure 5.29: 0.25 " Plate with Fan Gate

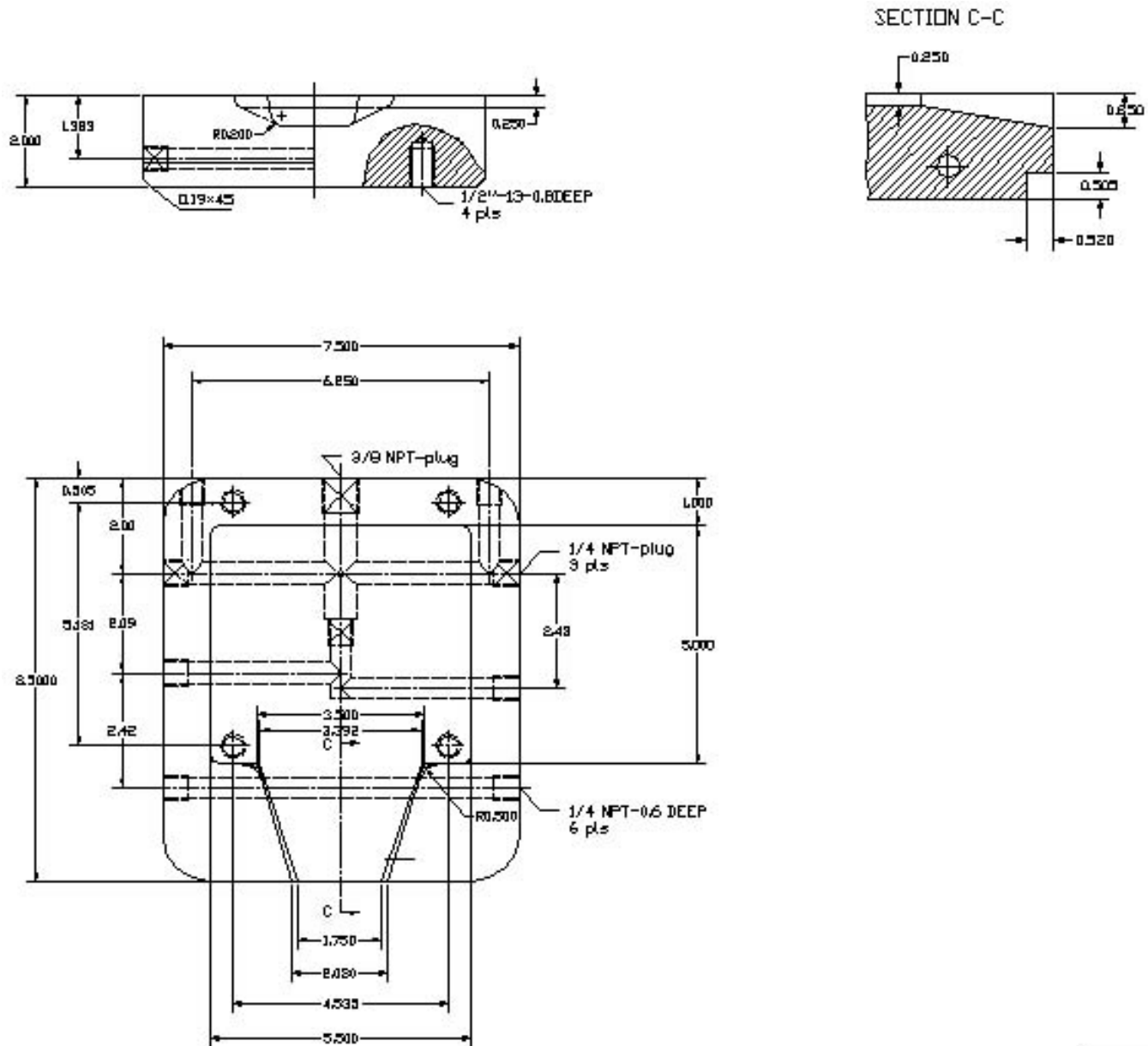
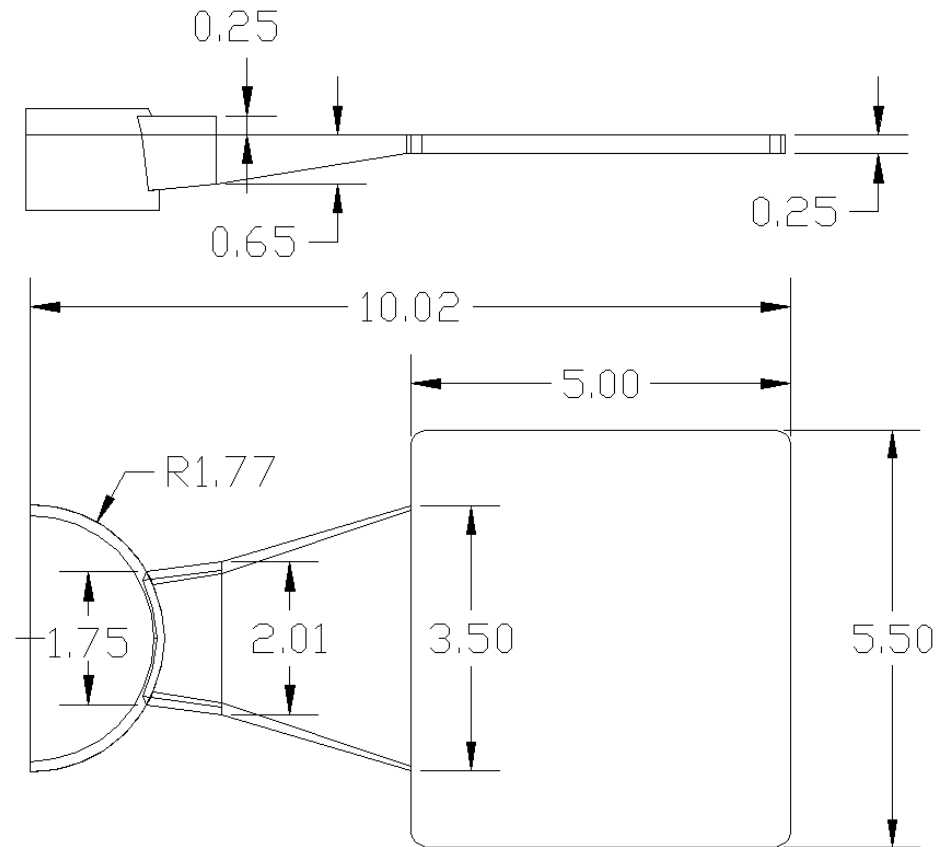
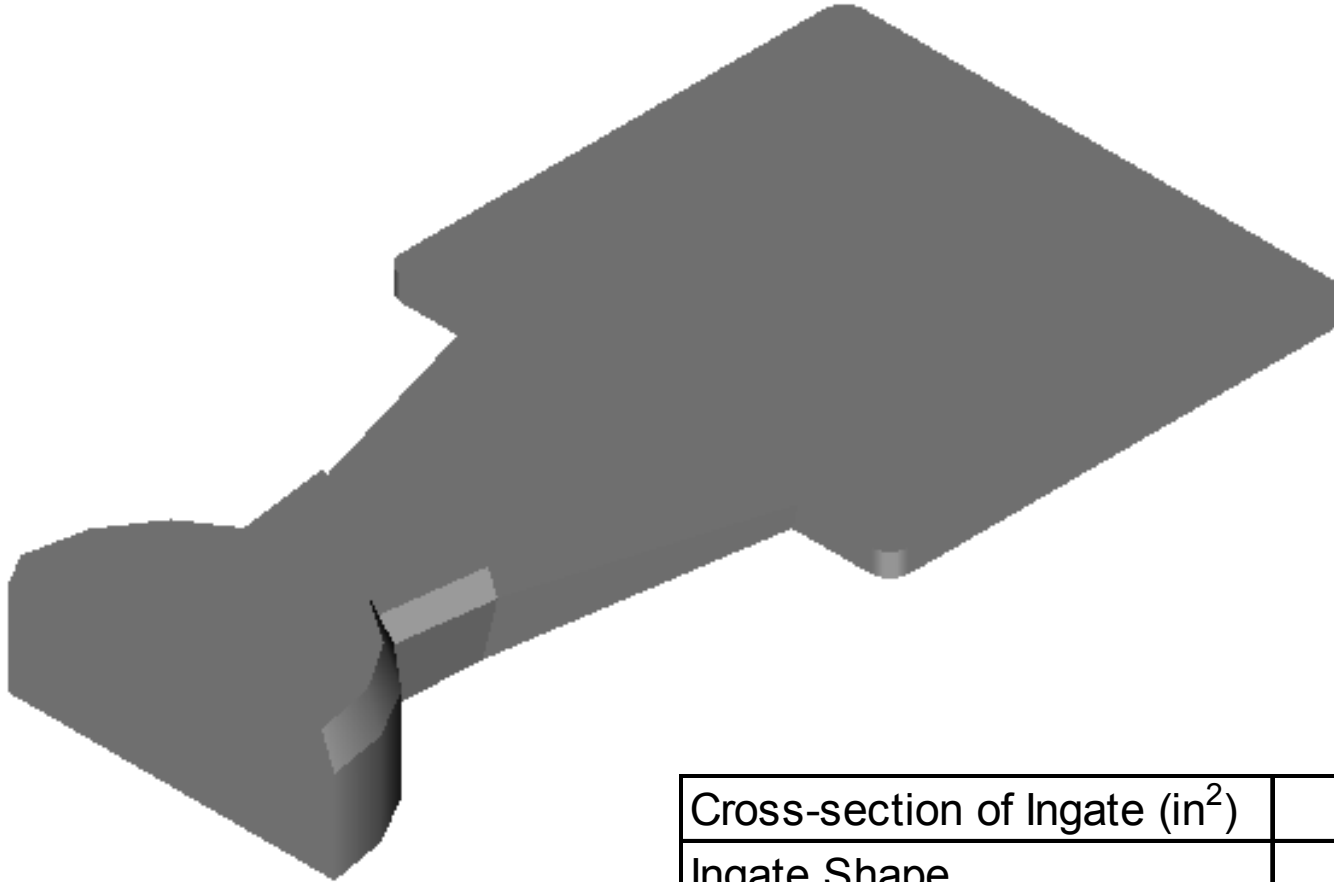


Figure 5.30: Dimensions of SC Plates



0.25" Plate

Figure 5.31: 0.25 " Plate with Fan Gate

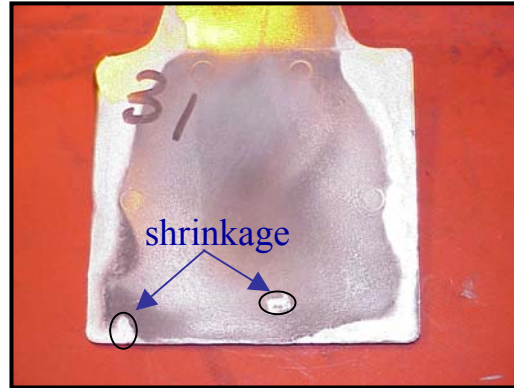


Cross-section of Ingate (in ²)	0.88
Ingate Shape	fanned
Volume of Casting (in ³)	6.87

Figure 5.32: Visual Rating of 0.25" SC Plate



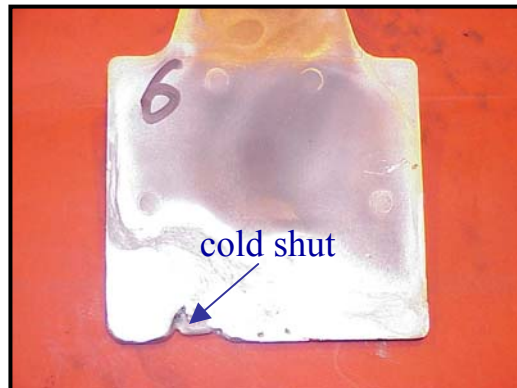
Rating = 6
Sound casting



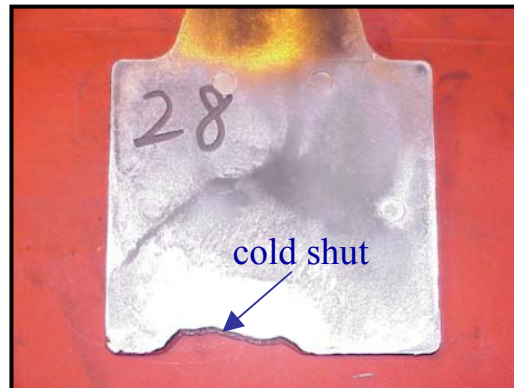
Rating = 5
Little shrinkage



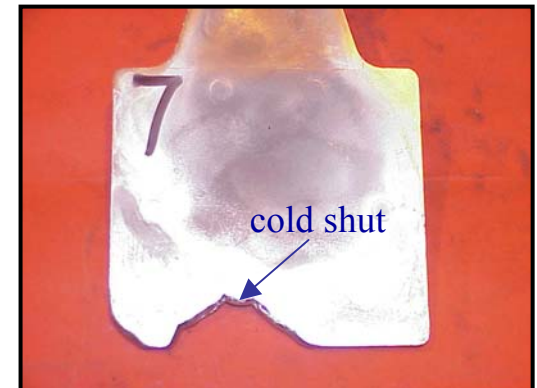
Rating = 4
Significant shrinkage



Rating = 3
Some cold shuts



Rating = 2
Significant cold shuts



Rating = 1
Partial filling

Figure 5.33: Visual Rating vs. Ingate Velocity
 (0.25 " plate with fan gate, Al356, with oil heater)

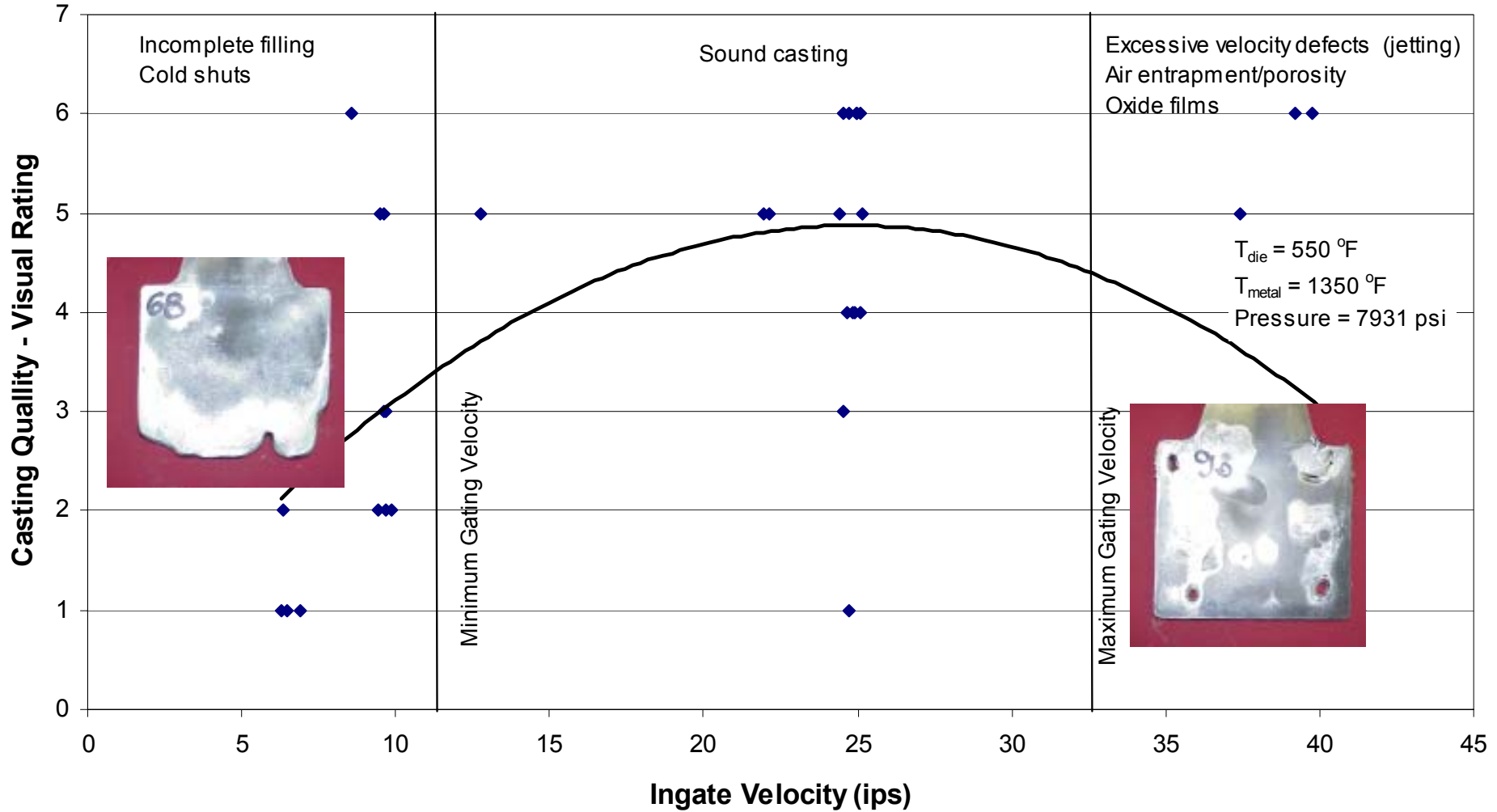


Figure 5.34: UTS and Elongation of SC A356 of 0.25" Plates-As Cast

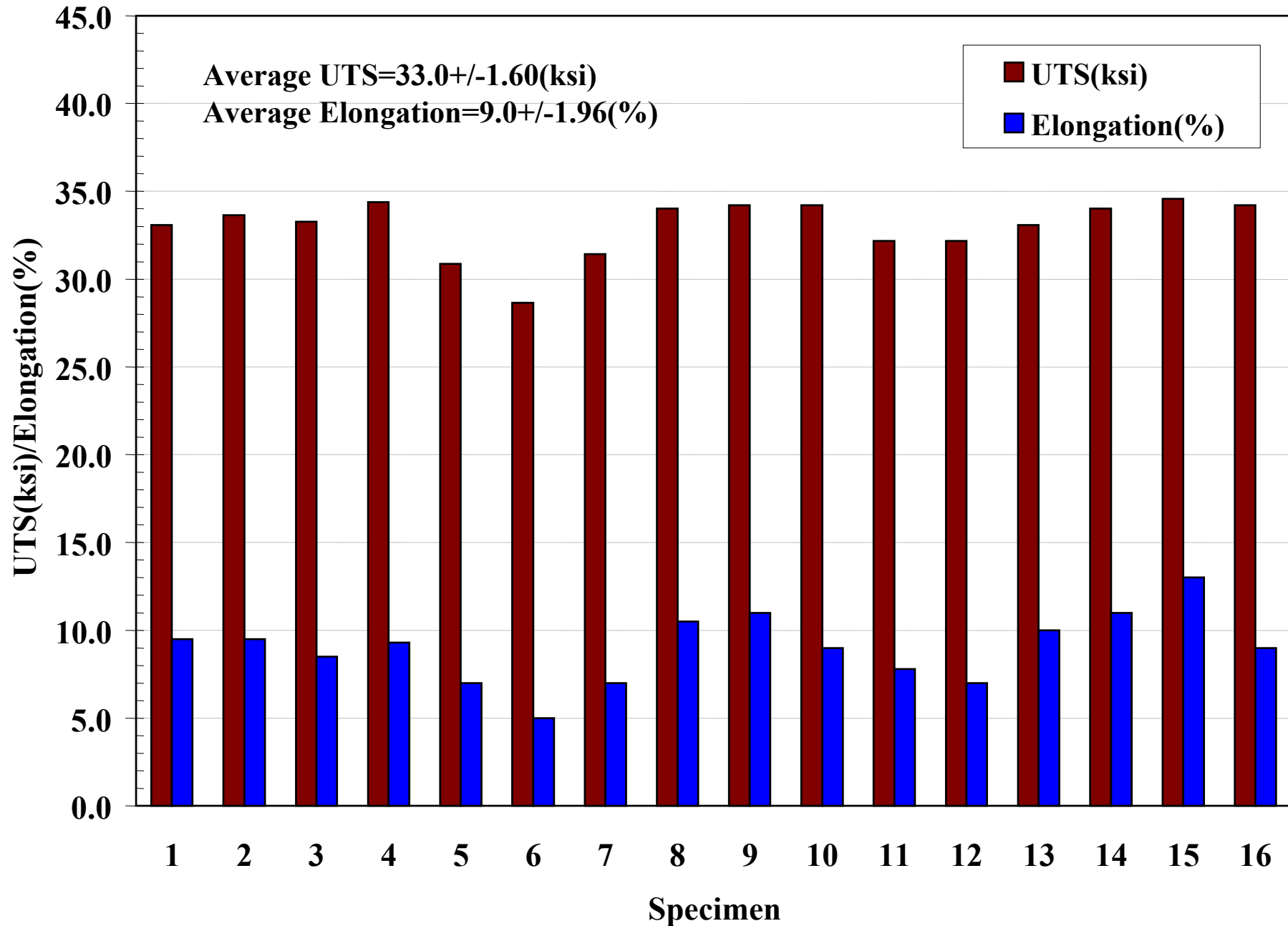


Figure 5.35: UTS and Elongation of SC A356 of 0.25" Plates-T6

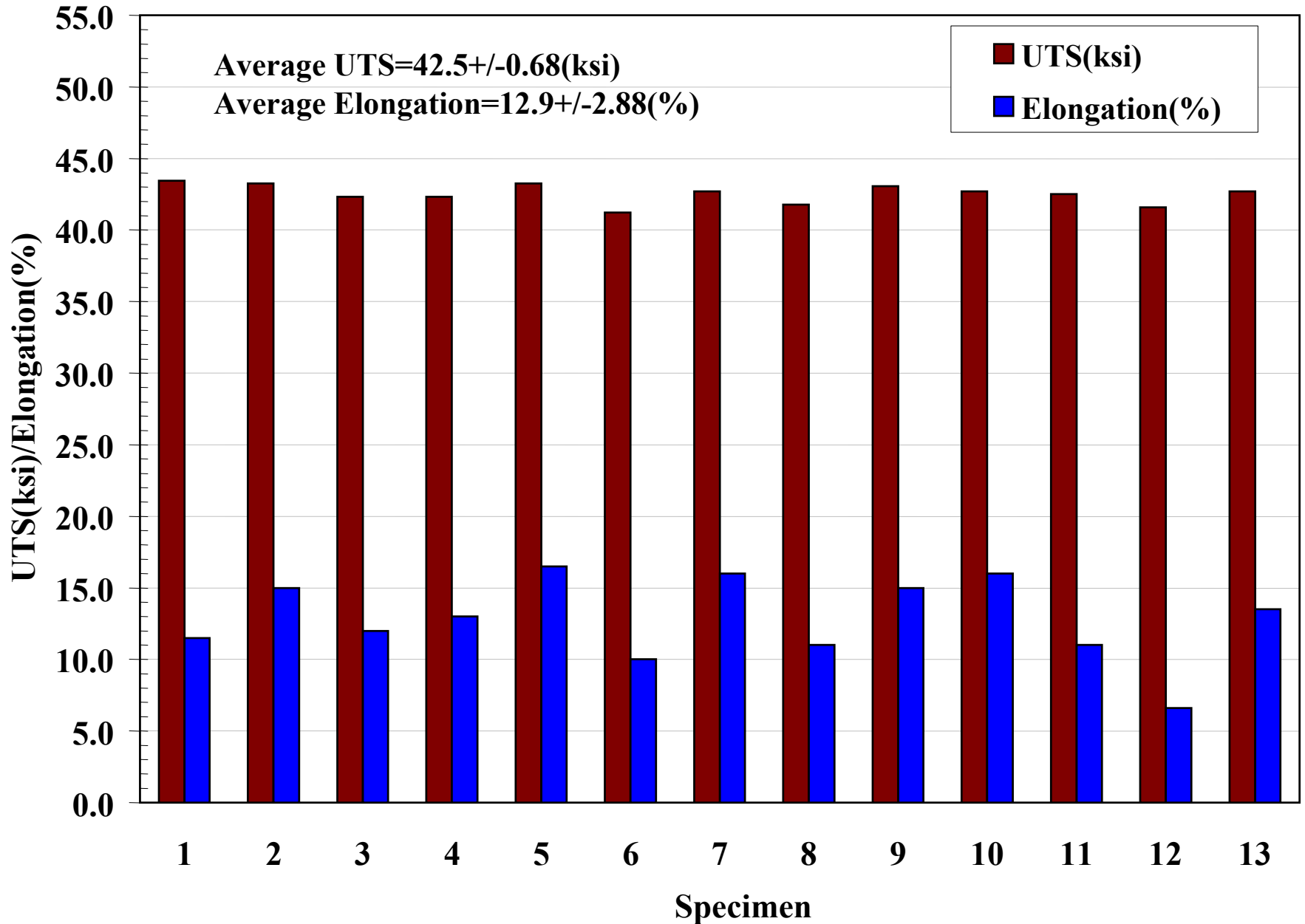
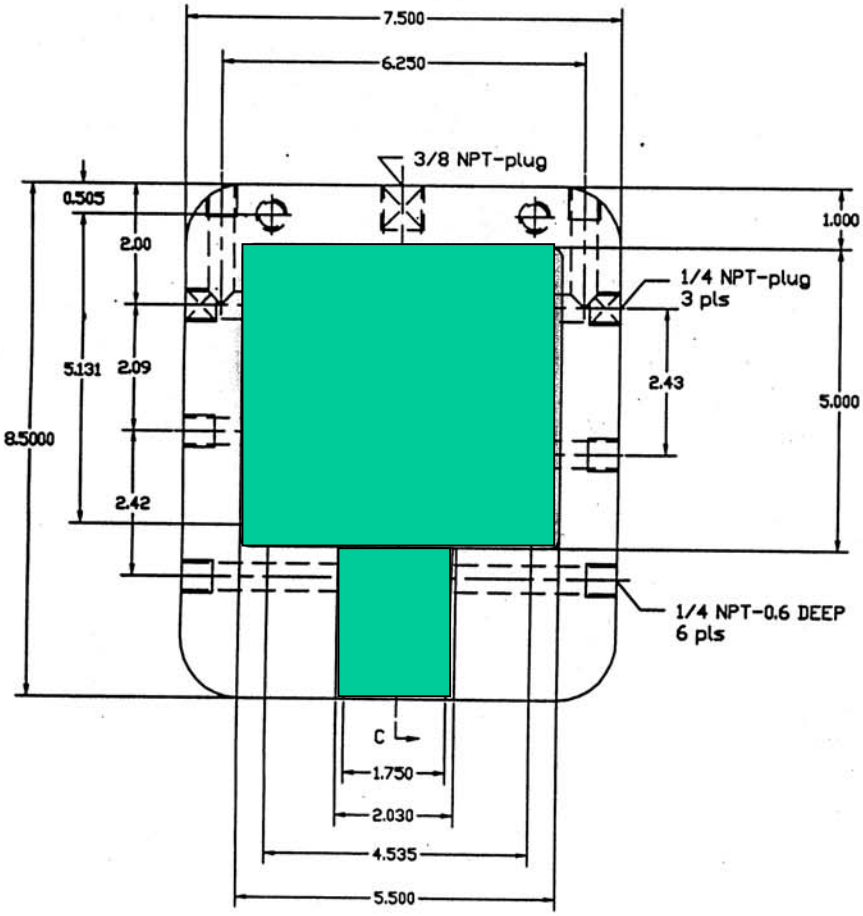


Figure 5.36: 0.5" Plate Insert (straight gate design)



SECTION C-C

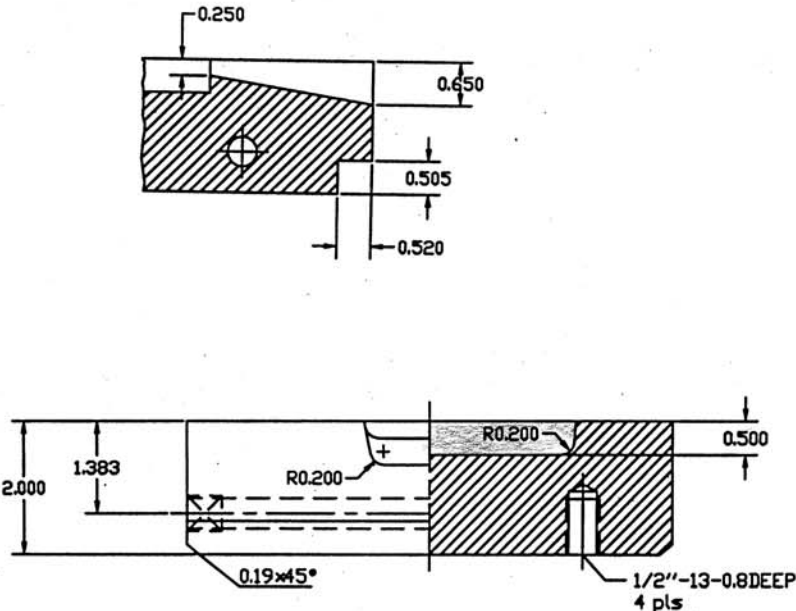
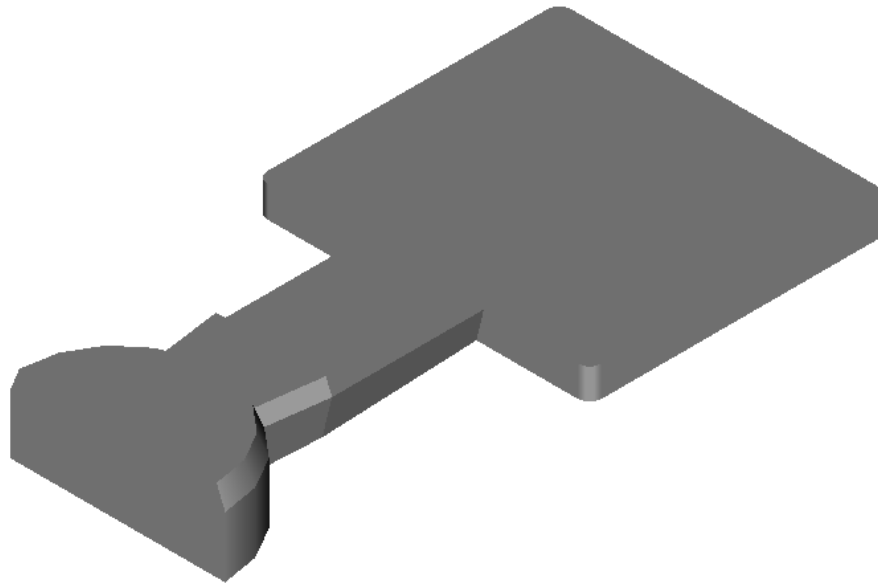
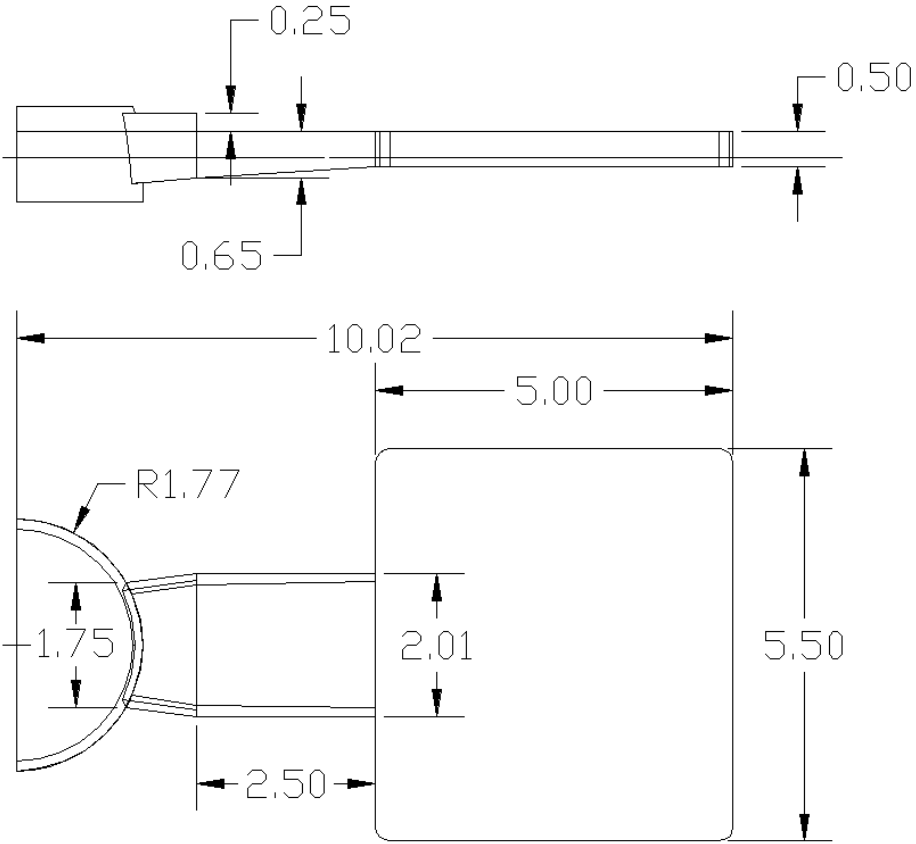


Figure 5.37: 0.5”Plate Insert (Straight Gate)



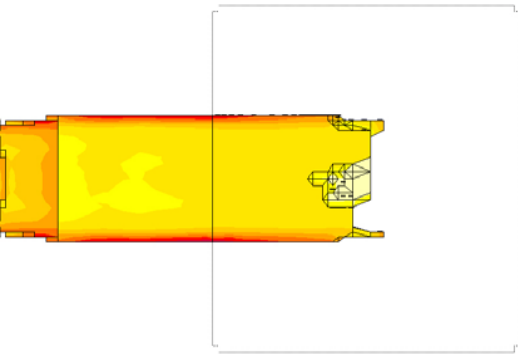
Cross-section of Ingate (in ²)	0.85
Ingate Shape	streight
Volume of Casting (in ³)	13.73

Figure 5.37: Dimensions of SC Plates

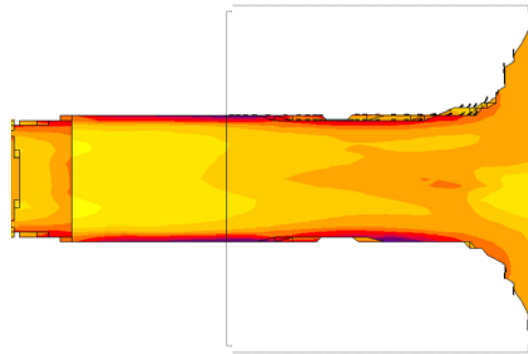


0.5 " Plate

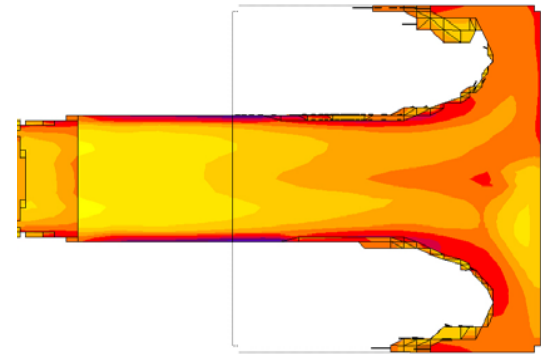
Figure 5.38 Flow Pattern in 0.5" SC Straight Fan Gate Plate
(Gate Velocity = 28 in/sec)



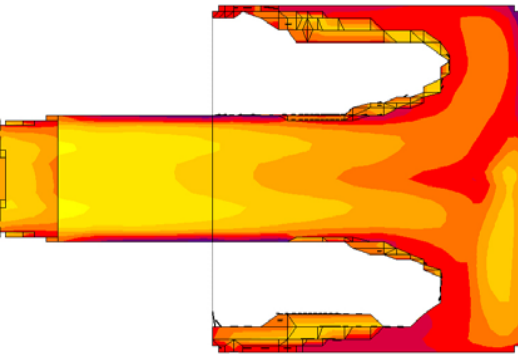
0.163 sec



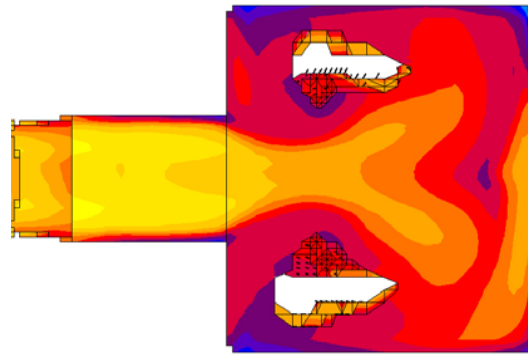
0.188 sec



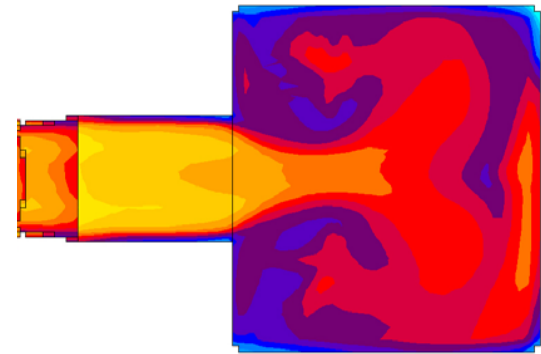
0.200 sec



0.212 sec

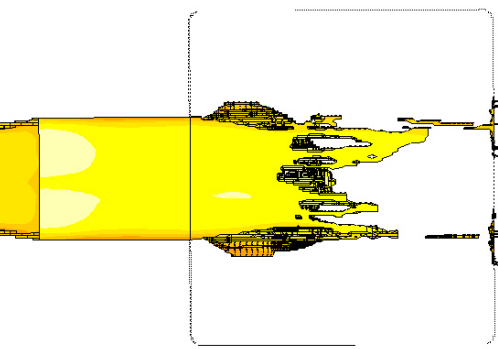


0.238 sec

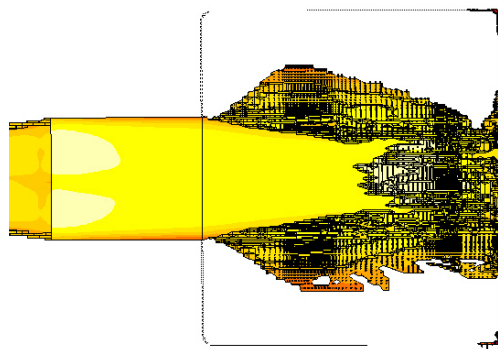


0.250 sec

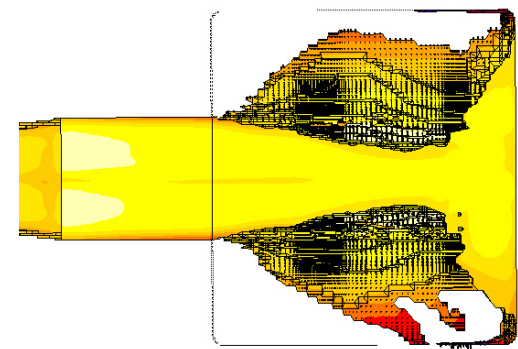
Figure 5.39 Flow Pattern in 0.5" SC Straight Gate Plate
(Gate Velocity = 7 in/sec)



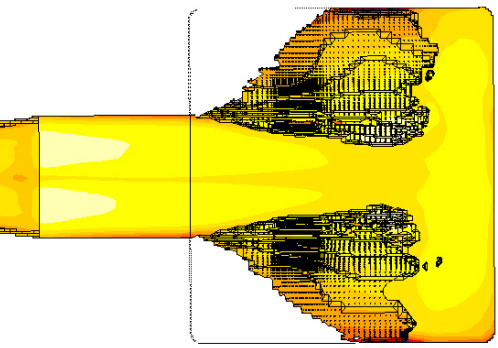
0.65 sec



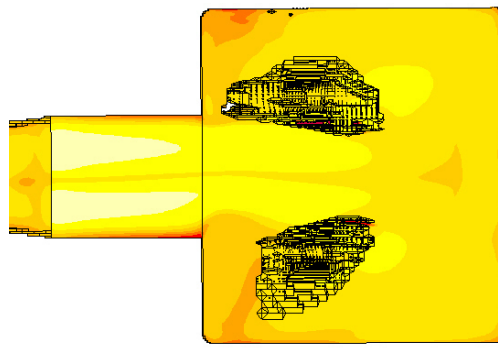
0.70 sec



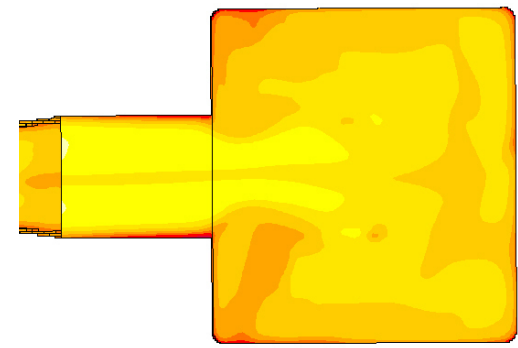
0.75 sec



0.80 sec

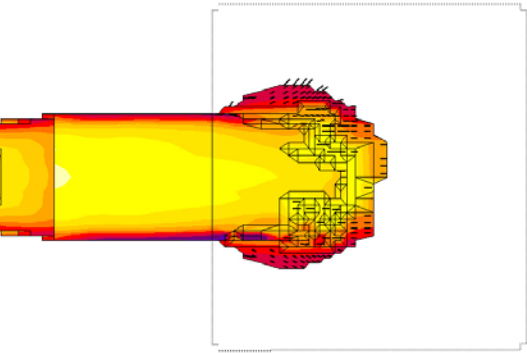


0.95 sec

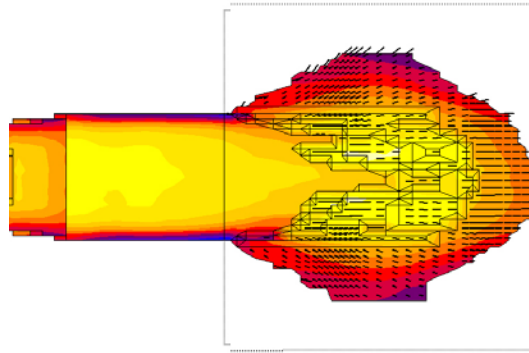


1.00 sec

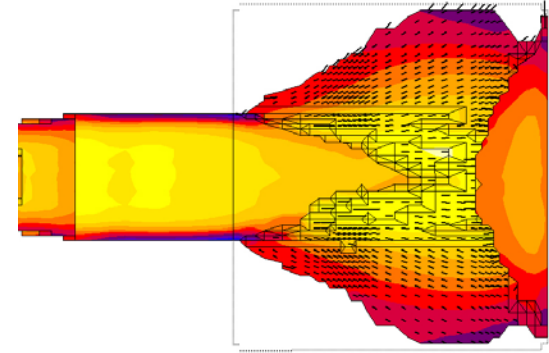
Figure 5.40: Flow Pattern in 0.5" SC Straight Gate Plate
(Gate Velocity = 5 in/sec)



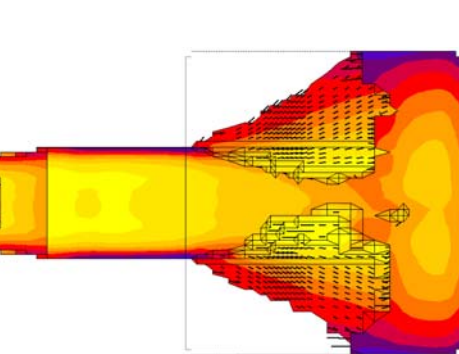
0.912 sec



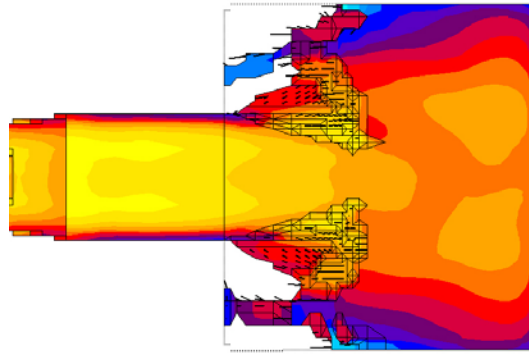
0.981 sec



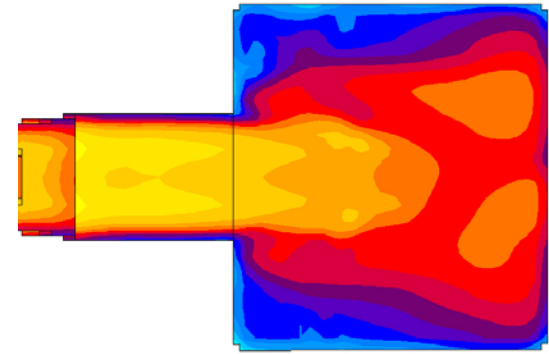
1.052 sec



1.121 sec

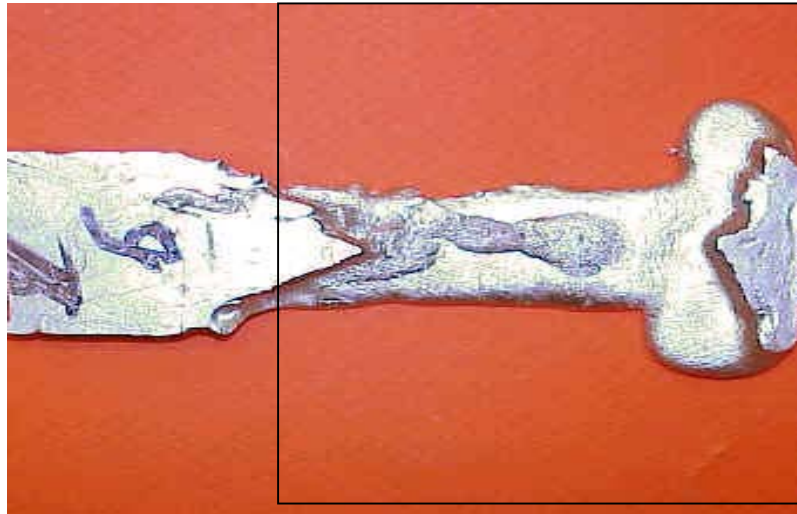


1.260 sec

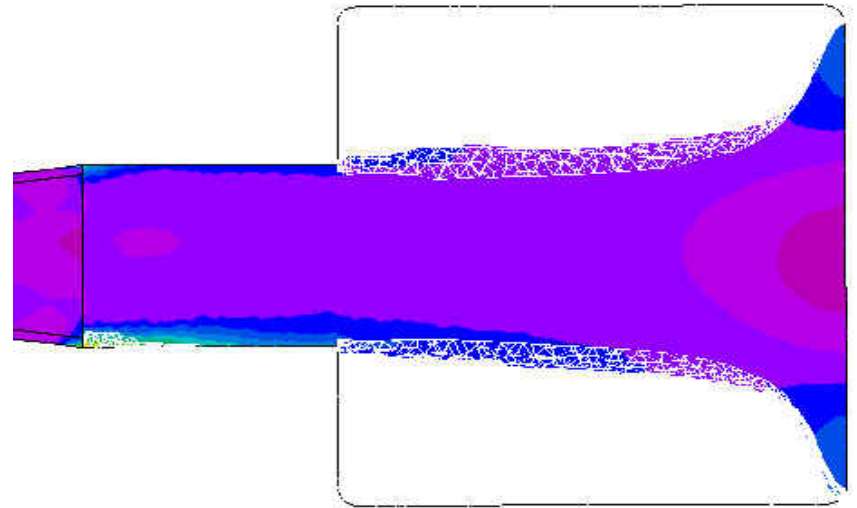


1.40 sec

Figure 5.41(a): Flow Pattern in 0.5" SC Plate
(Fast Gate Velocity = 50 in/sec)



Experimental



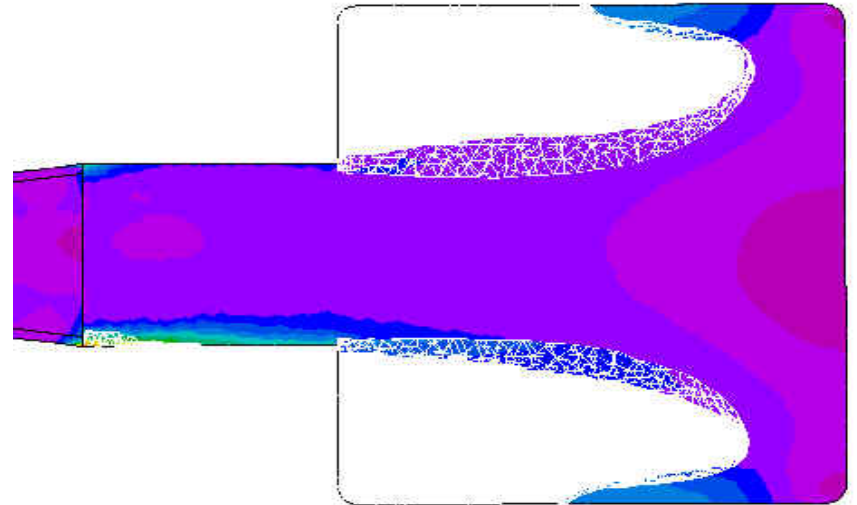
Computer Simulation

Filling Time : 0.2 sec

Figure 5.41(b): Flow Pattern in 0.5" SC Plate
(Fast Gate Velocity = 50 in/sec)



Experimental



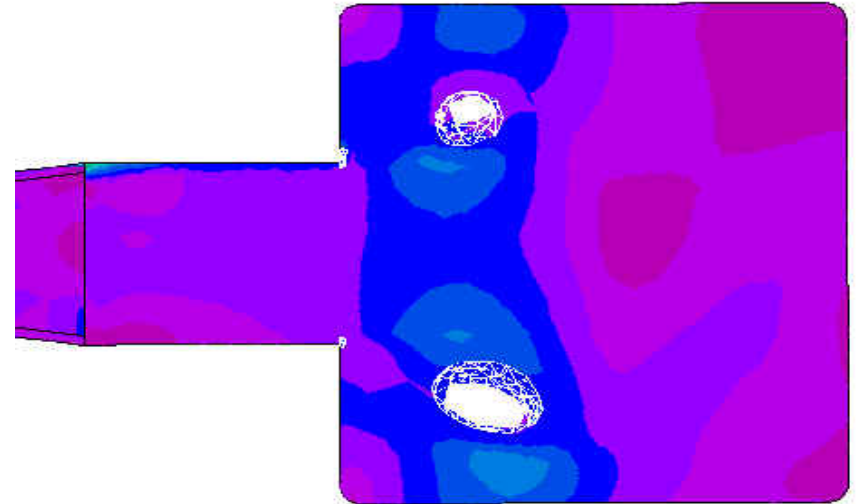
Computer Simulation

Filling Time : 0.5 sec

Figure 5.41(c): Flow Pattern in 0.5" SC Plate
(Fast Gate Velocity = 50 in/sec)



Experimental



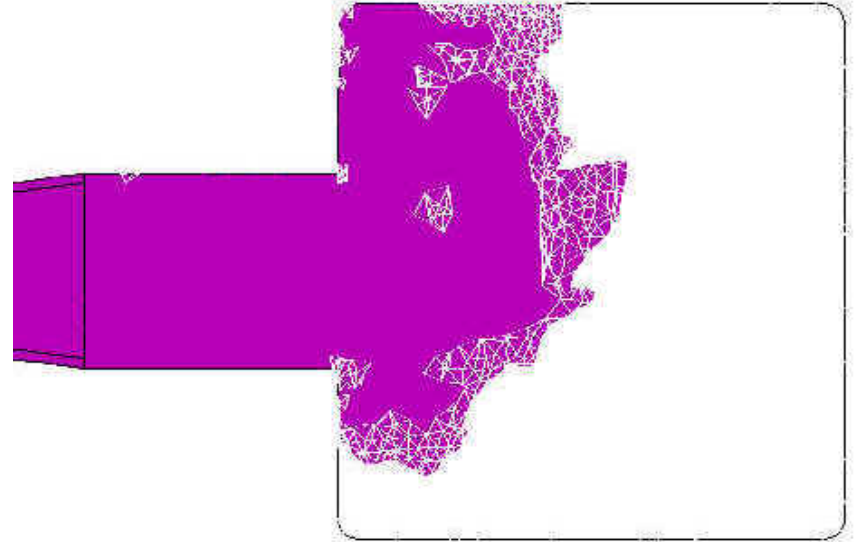
Computer Simulation

Filling Time : 1.4 sec

Figure 5.42(a): Flow Pattern in 0.5" Plate
(Slow Gate Velocity = 6.1 in/sec)



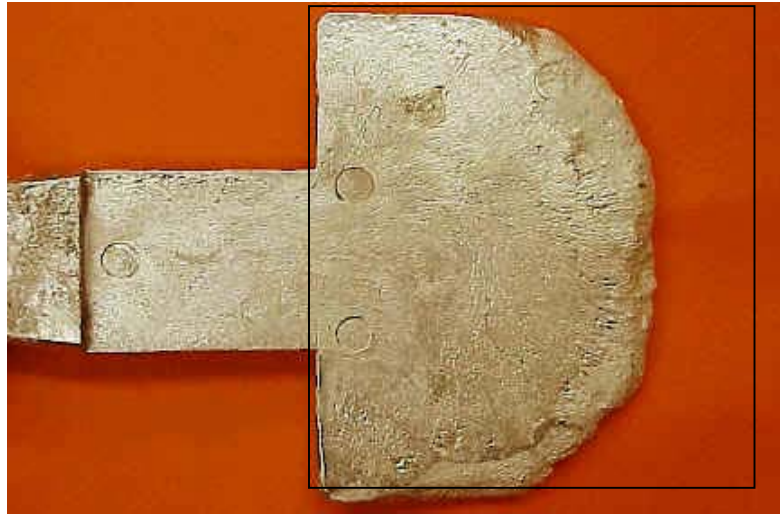
Experimental



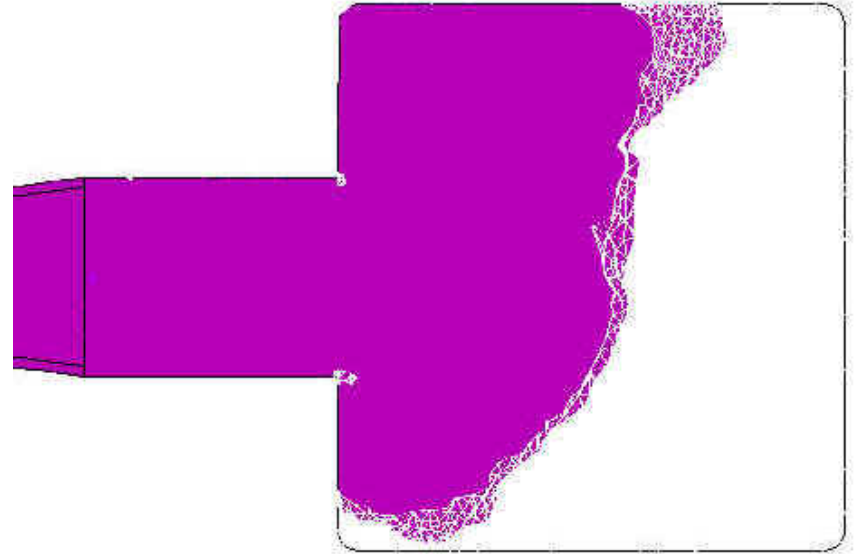
Computer Simulation

Filling Time : 2.1 sec

Figure 5.42(b): Flow Pattern in 0.5" Plate
(Slow Gate Velocity = 6.1 in/sec)



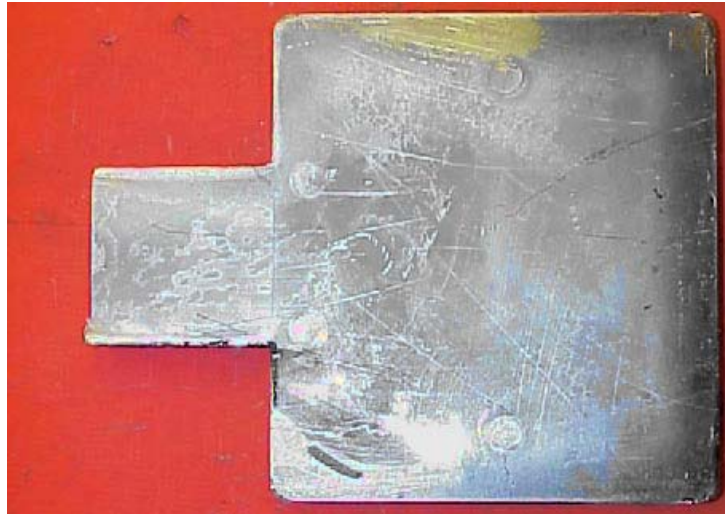
Experimental



Computer Simulation

Filling Time : 3.8 sec

Figure 5.42(c): Flow Pattern in 0.5" Plate
(Slow Gate Velocity = 6.1 in/sec)



Slow gate velocity
produce defect
free plates

Experimental

Filling Time : 4.3 sec

Figure 5.43: Visual Rating vs. Gate Velocity
 (0.5 " plate with Streight Ingate, Al356, with oil heater)

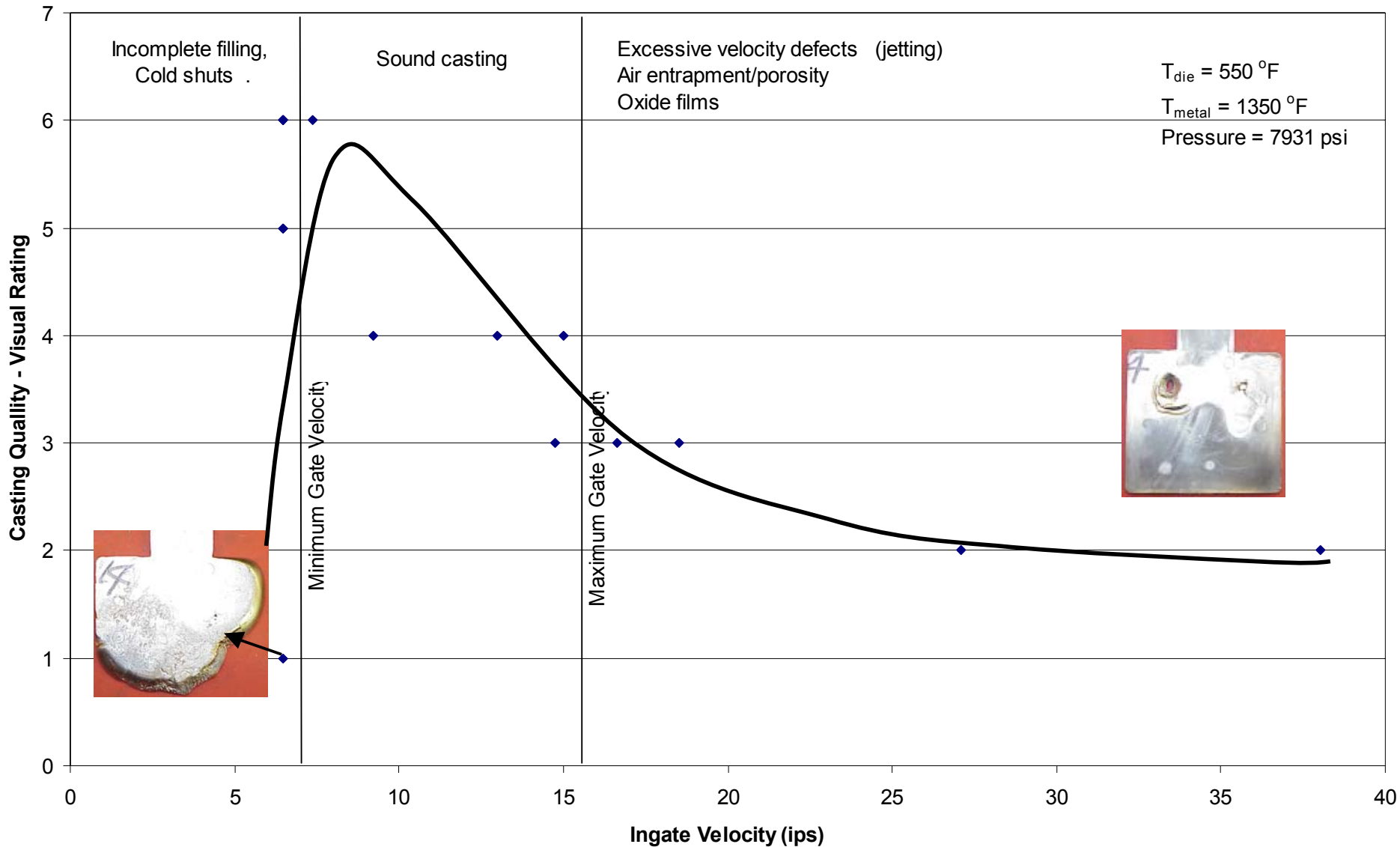
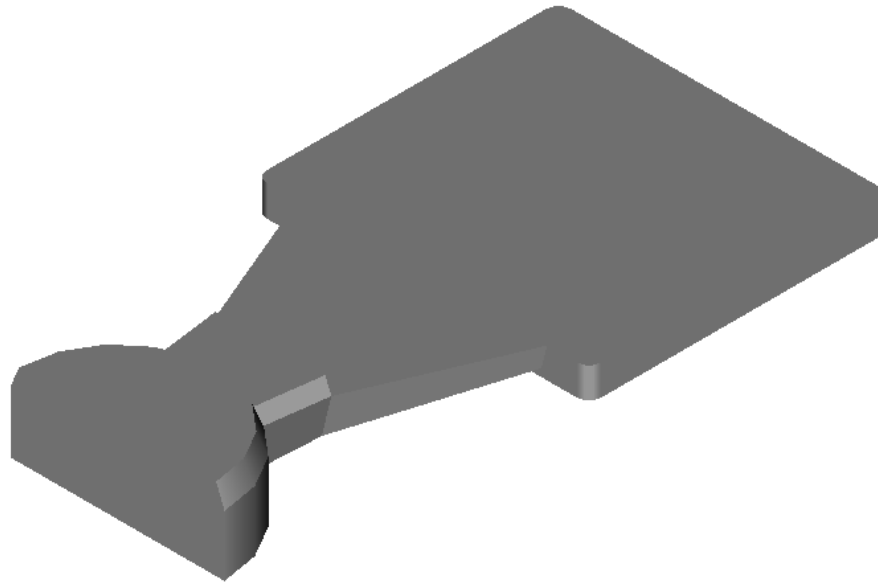
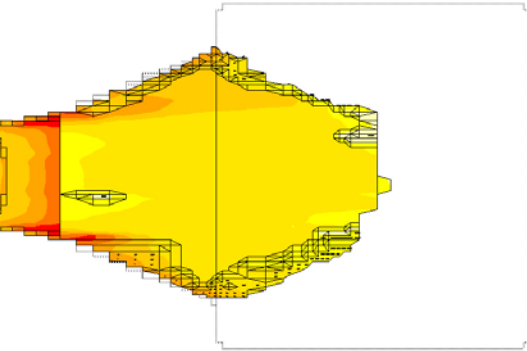


Figure 5.45: 0.5" Plate Insert (Fanned Gate)

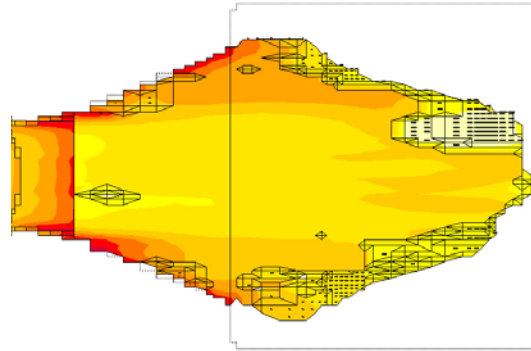


Cross-section of Ingate (in ²)	1.31
Ingate Shape	fanned
Volume of Casting (in ³)	13.73

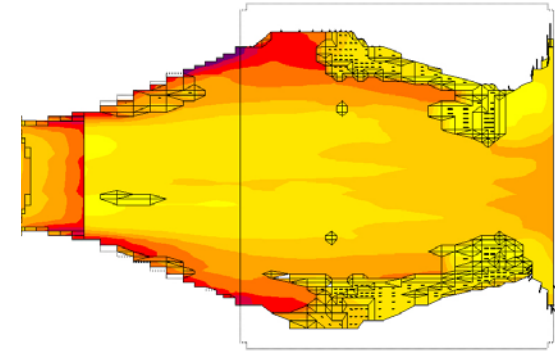
Figure 5.46: Flow Pattern in 0.5" SC Fan Gate Plate
(Gate Velocity = 28 in/sec)



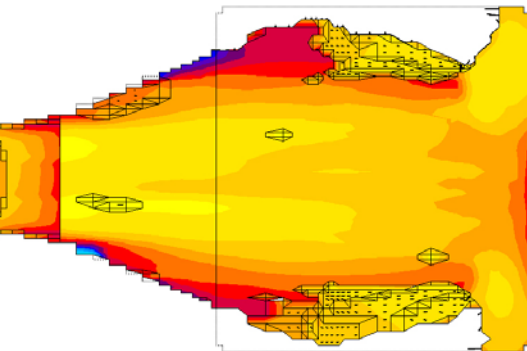
0.163 sec



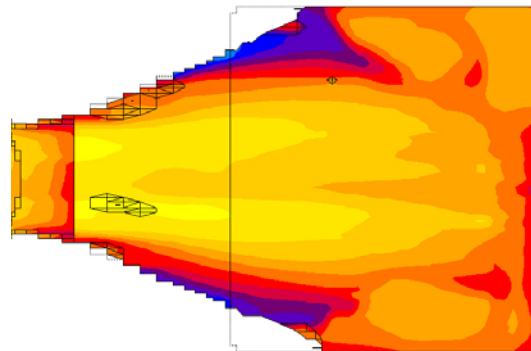
0.175 sec



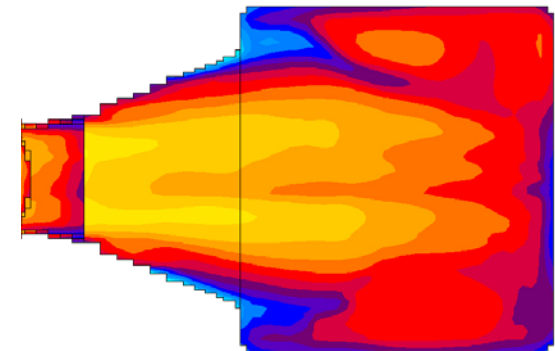
0.188 sec



0.200 sec

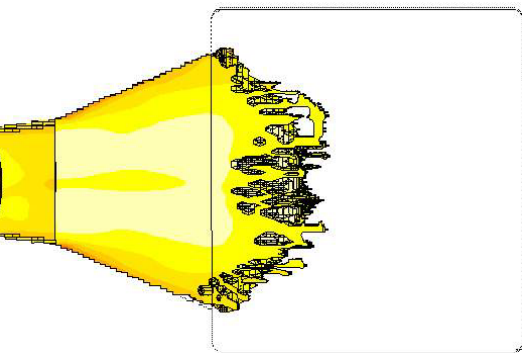


0.225 sec

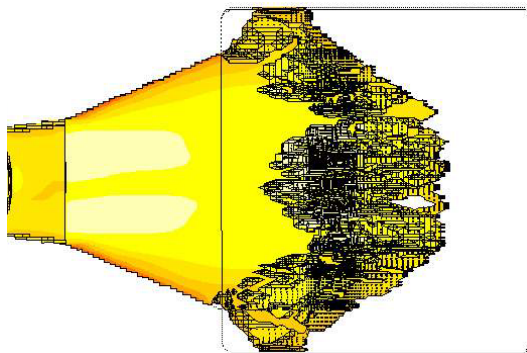


0.25 sec

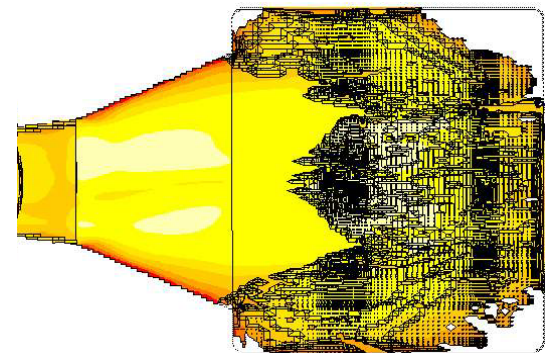
Figure 5.47: Flow Pattern in 0.5" SC Fan Gate Plate
(Gate Velocity = 7 in/sec)



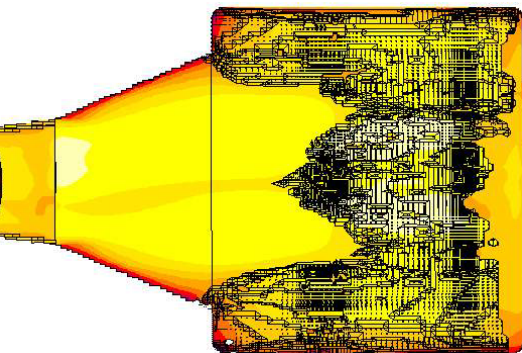
0.65 sec



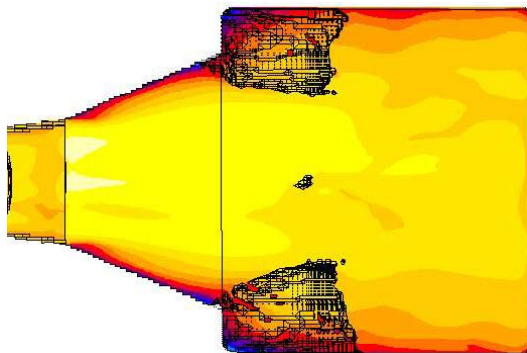
0.70 sec



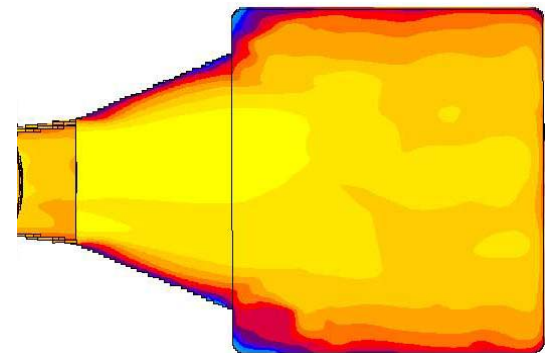
0.75 sec



0.80 sec



0.95 sec



1.00 sec

Figure 5.48: Visual Rating vs. Ingate Velocity
 (0.5 " plate with Fan Ingate, Al356, with oil heater)

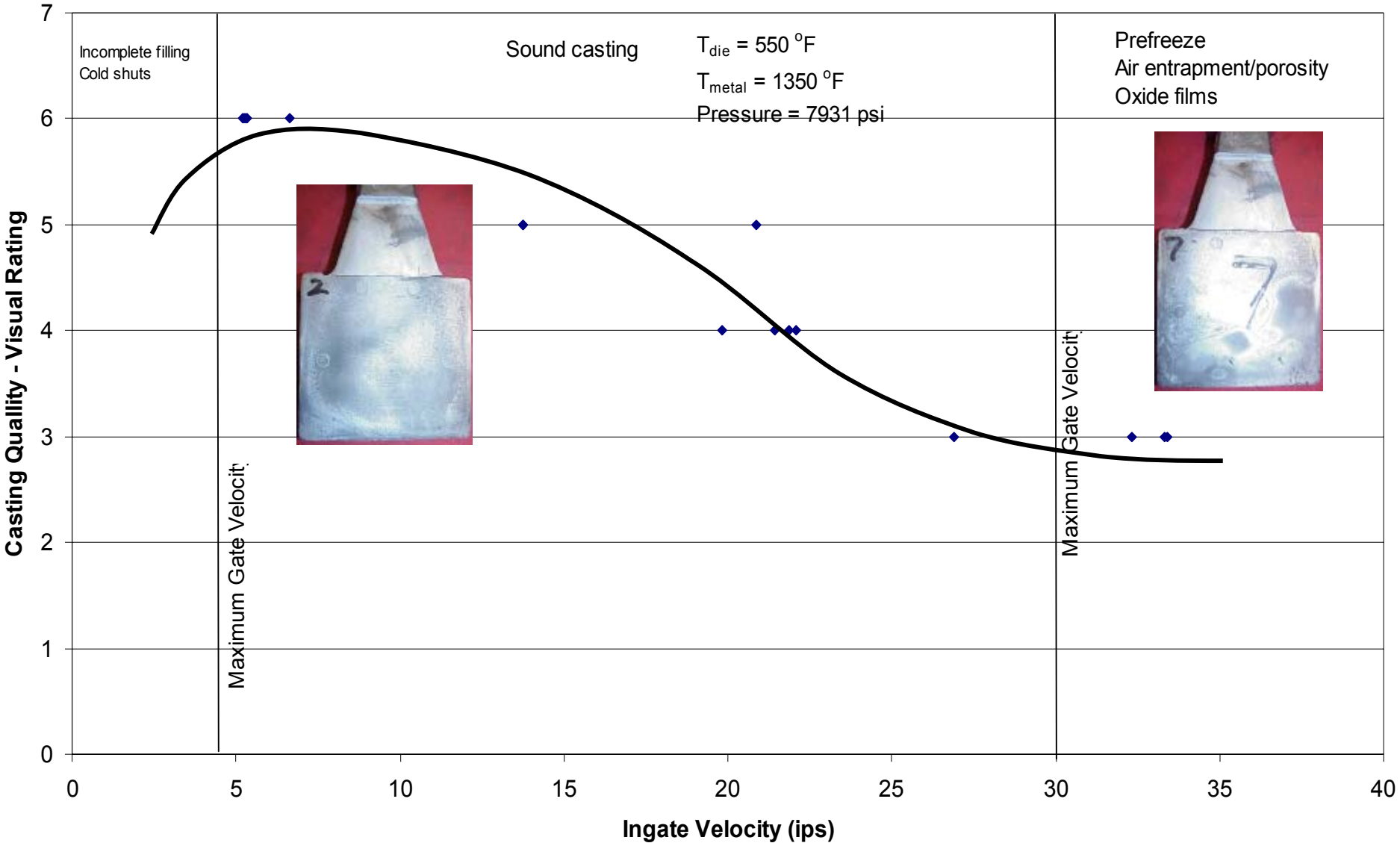


Figure 5.49: UTS & Elongation of SC A356 of 0.5" Plate-As Cast

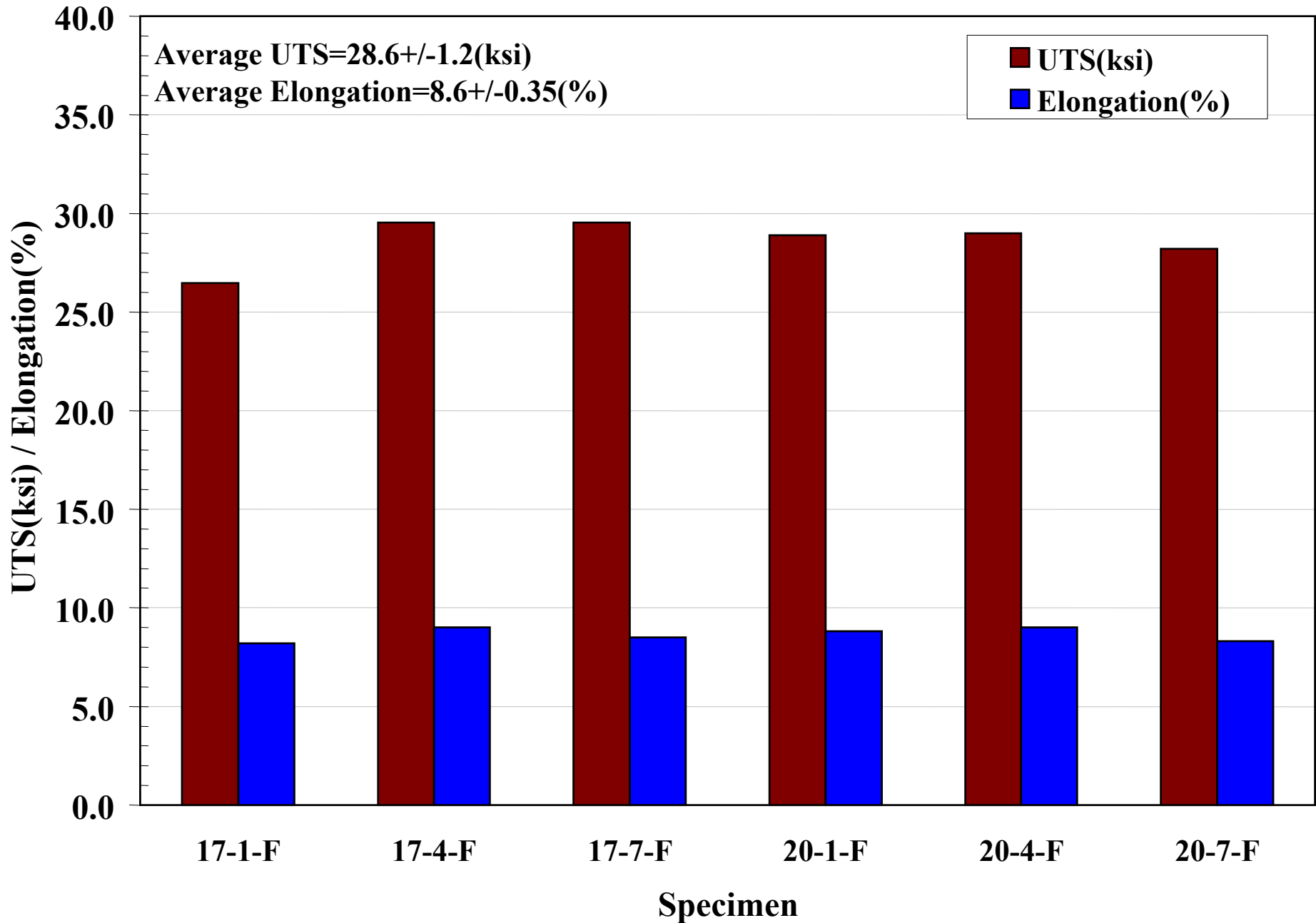


Figure 5.50: UTS & Elongation of SC A356 of 0.5" Plate-T6

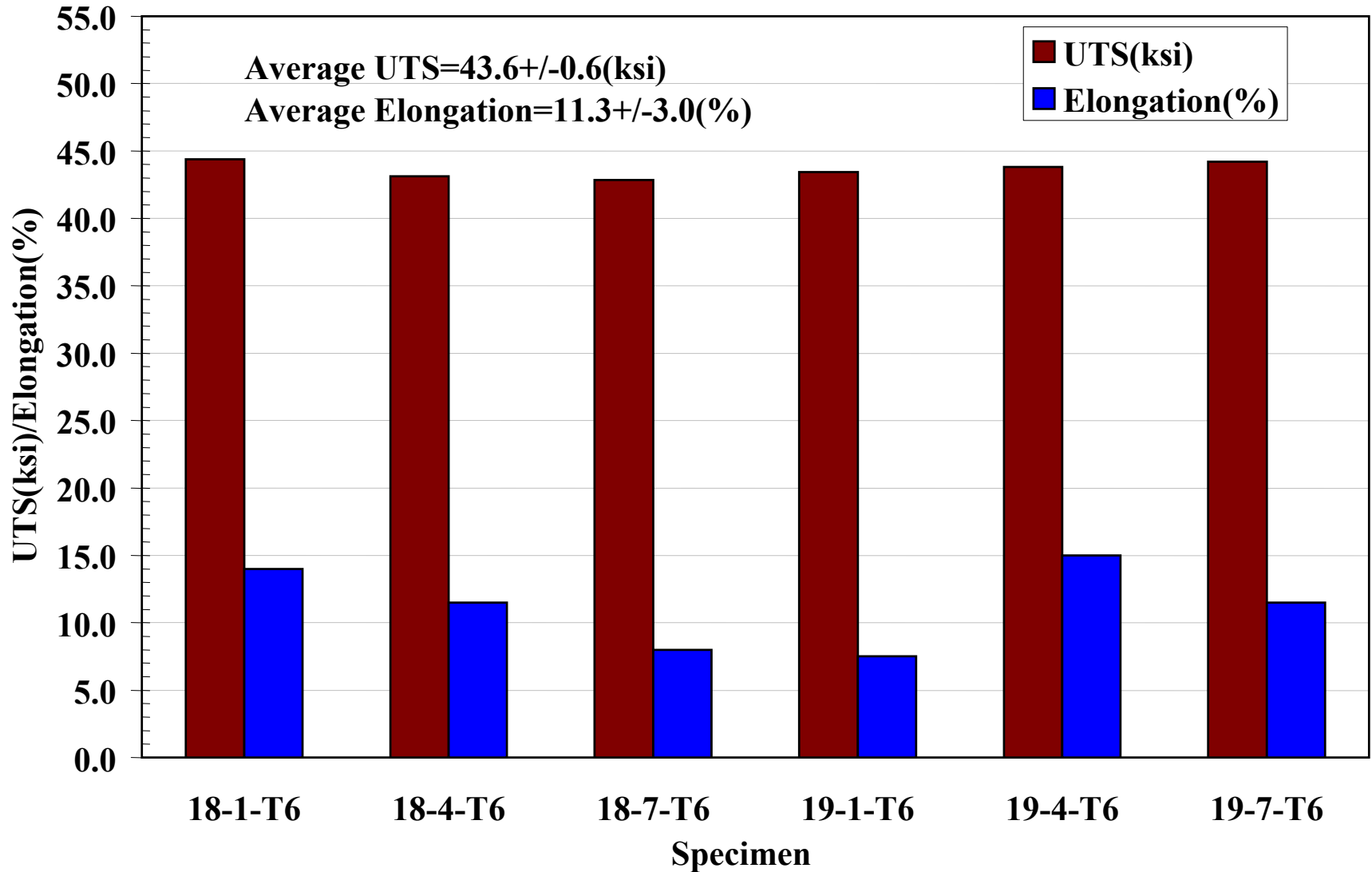


Figure 5.51: C-V-N Impact Strength of A 356 PM Test Bars & SC 0.5" Plates

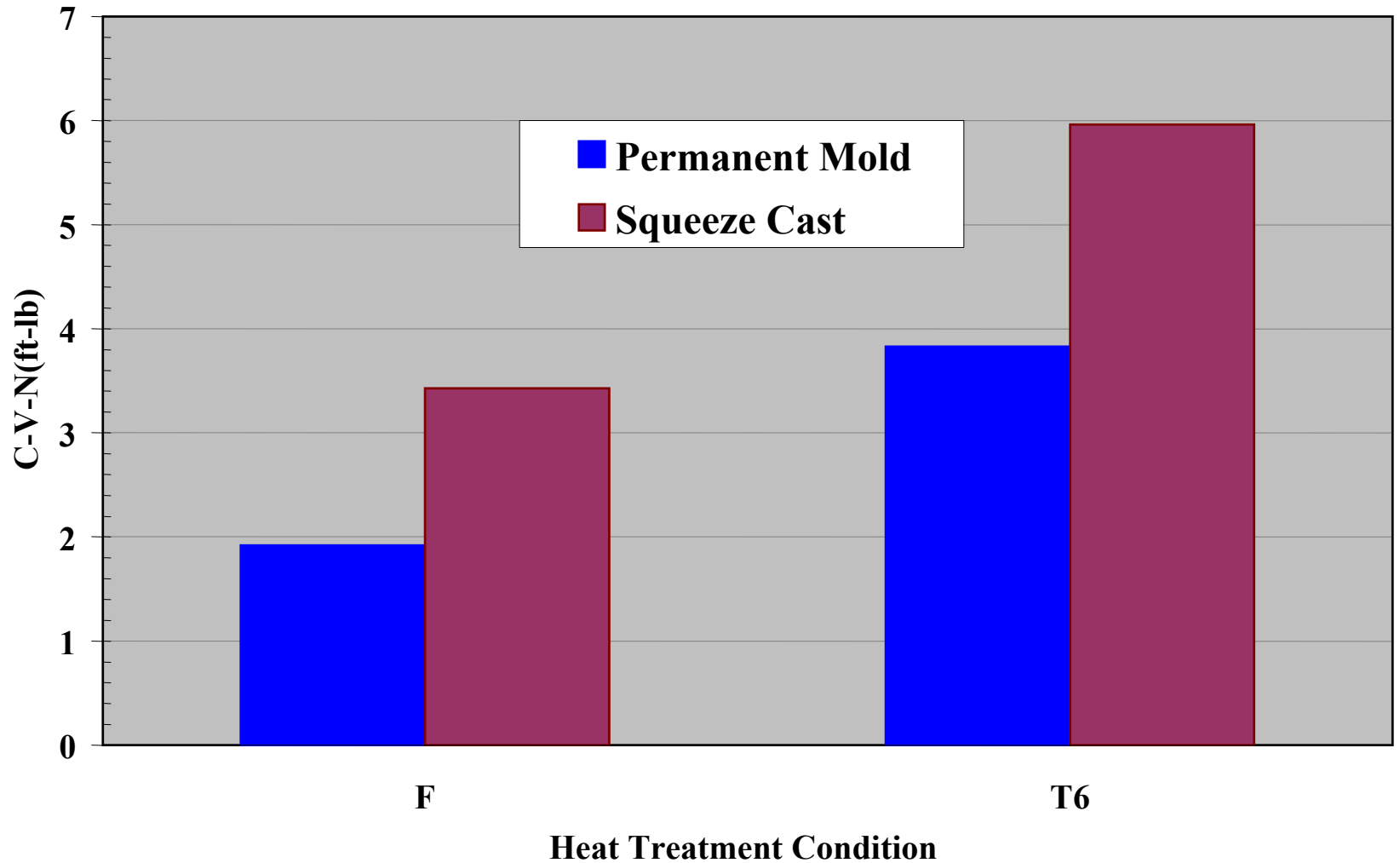
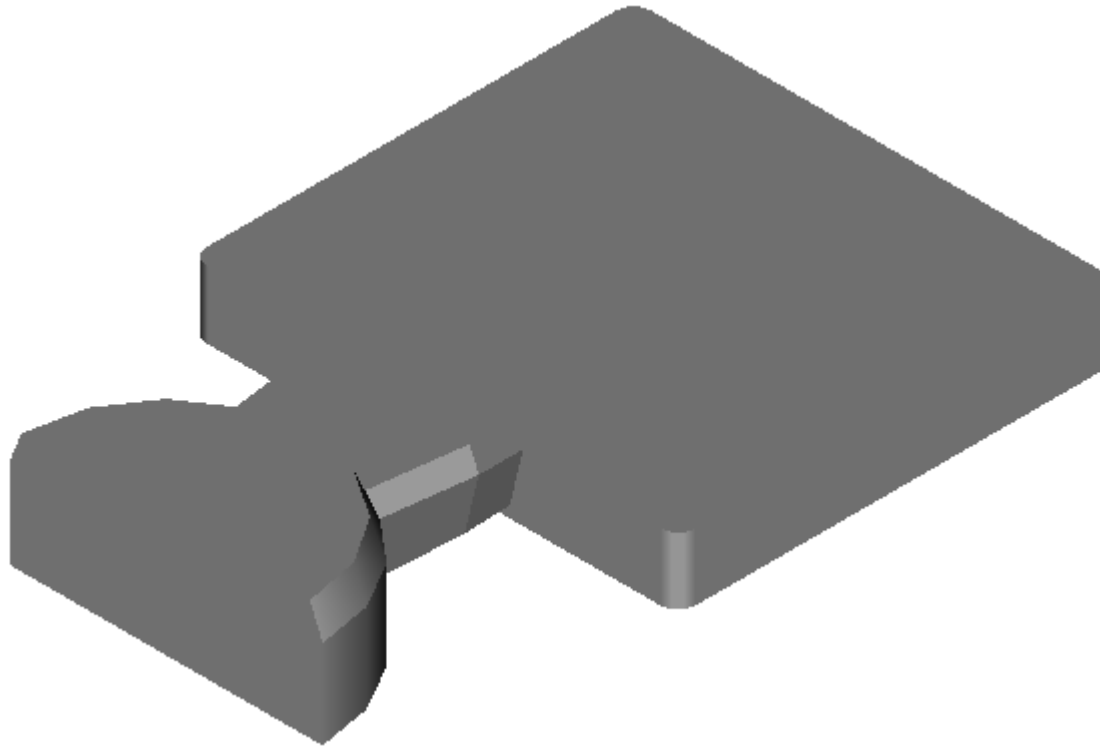


Figure 5.52: 0.75 ” Plate Insert



Cross-section of Ingate (in ²)	1.23
Ingate Shape	streight short
Volume of Casting (in ³)	20.60

Figure 5.53: Dimensions of 0.75 " SC Plates

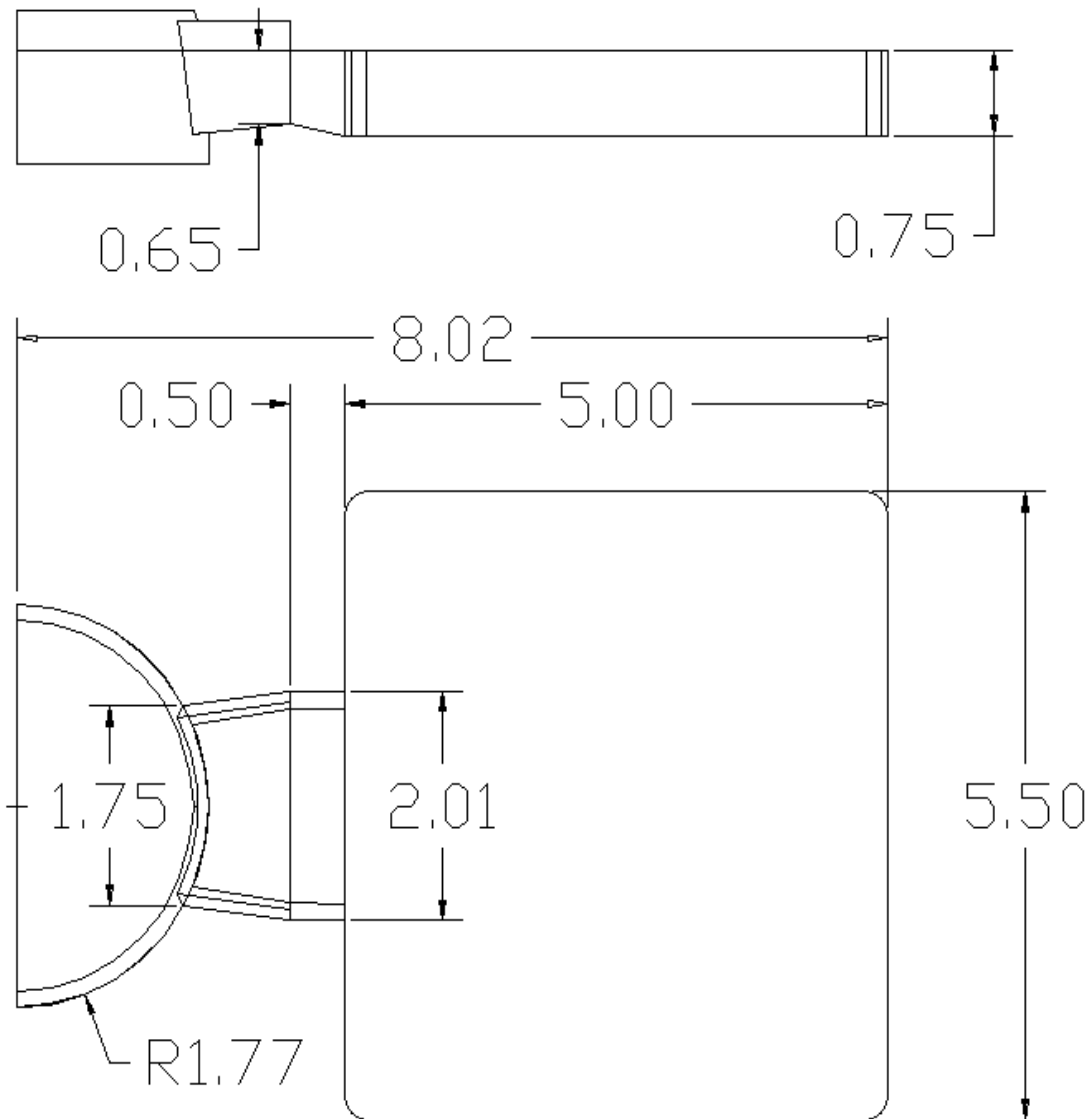
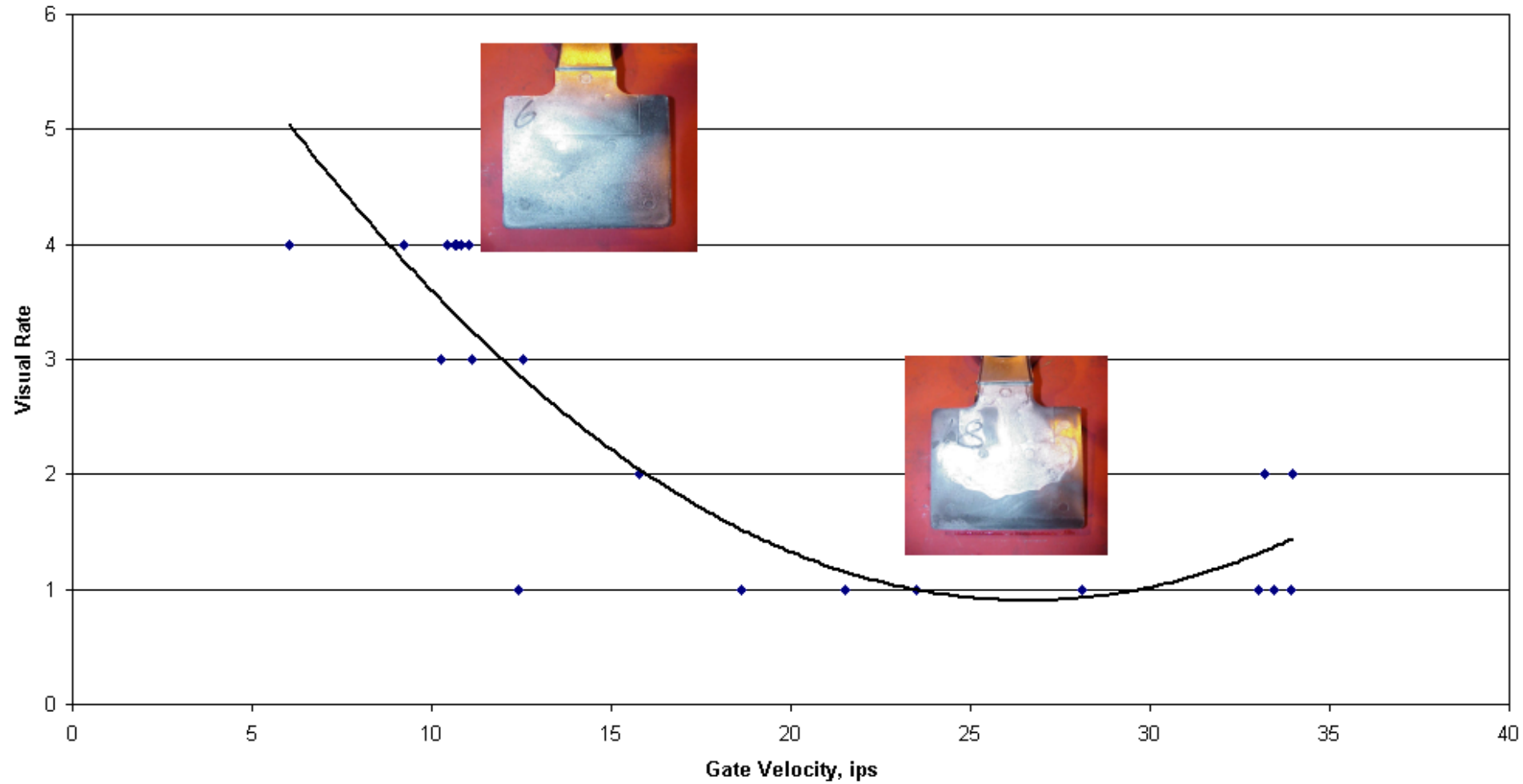


Figure 5.54

**Visual Rate VS. Gate Velocity
(0.75" Plate, Short Runner, Water Cooling)**



**Figure 5.55: Shrinkage Rating VS. Gate Velocity
(0.75 " Plate, Short Runner, Water Cooling)**

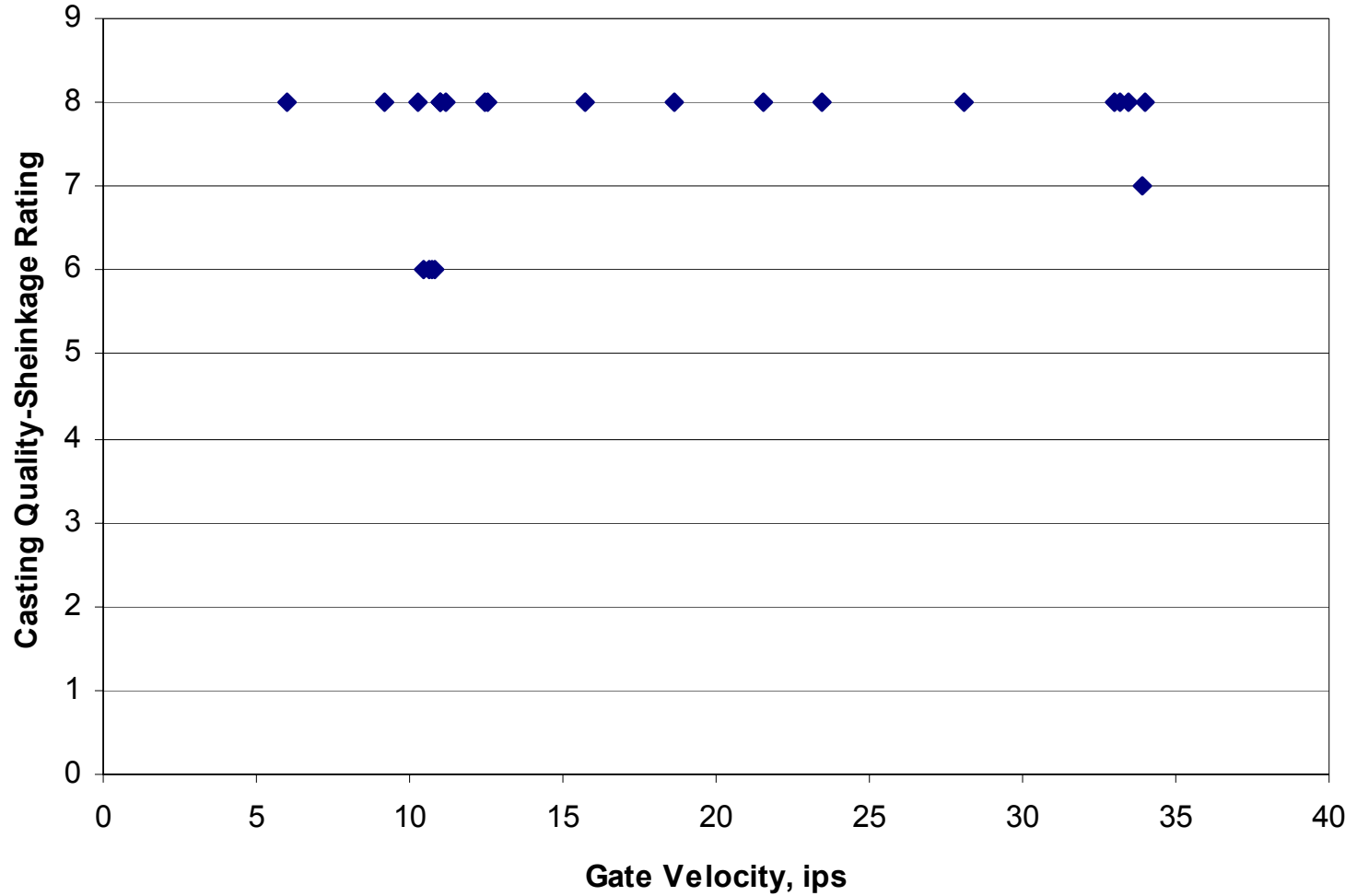


Figure 5.56: 1" Plate Insert (long and thin gate)

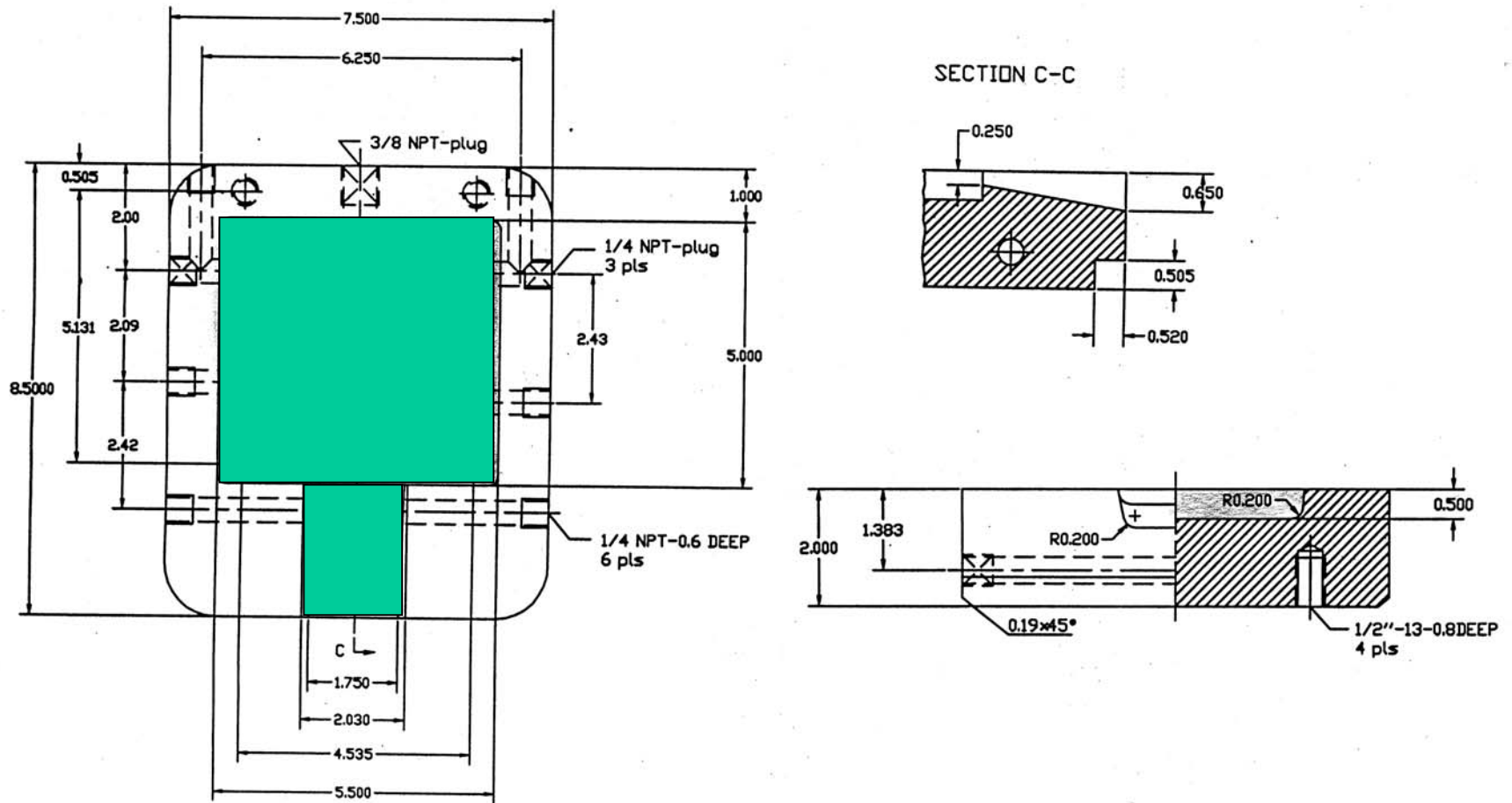
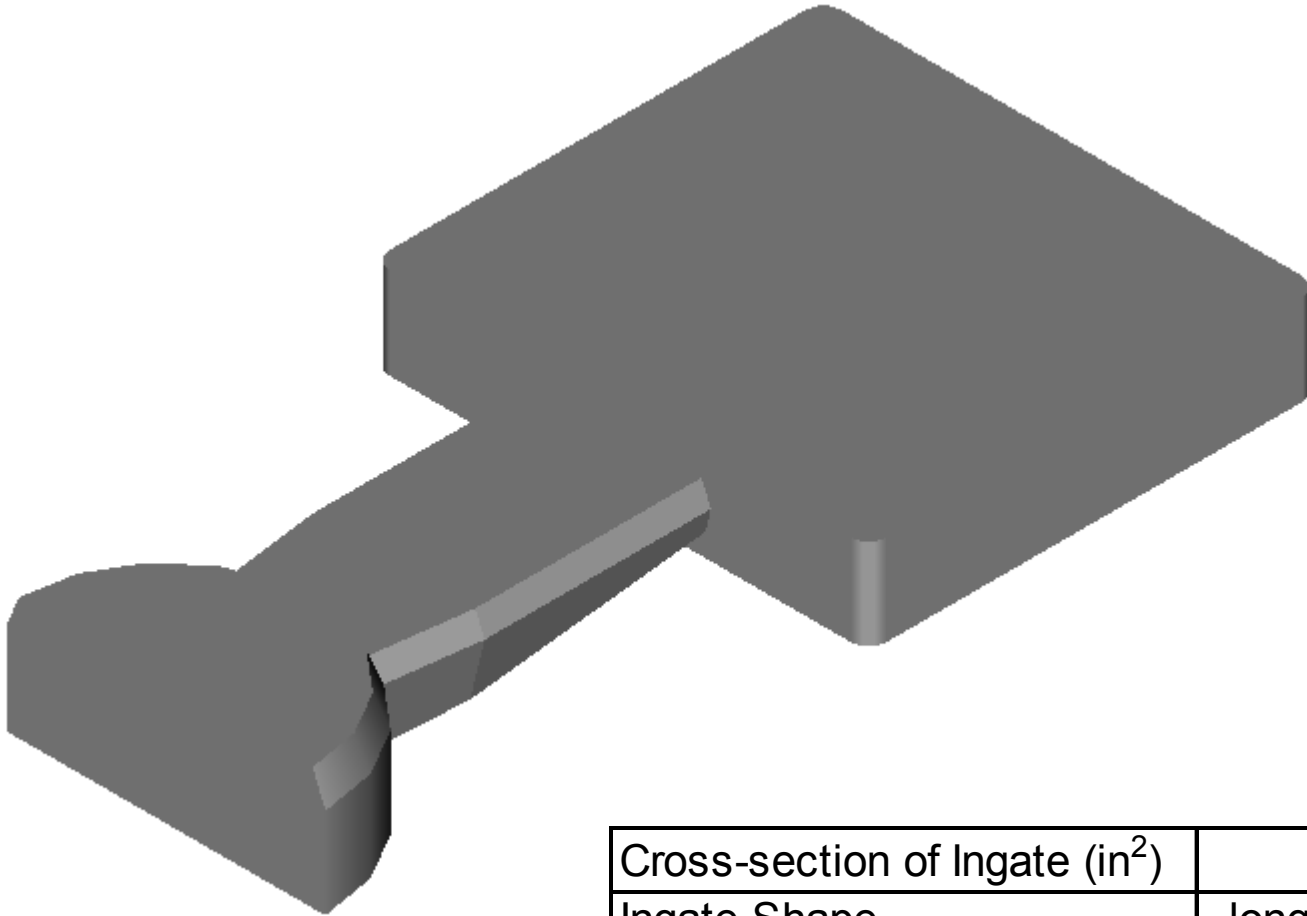


Figure 5.57: 1" Plate Insert (long and thin gate)



Cross-section of Ingate (in ²)	1.71
Ingate Shape	long and thin
Volume of Casting (in ³)	27.47

Figure 5.58: Dimensions of 1 " SC Plates

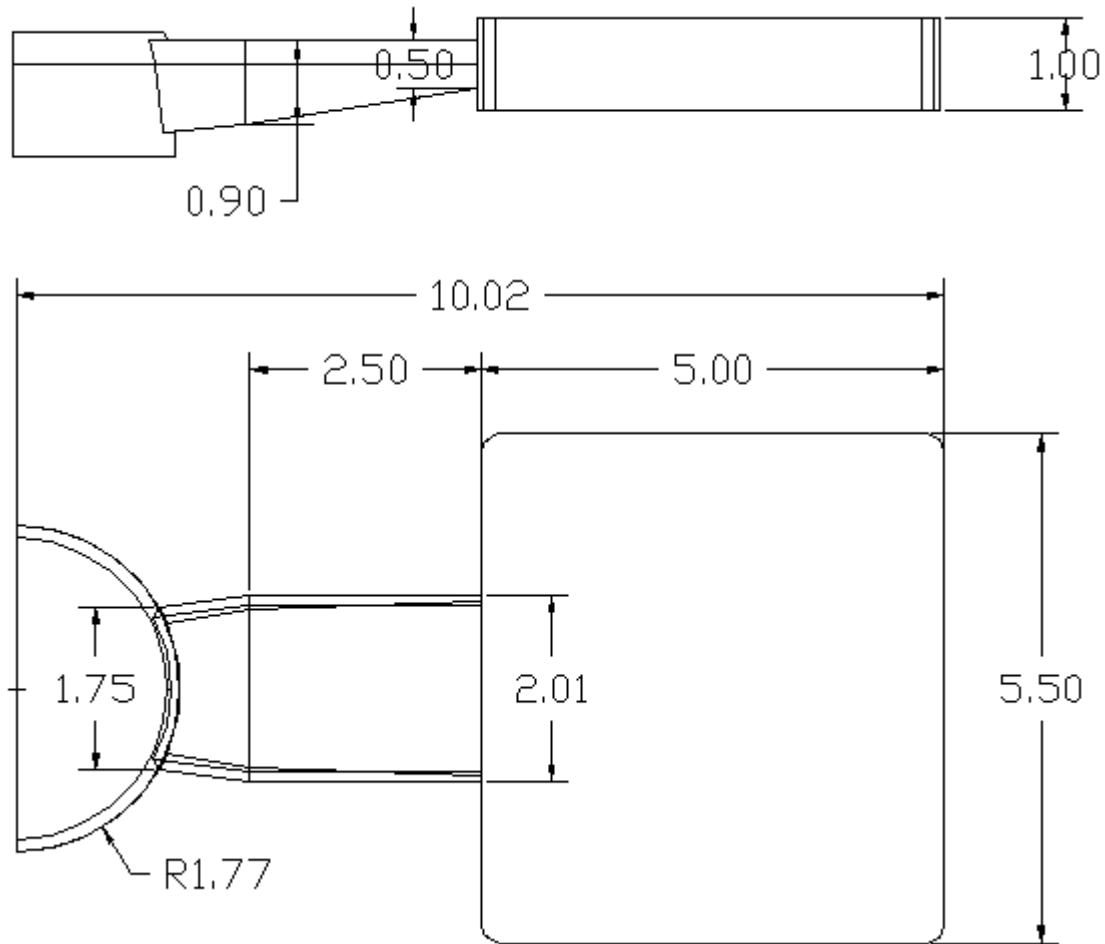
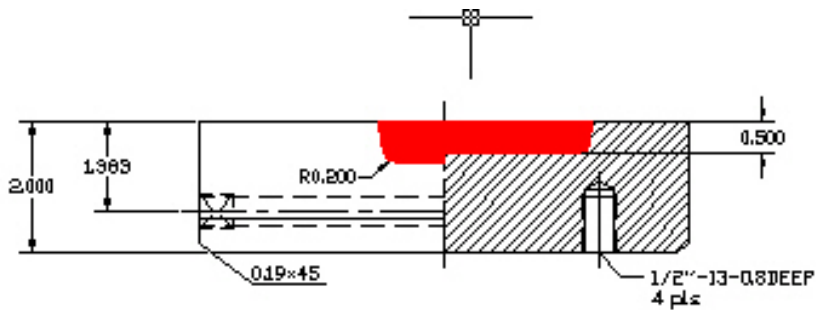
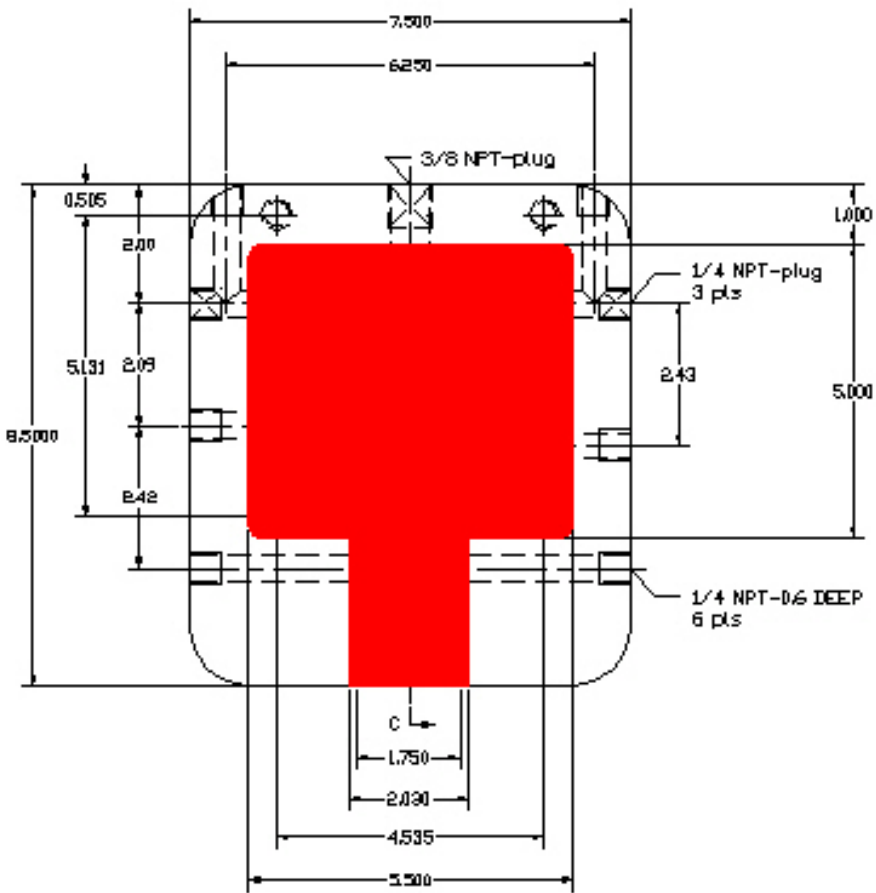
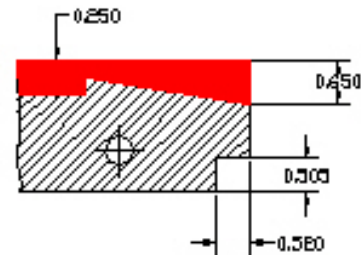


Figure 5.59: 1" Plate with Long and Thin Gate

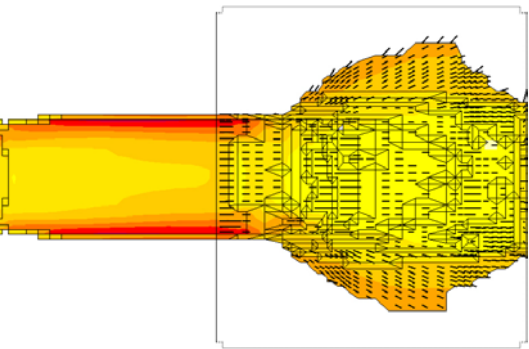


SECTION C-C

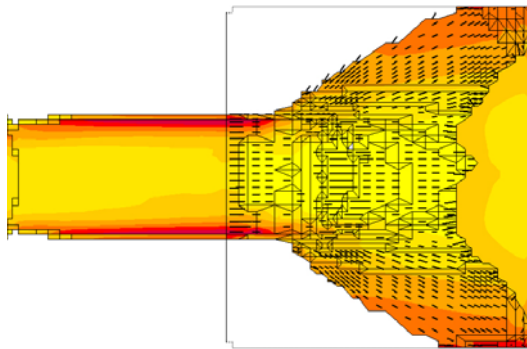


Gate freezes before casting; ineffective application of pressure during solidification

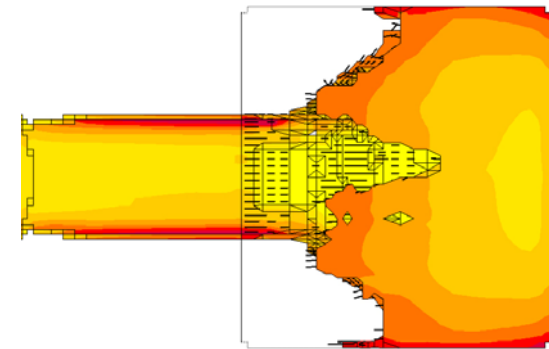
Figure 5.60: Flow Pattern in 1.0" SC w/Long Thin Gate
(Gate Velocity = 7 in/sec)



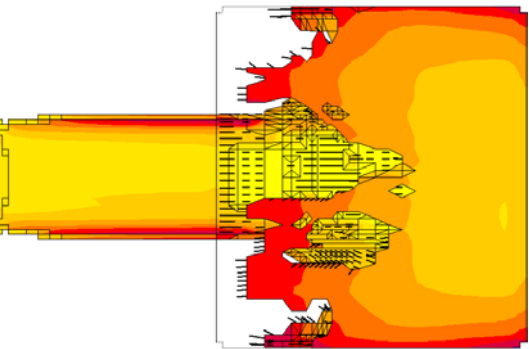
0.40 sec



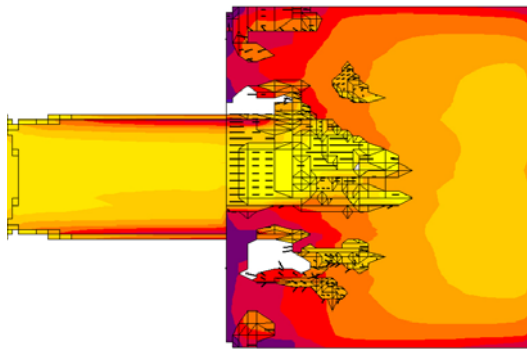
0.45 sec



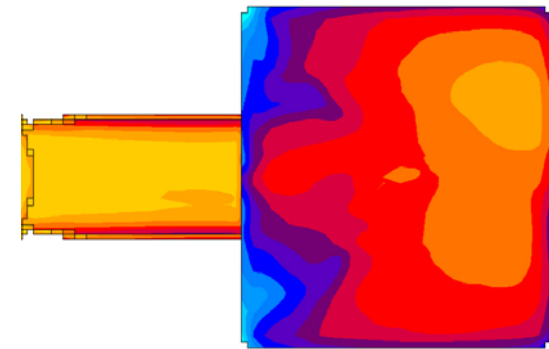
0.55 sec



0.60 sec

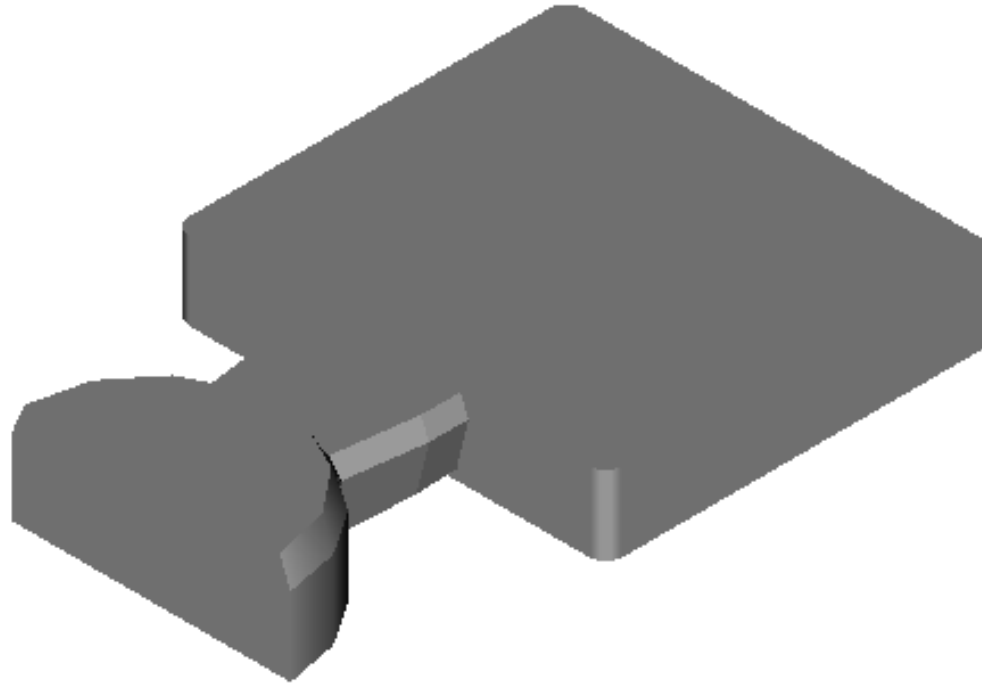


0.65 sec



1.00 sec

Figure 5.62: 1" Plate Insert (short and thick gate)



Cross-section of Ingate (in ²)	1.71
Ingate Shape	short and thick
Volume of Casting (in ³)	27.47

**Figure 5.63: Shrinkage Rate VS. Gate Velocity
(1" Plate, Short Runner, Oil Heating)**

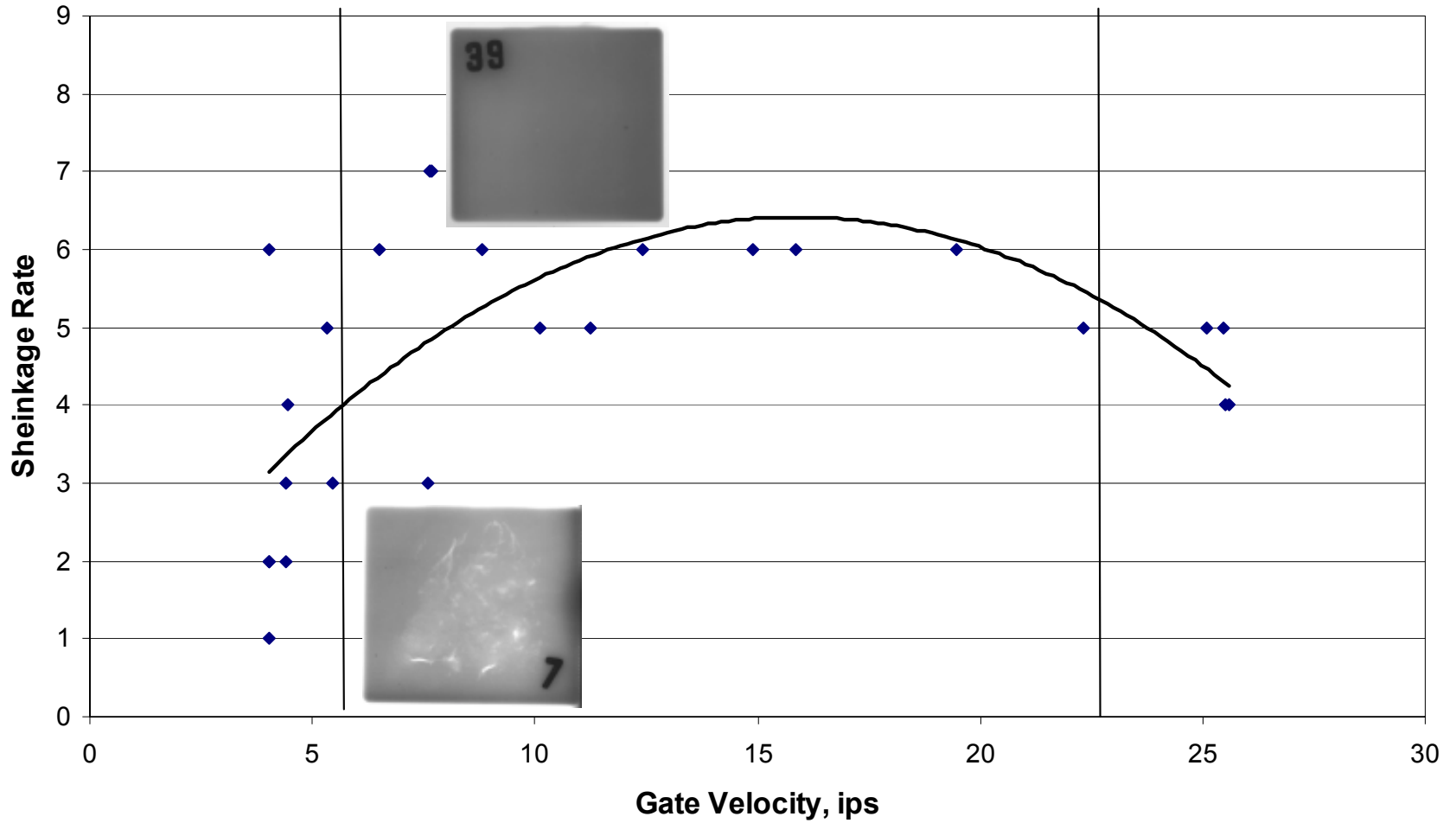


Figure 5.64: Shrinkage Rate VS. Gate Velocity
(1" Plate, Short Runner, Water Cooling)

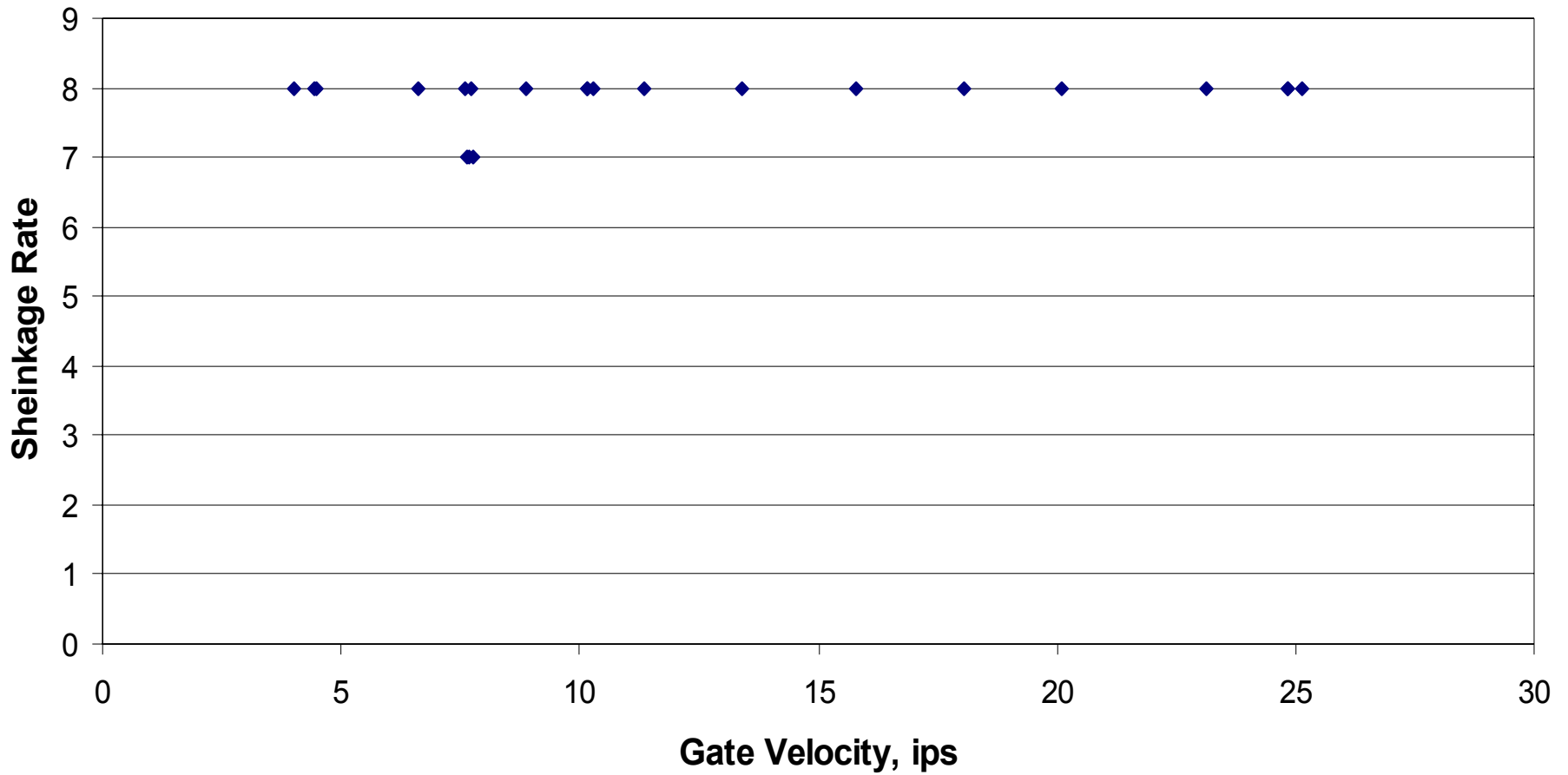


Figure 5.65: Computer simulation of solidification in a 0.75" plate

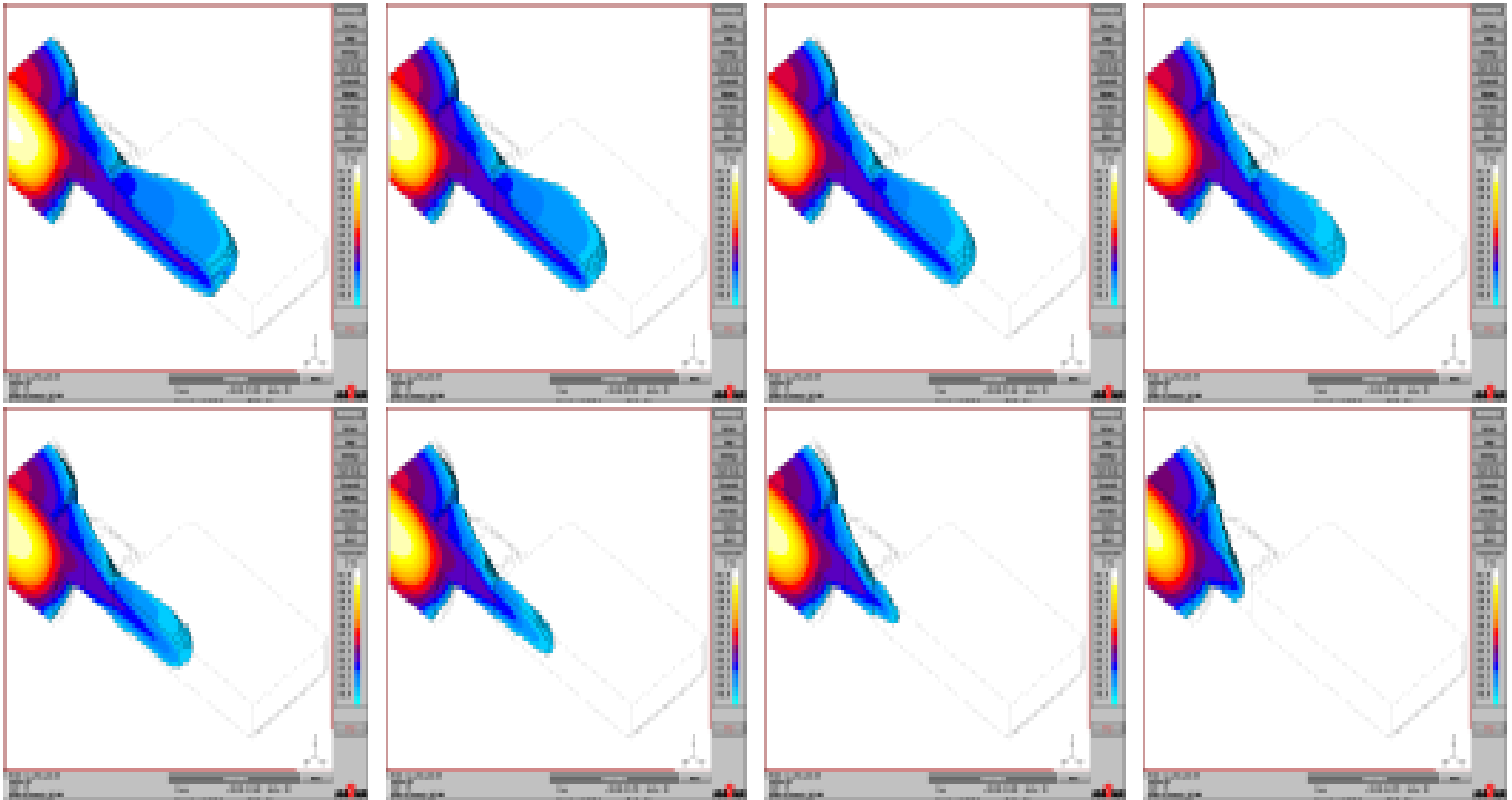


Figure 5.66: Location of Test Bars in Squeeze Cast Plate

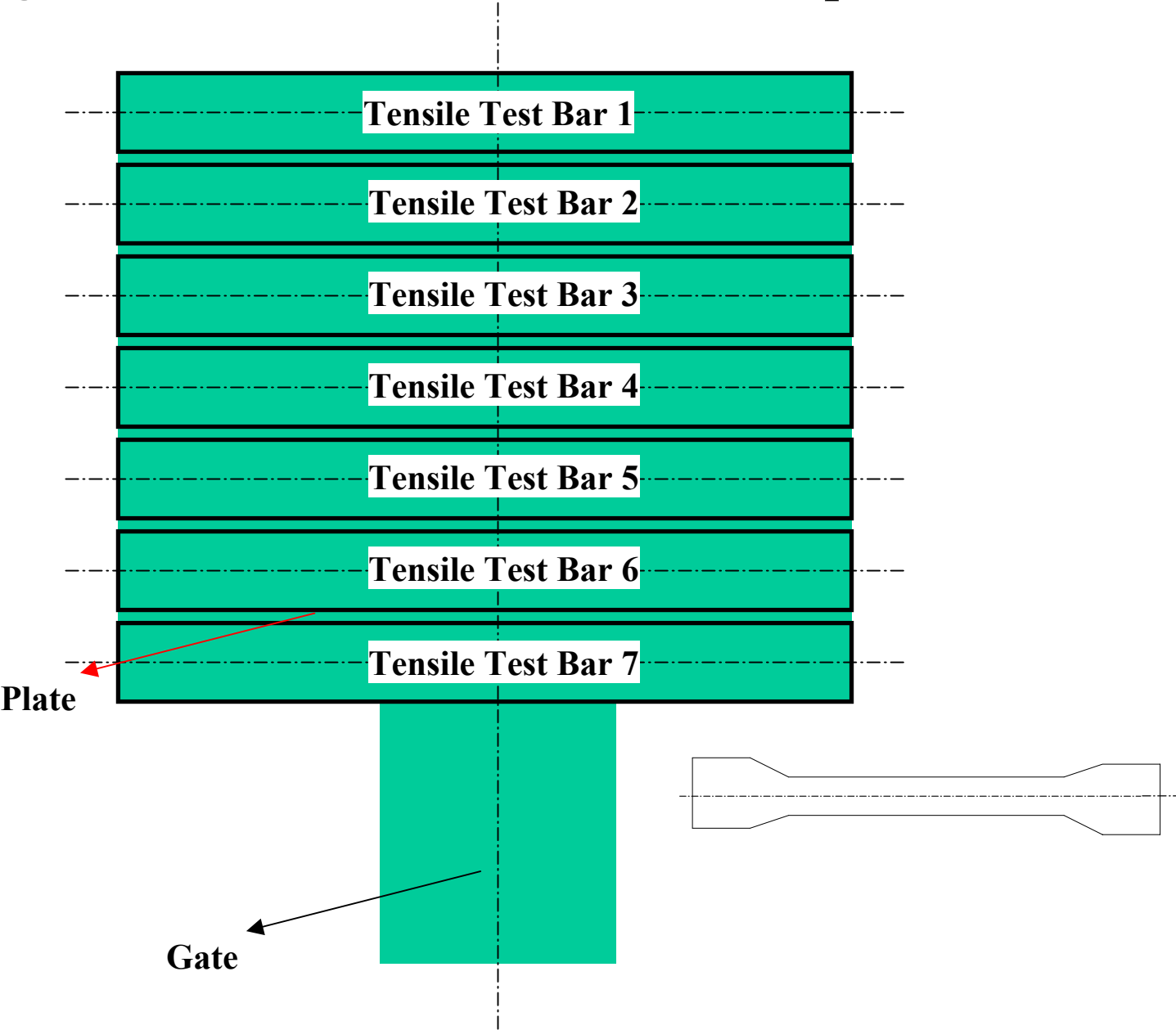


Figure 5.66: Effect of Test Bar Location on UTS of 0.75" and 1.0" Plate As-Cast

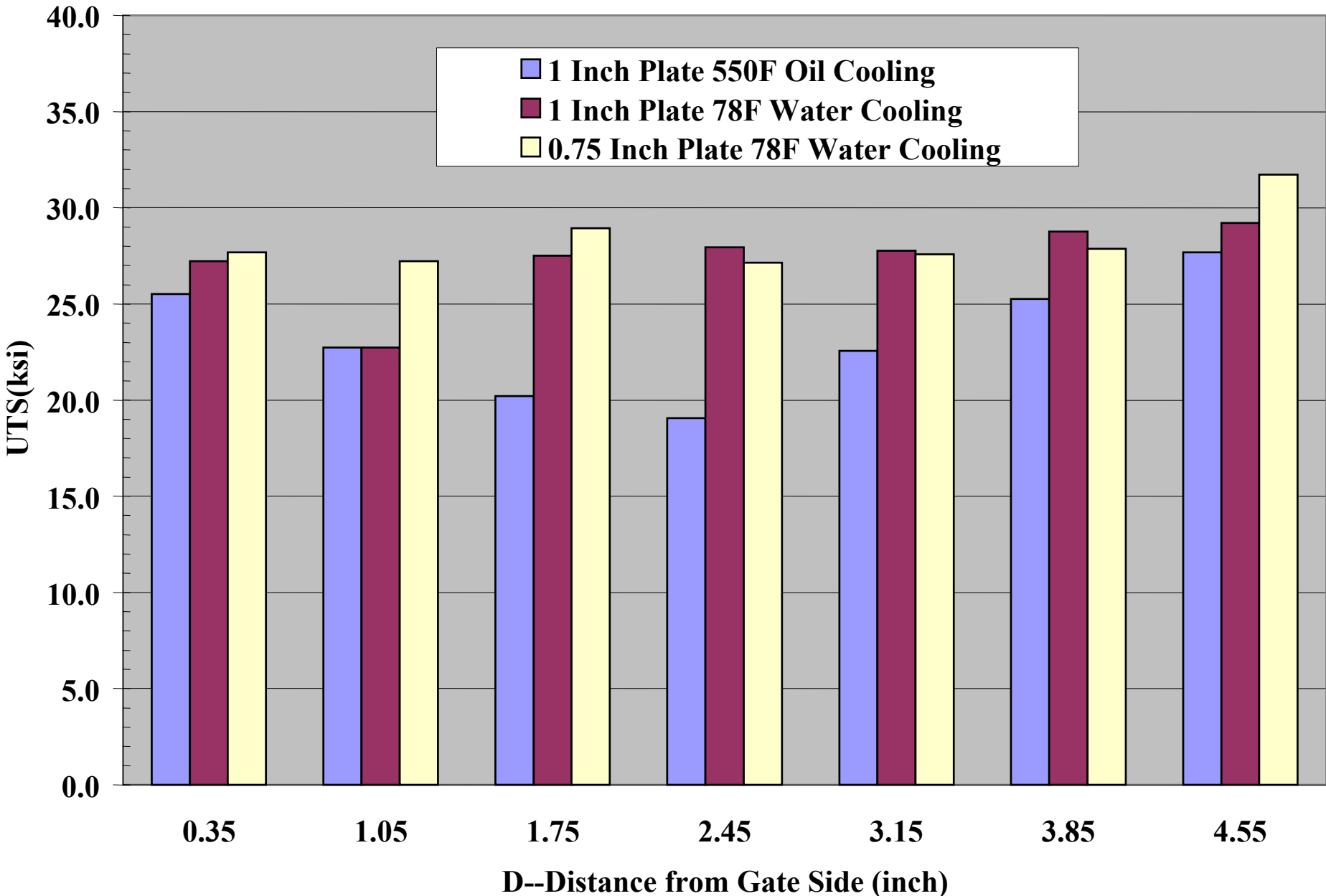


Figure 5.67: Effect of Test Bar Location on Elongation of 0.75" and 1.0" Plate As-Cast

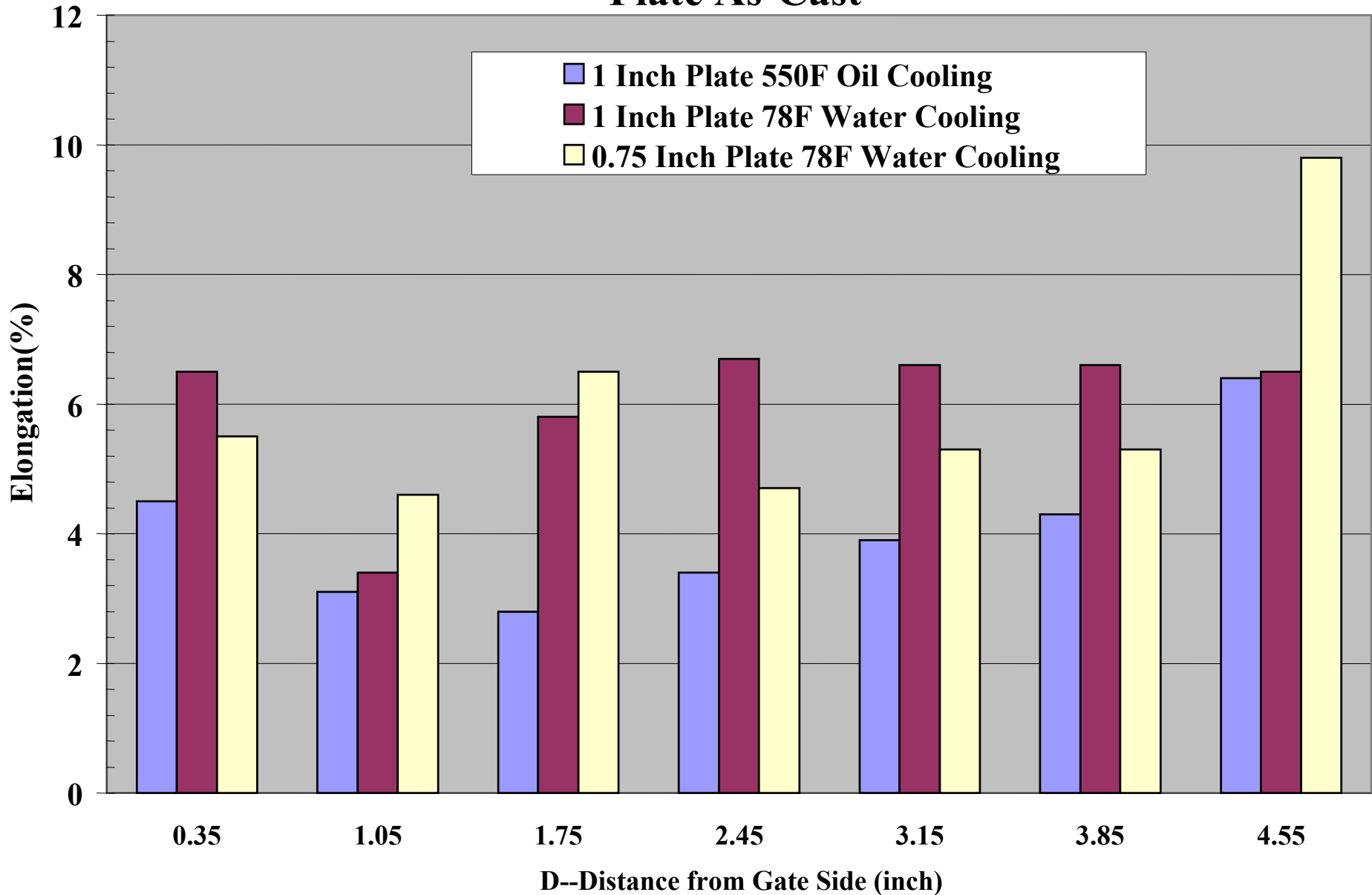


Figure 5.68: Effect of Test Bar Location on UTS of 0.75" and 1.0" Plate T6

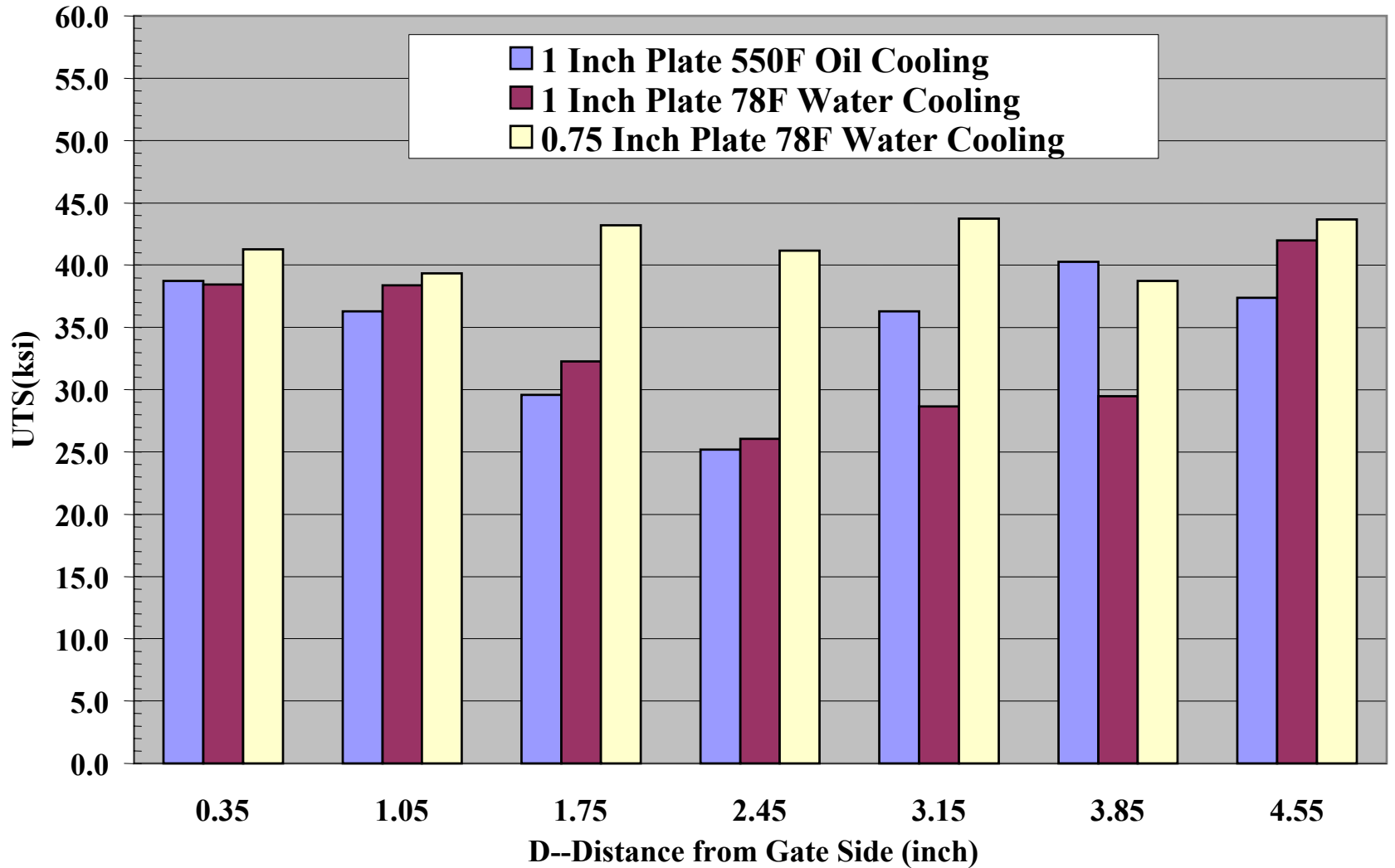
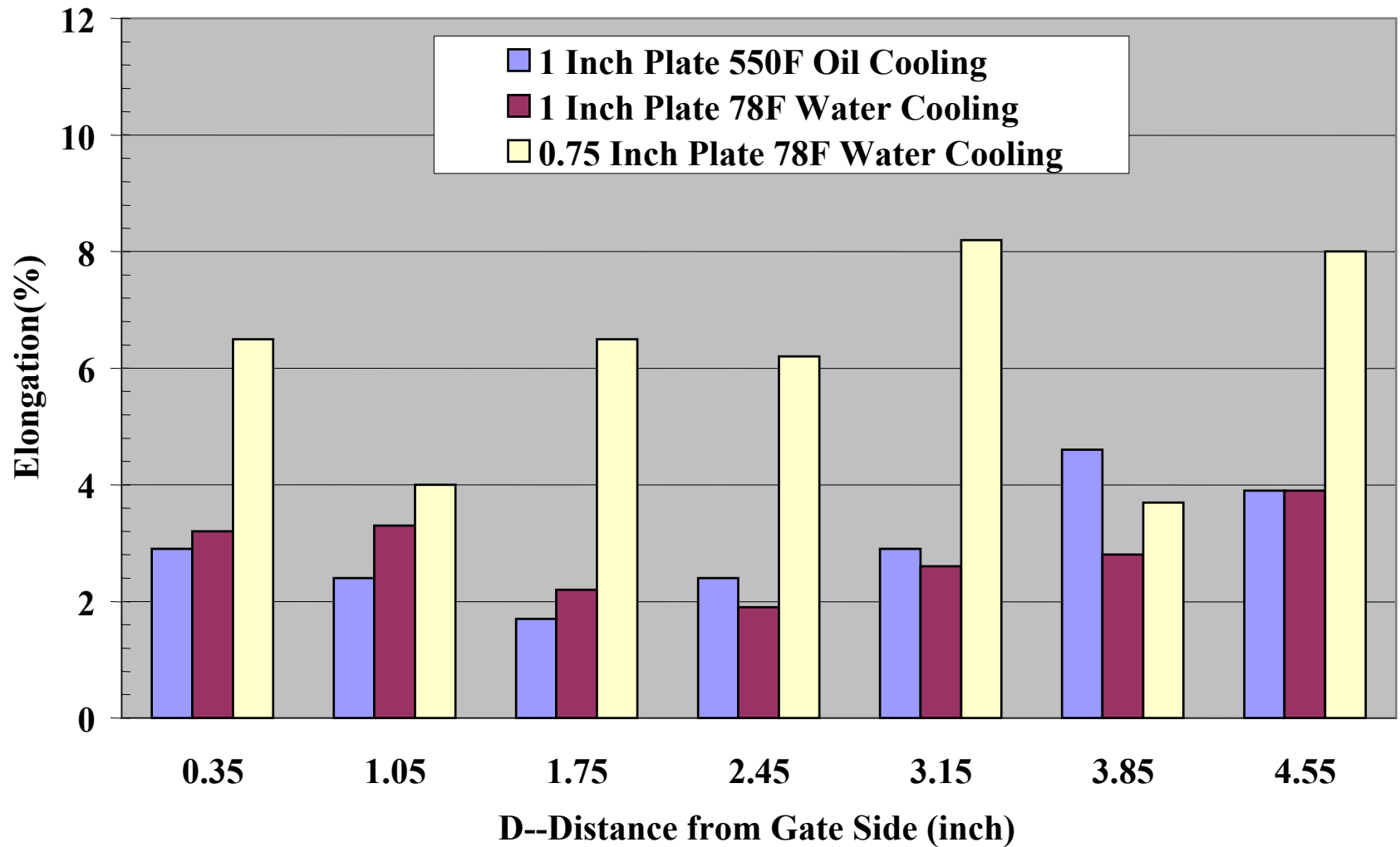


Figure 5.69: Effect of Test Bar Location on Elongation of 0.75" and 1.0" Plate T6



5:70: Velocity Range of SC Plate

Gate Design	Cross-section of Ingate (in ²)	Velocity Range (ips)		Best Velocity Range for Sound Casting			
		Plunger	Ingate	Plunger		Ingate	
				from	to	from	to
1/4" Fanned gate	0.875	0.74~4.93	6.19~41.9	1.16	3.2	12	30
1/2" straight gate	0.851	0.76~4.47	2.21~38.0	0.66	1.5	7	16
1/2" fanned gate	1.313	0.76~4.9	5.2~33.4	0.73	4.1	5	30
3/4" short straight gate	1.225	0.8~4.6	6.03~33.96	0.76	4.5	6	33
1" short straight gate (oil)	1.708	0.76~2.7	4~25.5	1.5	4.6	8	24
1" short straight gate(water)	1.708	0.76~4.75	4.8~25.58	0.75	4.7	4	25

Note:

Area of Plunger Tip : 9.027 in²

Figure 5.71: Velocity Range for Sound Casting

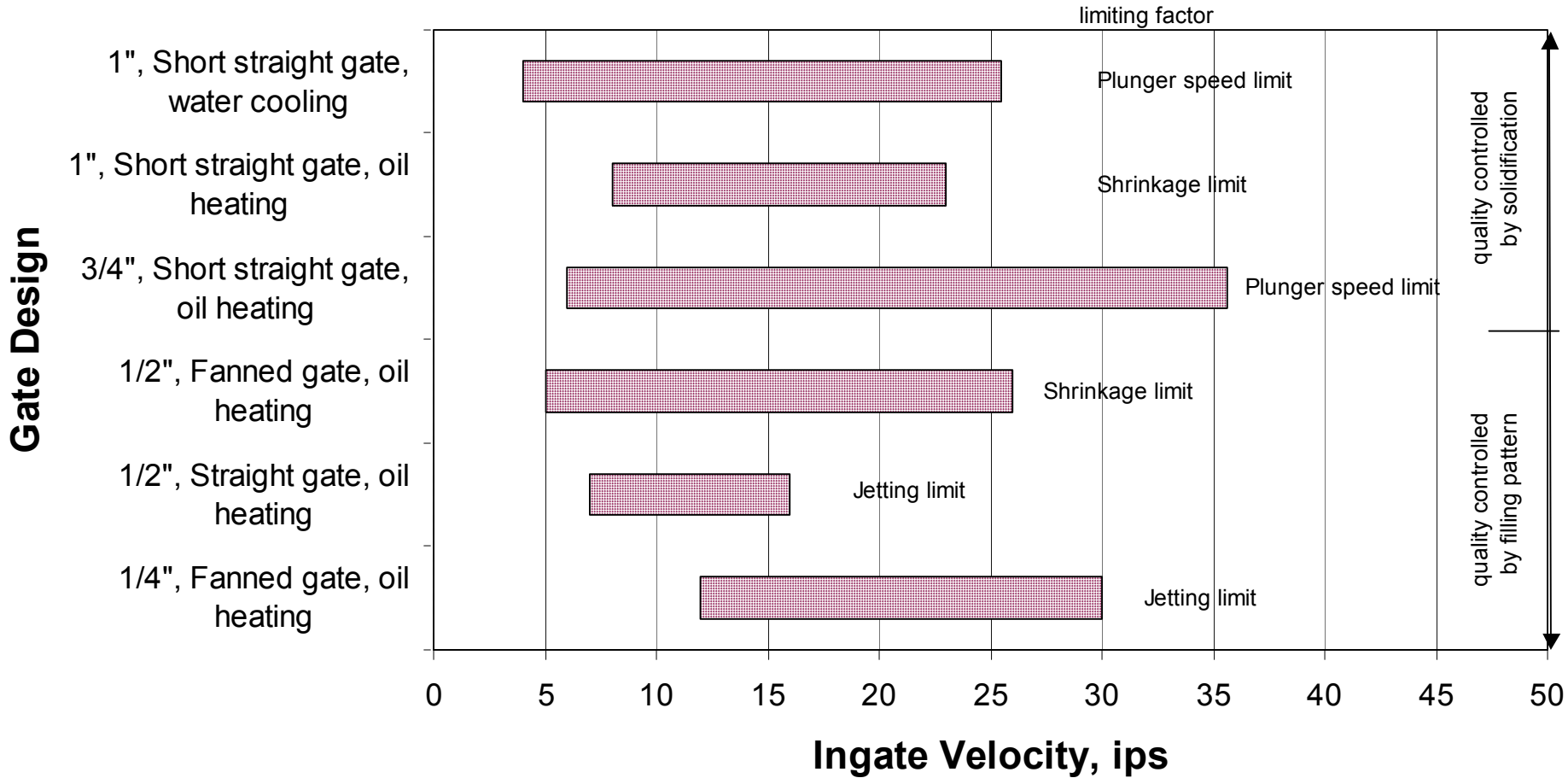


Figure 5.72: Velocity Range for Sound Casting

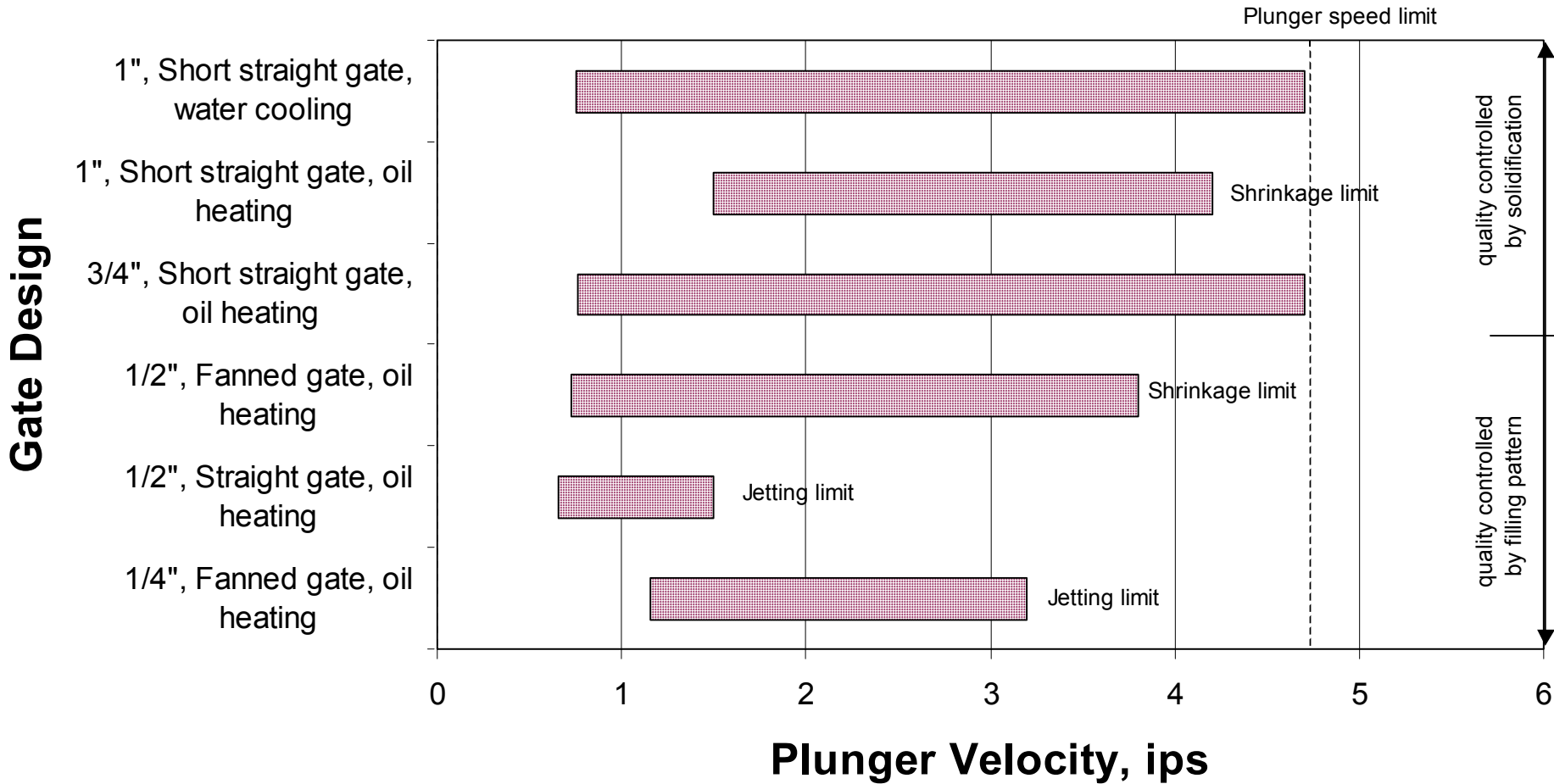


Figure 5.73: Average Visual Rating of 0.5" Plate with Large Gate vs Metal Pressure

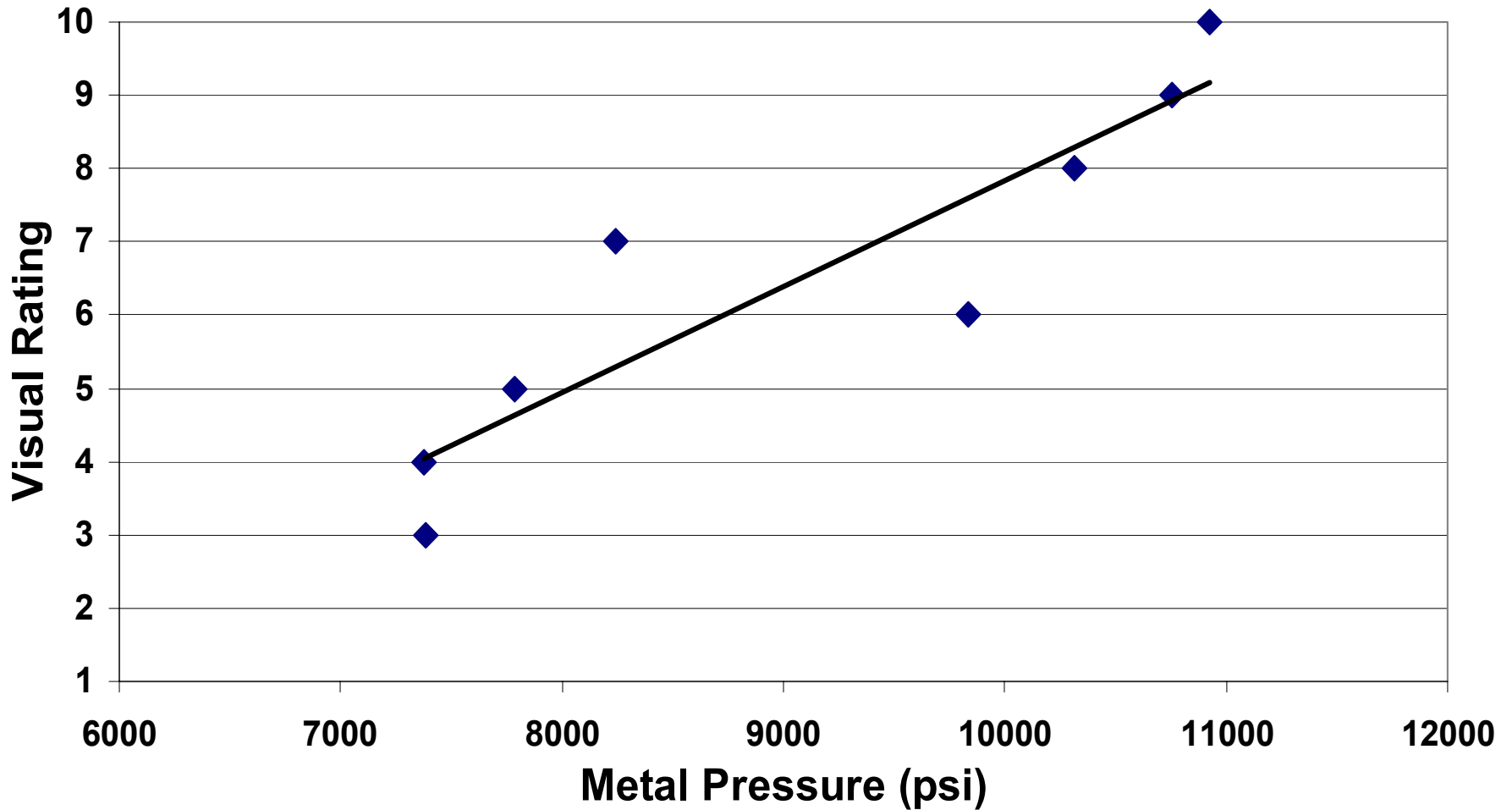


Figure 5.74: Effect of Pressure on Density

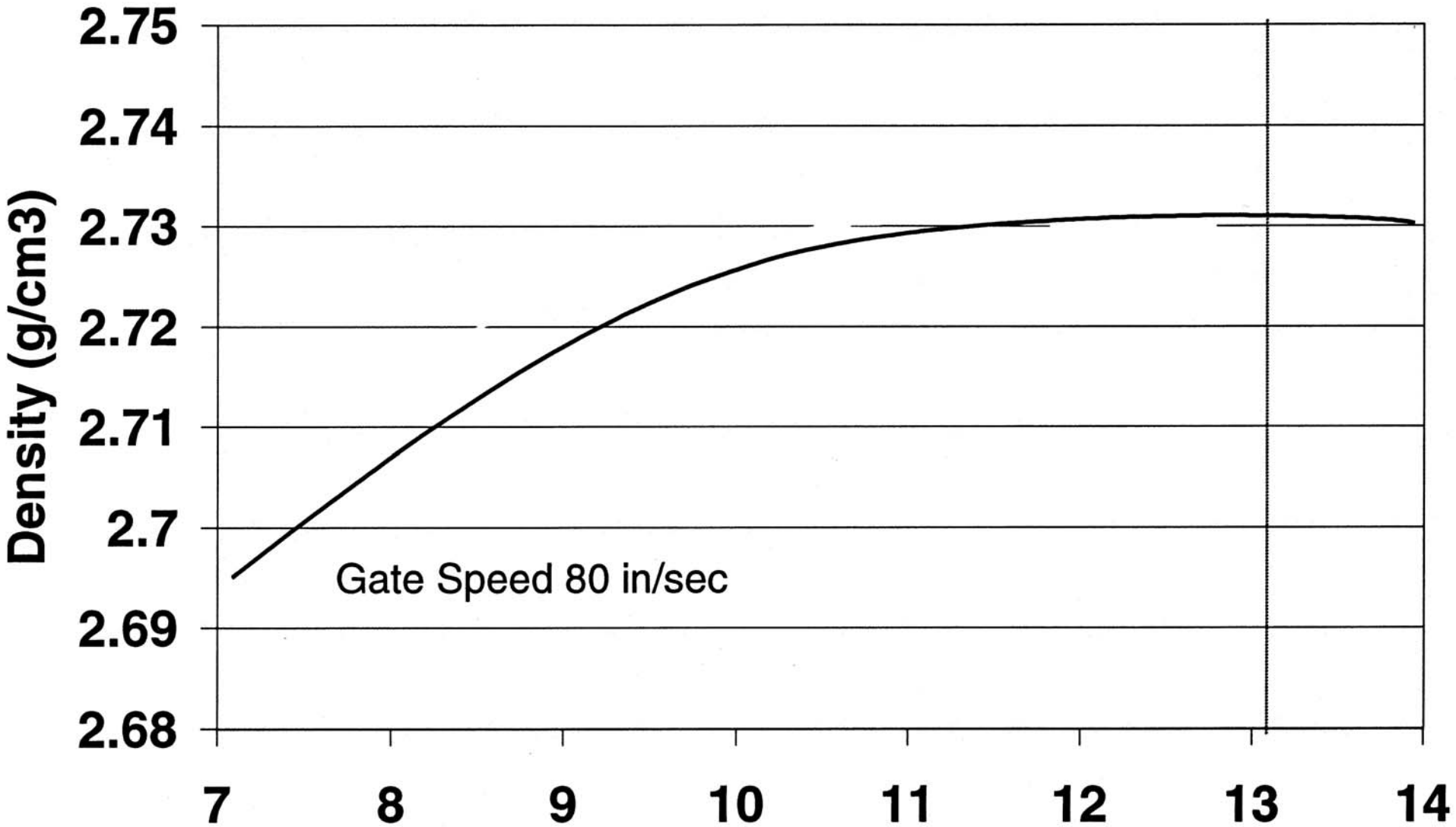


Figure 5.75: Ribbon Insert

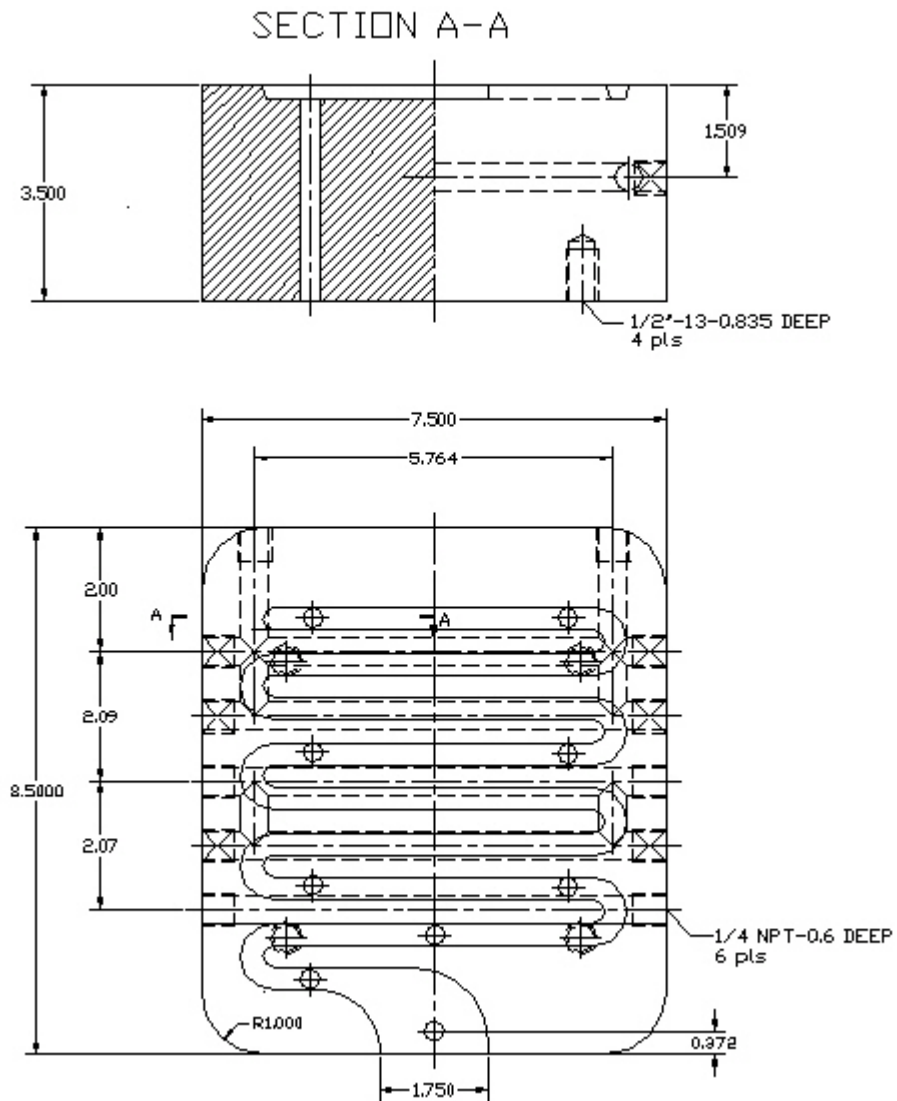
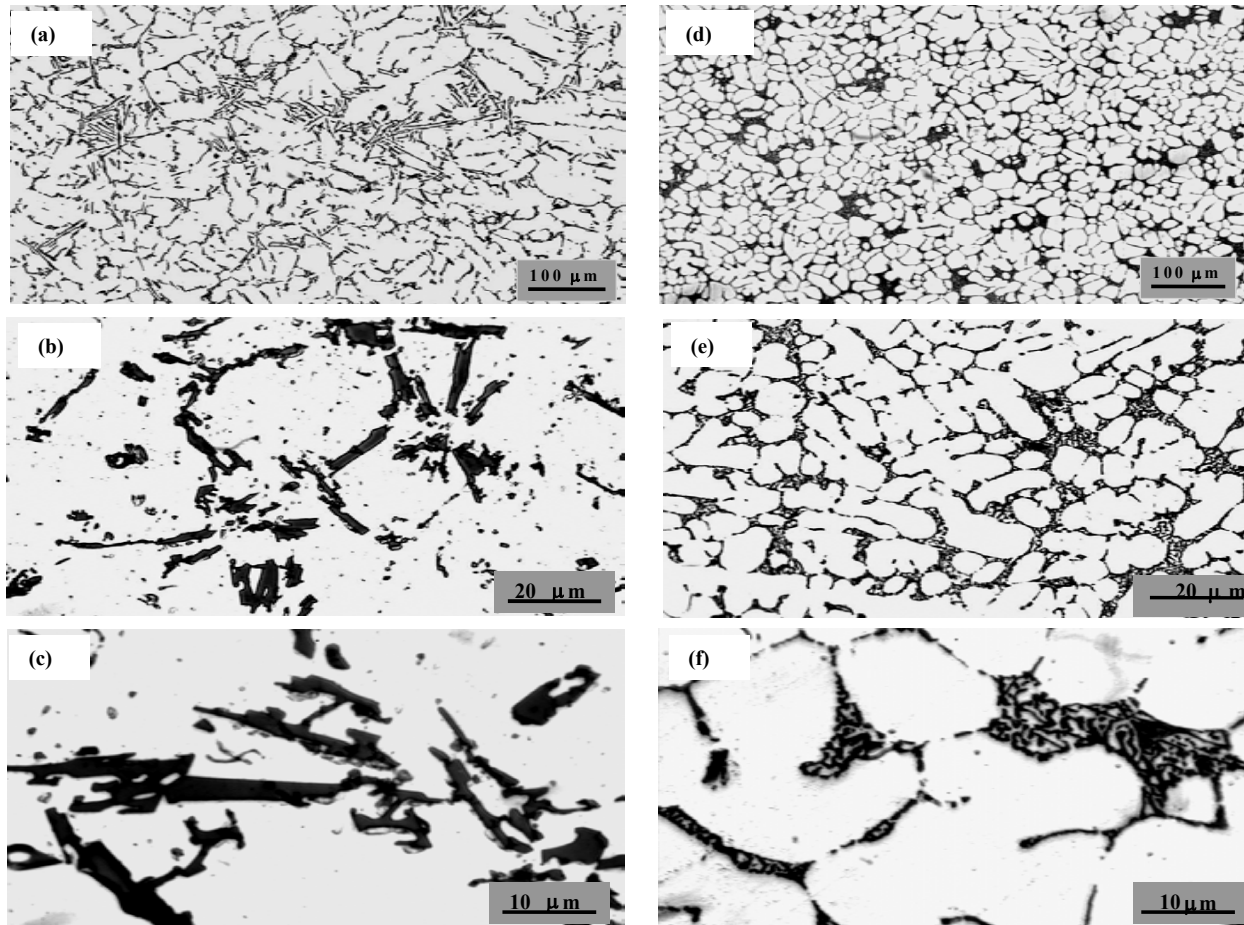


Figure 5.76: Flow distance in Ribbon



Figure 5.77: Microstructures of permanent mold and squeeze cast as-cast condition



**(a), (b) and (c) are permanent mold with magnification of 100, 500 and 1000
(d), (e) and (f) are squeeze casting with magnification of 100, 500 and 1000**

Figure 5.78: Impact fractures of permanent mold and squeeze casting in as-cast and T6 conditions
PM--permanent mold, SC--squeeze cast, F--as-cast.

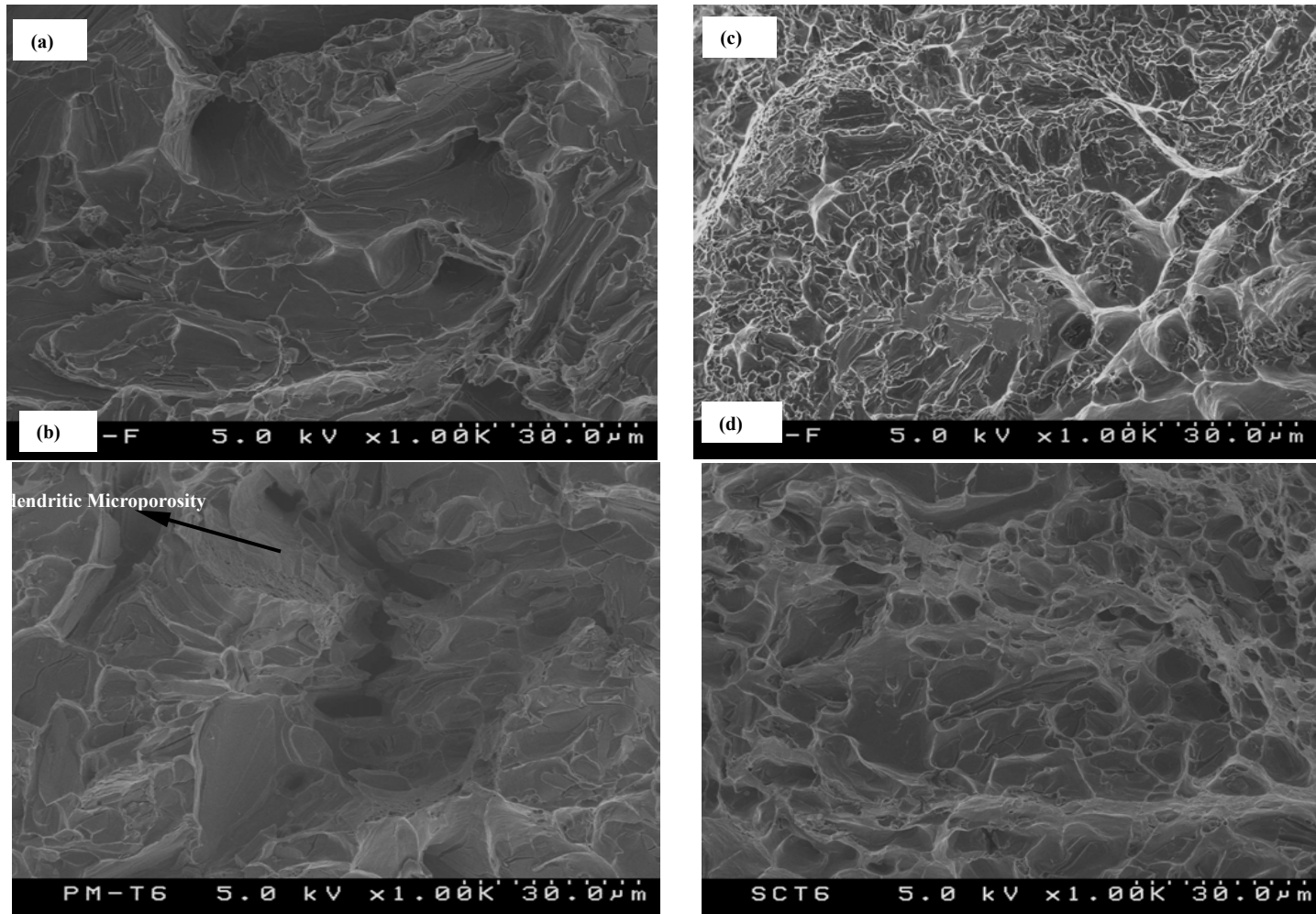
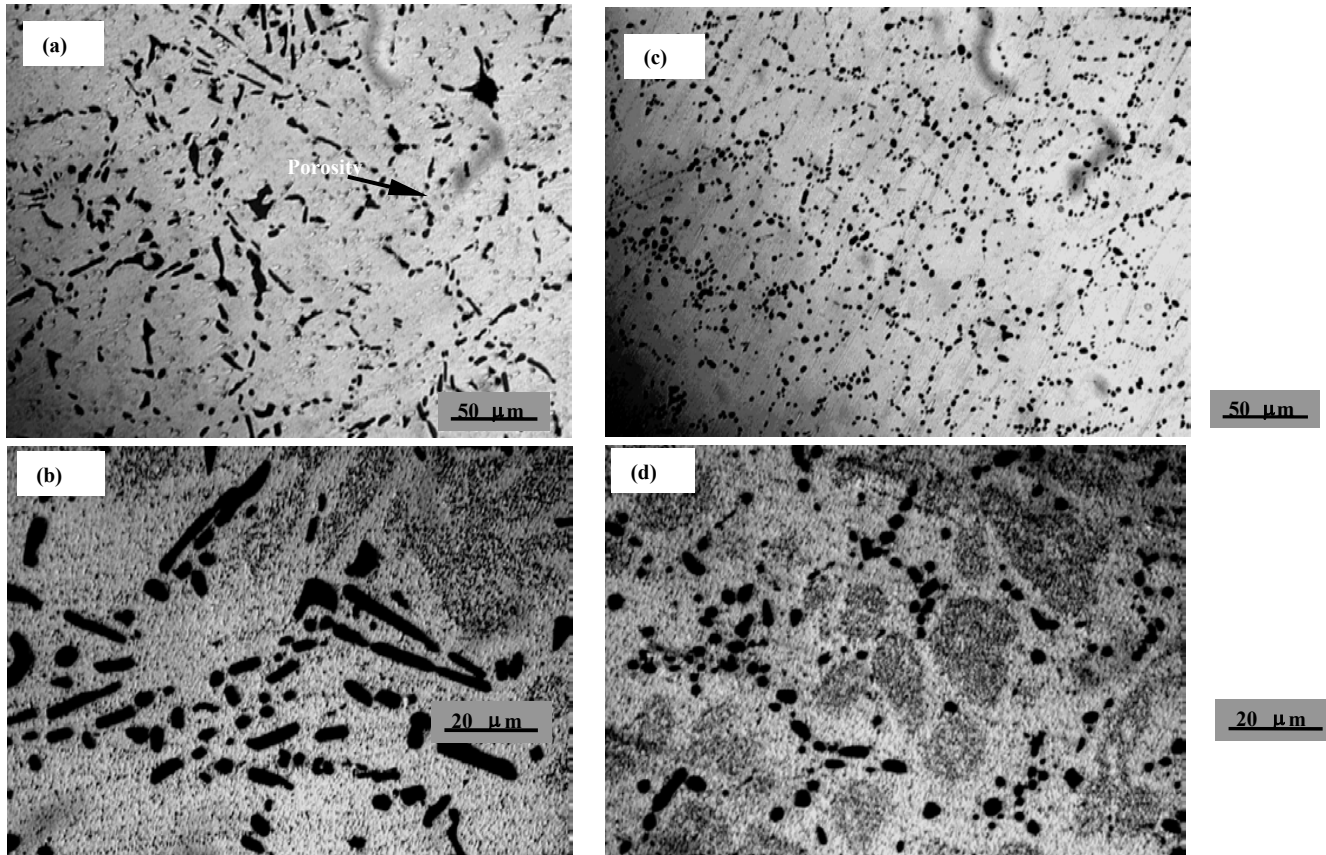
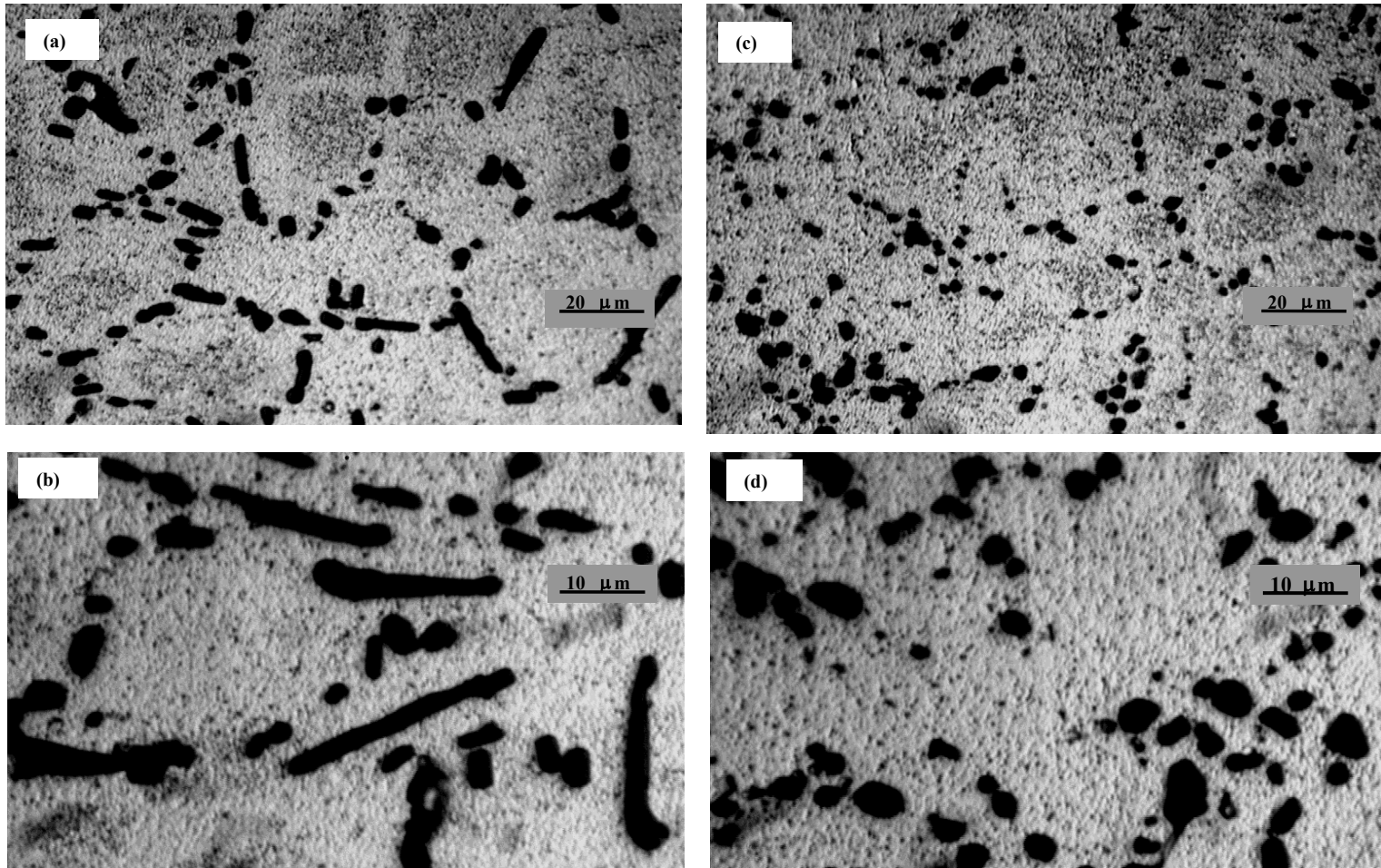


Figure 5.79: Microstructures of permanent mold and squeeze casting in T4 condition



**(a) and (b) are permanent mod with magnification of 200 and 500
(c) and (d) are squeeze casting with magnification of 200 and 500**

Figure 5.80: Microstructures of permanent mold and squeeze casting in T6 condition



**(a) and (b) are permanent mod with magnification of 200 and 500
(c) and (d) are squeeze casting with magnification of 200 and 500**